12-2011

Toward Personalized Medicine: The potential role of RNA interference in Plasma Cell Dyscrasia

Jonathan E Phipps
jphipps@utk.edu

To the Graduate Council:

I am submitting herewith a dissertation written by Jonathan E Phipps entitled "Toward Personalized Medicine: The potential role of RNA interference in Plasma Cell Dyscrasia." I have examined the final electronic copy of this dissertation for form and content and recommend that it be accepted in partial fulfillment of the requirements for the degree of Doctor of Philosophy, with a major in Comparative and Experimental Medicine.

<div align="right">

Jonathan S. Wall, Major Professor

</div>

We have read this dissertation and recommend its acceptance:

Daniel P. Kestler, Robert Donnell, Steven J. Kennel

<div align="right">

Accepted for the Council:
Carolyn R. Hodges

Vice Provost and Dean of the Graduate School

</div>

(Original signatures are on file with official student records.)

Toward Personalized Medicine:
The potential role of RNA interference in Plasma Cell Dyscrasia

A Dissertation Presented for
the Doctor of Philosophy
Degree
The University of Tennessee, Knoxville

Jonathan Earl Phipps

December 2011

Dedication

This work is dedicated to my family, who never said "You can't do that", and always said

"We're here for you".

This is also dedicated to my wife Dr. Jada Phipps, who has been my cheerleader and my

cornerstone.

Finally, to our Son, who gave me the motivation I needed to make it through.

Acknowledgements

I would like to express my deepest gratitude to Dr. Robert Donnell Dr. Steve Kennel for their guidance and support over the term of this project. I would also like to thank Dr. Daniel Kestler for the years of training, which I am sure, will prepare me for any work environment. I also wish to thank Dr. Alan Solomon for his support and help during my time with his group. I express my gratitude to Steve Foster, who has helped with designing experiments and taught me a variety of techniques. Thank you as well to Tina Richey of the HICP program, who provided care for and patiently taught me how to handle the animals used herein and graciously collected sera for the experiments. I would also like to thank Sallie Macy, for her support and whose brilliance with preparing immunohistochemical stains truly is an art. I would also like to thank my major professor, Dr. Jonathan S. Wall for nothing*.

* Whereas nothing refers to being a great advisor, wonderful friend, and a true mentor. Dr. Wall has always seemed to know when to offer a word of support or a kick in the pants. Without his support and stubborn faith in my abilities, I would have never had the opportunity to start down this path. To that I say "thank you, sir".

Abstract

A major contributor to mortality in patients with plasma cell dyscrasias (PCDs); i.e., multiple myeloma, light chain deposition disease and AL amyloidosis is the deposition as insoluble aggregates of monoclonal immunoglobulin light chain proteins (LC) in the kidneys and other organs. Currently anti-plasma cell chemotherapies are used to reduce LC synthesis, and slow deposition. While effective, these treatments are toxic, non-specific, expensive, and might not be appropriate in all cases, making the identification of an alternate means of reducing toxic LC species desirable. To this end, we have investigated whether RNA interference (RNAi) could achieve these goals.

Human (RPMI 8226, Bur) and transfected mouse myeloma (SP2/O-lambda 6) cells which produce measureable quantities of human LC protein were used as model systems for testing the efficacy of both synthetic small interfering RNAs (siRNAs) and short hairpin RNA (shRNA) expression vectors in reducing LC synthesis. Sequencing of LC genes provided the basis for design of siRNA duplexes targeting either the variable (V) or joining (J) regions of individual LCs, or the constant (C) region of either kappa or lambda LC isotypes. Myeloma lines were transfected with siRNAs using lipid-based transfection media. Cells receiving non-silencing siRNAs served as controls. Exposure of myeloma lines to siRNAs was well tolerated and no cytotoxicity was observed. LC mRNA expression was shown to be reduced $\geq 40\%$ in 8226 and SP2/O- lambda 6 cell lines receiving siRNA treatment as compared with untreated controls. Exposure to siRNAs was also effective in significantly reducing both intracellular and secreted LC protein levels in cell lines tested as evidenced by flow cytometry or enzyme-linked immunosorbent assays (ELISAs).

Effective siRNA nucleotide sequences were used to generate shRNA cassettes which were ligated into lentiviral expression vectors under the control of the RNA polymerase III promoter,

iv

U6. These expression systems were used to generate replication incompetent lentiviral particles.

Exposure of 8226 to lentiviral particles resulted in significant knockdown of LC mRNA and

protein both *in vitro* and in xenograft tumor bearing immune compromised mice. These results

provide positive evidence for the ability of RNAi based approaches to reduce LC secretion in

models of PCD.

Table of Contents

Table of Figures

List of Tables

List of Abbreviations

ABTS	2,2'-azino-bis(3-ethylbenzthiazoline-6-sulphonic acid
Ago	Argonaute proteins
AL	Light chain amyloidosis
ASCT	Autologous stem cell transplant
$\beta_2 M$	Beta-2 microglobulin
BCR	B-cell receptor
BJP	Bence Jones Protein
BSA	Bovine serum albumin
C	Constant region
cDNA	complimentary DNA
CMV	Cytomegalovirus
D	Diversifying region
DMEM F-12	Dulbecco's Modified Eagles Media Formulation-12
dNTP	deoxynucleotide tri-phosphate
dsRNA	double stranded RNA
EDTA	Ethylenediaminetetraacetic acid
EGFP	Enhanced green fluorescent protein
ELISA	Enzyme Linked Immunosorbent Assay
FLC	Free light chain
GAPDH	Glyceraldehyde-3-phosphate dehydrogenase
GFP	Green fluorescent protein
HC	Immunoglobulin heavy chain
HRP	Horseradish peroxidase
IACUC	Institutional Animal Care and Use Committee
Ig	Immunoglobulin
i.p.	Intraperitoneal
i.t.	Intratumoral
J	Joining
LC	Immunoglobulin light chain
LCDD	Light chain deposition disease
miRNA	micro RNA
MGUS	Monoclonal gammopathy of undetermined significance
MM	Multiple Myeloma
mRNA	Messenger RNA
PBS	Phosphate Buffered Saline
PCD	Plasma cell dyscrasia
PTGS	Post transcriptional gene silencing
RAG	Recombinase activating gene
s.c.	Sub-cutaneous
SEER	Surveillance Epidemiology End Results
shRNA	Short hairpin RNA
SHM	Somatic hypermutation
siRNA	Short interfering RNA

SWOG	Southwestern Oncology Group
TAE	Tris acetate EDTA
TBS	Tris buffered saline
THP	Tamm-Horsefall protein
V	Variable
VAD	Vincristine, Adriamycin, Dexamethasone

Chapter 1

Review of the Literature

1.1 Post transcriptional gene silencing by RNA interference

Recently, new light was shed on the process by which eukaryotic cells moderate the expression of genes following transcription (post-transcriptional gene silencing; PTGS). This process, namely, RNA interference (RNAi) is enacted by a conserved family of proteins that, upon activation by the presence of short double stranded RNA sequences, abrogate translation of messenger RNA (mRNA) in a sequence dependant manner.

The process of RNA mediated conditional gene silencing was first posited in the early nineties with observations made in plants which were infected with viral constructs designed to express short mRNAs encoding the chalcone synthase gene, with the intended goal of enhancing petal colors in petunias by overexpression of the gene product. Results from these experiments were contradictory to this hypothesis as transgenic plants generated in these experiments exhibited either a total or a variegated loss of pigment within the petals (1). This loss of pigment was found to correlate with suppressed levels of both endogenous and exogenous chalcone synthase mRNAs, thus the process was originally termed co-suppression (1). Following these observations, a series of studies were enacted to determine if co-suppression was present in other organisms (2) (3). In 1997 two American researchers Andrew Fire and Craig Mello demonstrated that small double stranded RNAs (dsRNA) were the initiating factors of RNA interference in the invertebrate *C. elegans* in a nature publication and were later awarded the nobel prize for this work (4).

The process of RNAi is highly conserved among eukaryotes and has been posited to have arisen as part of a cellular innate immune defense to viral infection and harmful transposable genetic elements (5). Similarly, endogenous siRNAs may be produced which are used to modulate normal gene expression. These so-called microRNAs (miRNAs) were first identified in developmental models and were originally termed short-temporal RNAs due to their pattern of expression, and have since been shown to mediate tissue and cell cycle specific post transcriptional regulation of self proteins (6-9).

Overview of RNA interference

Initation of the RNAi pathway coincides with the introduction of short dsRNA molecules to the cytoplasm of a eukaryotic cell which act as guides for silencing (10) (figure 1.1). Also known as a short interfering RNAs (siRNAs), these molecules are palindromic, double stranded 21-28 bp RNA sequences showing either complete or nearly complete complimentarity and possessing a characteristic 2-4 nucleotide overhang on the 3'end of each strand (11, 12). Generation of siRNAs is the result of a multi-protein complex, whose enzymatically active member, known as Dicer belongs to the RNase III family of proteins. Dicer is capable of generating double strand endonucleic cleavages along longer dsRNA transcripts produce the characteristic siRNAs described above (13). Dicer, along with mature siRNAs, then acts as a nucleus which triggers the association of several specialized proteins into a larger multi-protein complex known as the RNA Induced Silencing Complex (RISC). As the RISC assembles Dicer transfers the siRNA to a protein belonging to the Argonaute (Ago) family (of which there are four in humans), and the siRNA is cleaved into its component nucleotide "guide" and "passenger" strands, with the strand

2

showing the lowest thermodynamic stability at the 5' end being preferentially transferred (14, 15). Proteins of the Ago family (Ago 2 in humans) have been found to have both an RNA binding domain (PAZ) as well as an active RNase site (PIWI) and are thought to be the enzymatically active portion of RISC, details of which are summarized in (Figure 1.2) (14). Using the guide strand to locate target mRNA molecules by complimentary bp binding RISC prevents translation and protein synthesis in several ways; In the case of siRNAs, the perfect pairing of guide to target triggers allows cleavage of the mRNA by the PIWI domain of the Ago protein (579). The guide strand also acts in concert with Ago as a "molecular ruler", generating cleavage sites which are defined in relation to the siRNA 3' end, occurring between the 10th and 11th nucleotide of the bound portion of the mRNA strand (16). Imperfect base among partner RNA strands may induce silencing as well, as is the case with another class of interfering RNA molecules, the miRNAs. These act along a parallel pathway as siRNAs, however, bulges generated by imperfect pairing prevent cleavage by RISC. Silencing generated by miRNAs is a result of inhibition of translation by the bound RISC complex. These bound mRNAs may also be removed to cytoplasmic storage centers called "processing bodies" (p-bodies) for degradation or future release (15).

Endogenous interfering RNAs

Endogenous short dsRNA sequences are transcribed from stretches of non-coding DNA by either RNA pol-II in the case of miRNAs or RNA pol-III enzymes as with shRNA molecules. Of the endogenous silencing RNAs, ShRNAs are perhaps the simplest consisting of two complimentary 21-28nt sequences which are separated by an intervening stretch of non-complimentary nucleo-
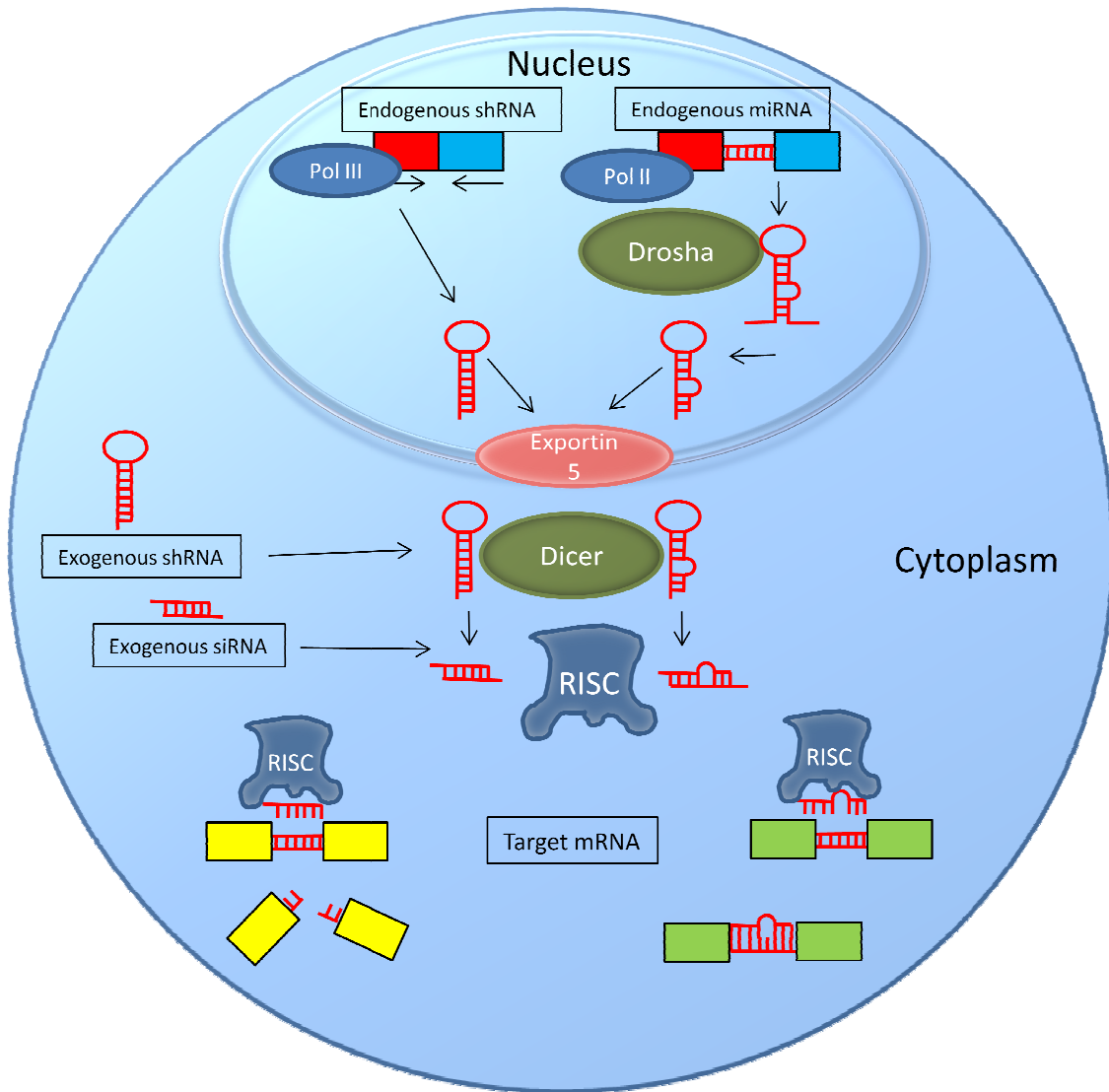
Figure 1.1 Outline of RNA interference. RNA polymerase III enzymes generate ~60nt short hairpin RNA molecules with 2nt 3' overhangs, while RNA polymerase II enzymes synthesize longer primary miRNAs (pri-miRNA). Pri-miRNAs are processed by the RNase enzyme Drosha to mature miRNAs containing hairpin loops and 2nt 3' overhangs. Structural recognition of the 3' end overhang by the nuclear export protein exportin 5 allows transfer of the nucleic acid to the cytoplasm. Processing by nuclease enzyme Dicer removes loop portion, leaving short dsRNA molecules upon which the RNA induced silencing complex (RISC) forms. Further processing removes passenger strand RNA while the guide strand remains associated with RISC and identifies target mRNA strands. Perfect homology results in cleavage of target sequence, while imperfect pairing results in inhibition of translation or sequestering to p-bodies. Figure adapted from (17).
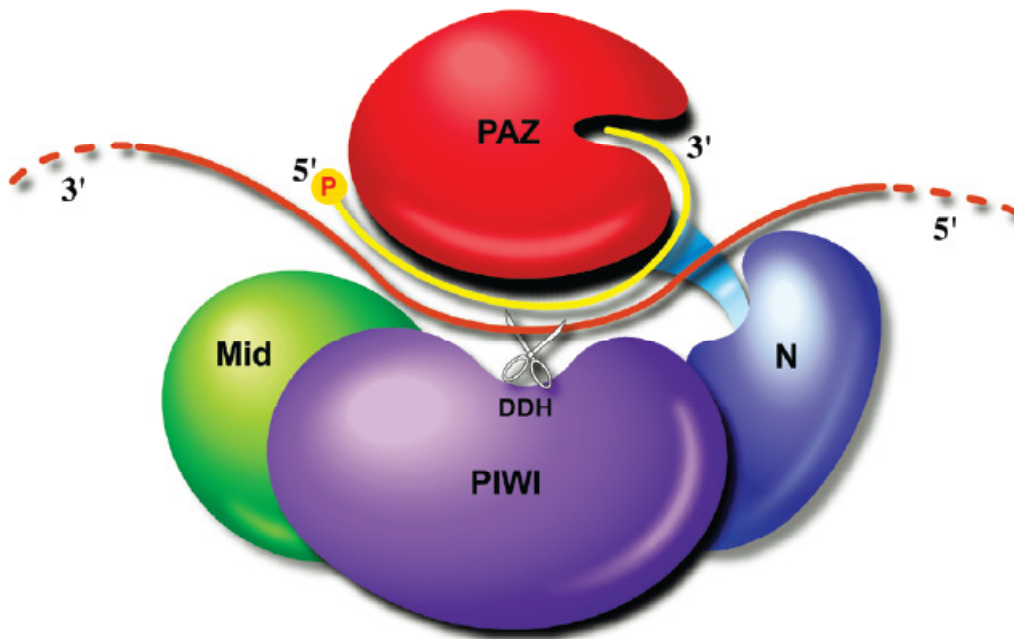
Figure 1.2 Schematic depiction of the model for siRNA-guided mRNA cleavage by Ago.
Within the Ago protein (Red, Green, Purple, Blue) the siRNA (yellow) binds with its 3' end in
the PAZ cleft (red) and is directed along a groove which facilitates duplex binding between PAZ
and the RNase domain PIWI (purple). The 5' phosphate group interacts with a second site on
PAZ to stabilize the interaction between siRNA and Ago, as well as to produce the crucial
binding region for target mRNA loading, known as a "seed region" this area corresponds to
nucleotides 2 through 8. Target mRNA is introduced between the amino terminal (blue) and
PAZ, exiting between PAZ and the middle domain (green). Cleavage of target mRNA occurs at
a conserved site containing two aspartate and single histadine residue (scissors) found within the
PIWI domain (purple). Taken and summarized from (14).

tides. Upon transcription, shRNA gene products self-anneal to generate a stem-loop structure with a short overhanging sequence found at the 3' terminus. Recognition of the overhang region by the protein Exportin-5 facilitates transfer from the nucleus to the cytoplasm (18-21).

Initial transcription of miRNA genes produce longer (up to several kilobases) primary-miRNAs (pri-miRNA) which are processed by the RNase III-like enzyme Drosha to ~70 nt shRNAs complete with 3' overhang (22-24). In contrast with shRNAs, miRNAs contain short regions of mismatch between strands causing bulges to form during folding. As with shRNAs the nuclear export protein, Exportin-5, recognizes the 3' overhang and transports the nucleic acid to the cytoplasm where it is processed by Dicer and incorporates to RISC as above (21). Schematic representations of each species are illustrated in Figure 1.3.

Exogenous siRNAs

Since their discovery over a decade ago countless studies have utilized the phenomenon of RNAi as a means to probe gene function within the laboratory and have postulated their use in the clinical setting to target gene products associated with a variety of pathologies (25). Design of these molecules has been optimized based on the characteristics of naturally occurring siRNAs, shRNAs, and miRNAs to allow efficient incorporation to the RNAi pathway (26, 27). Introduction of functional interfering RNAs has been shown possible using a variety of transfection methods each with their own strengths and weaknesses (Table 1.1). These user generated siRNAs may be synthesized and pre-annealed siRNAs and introduced to the cytoplasm
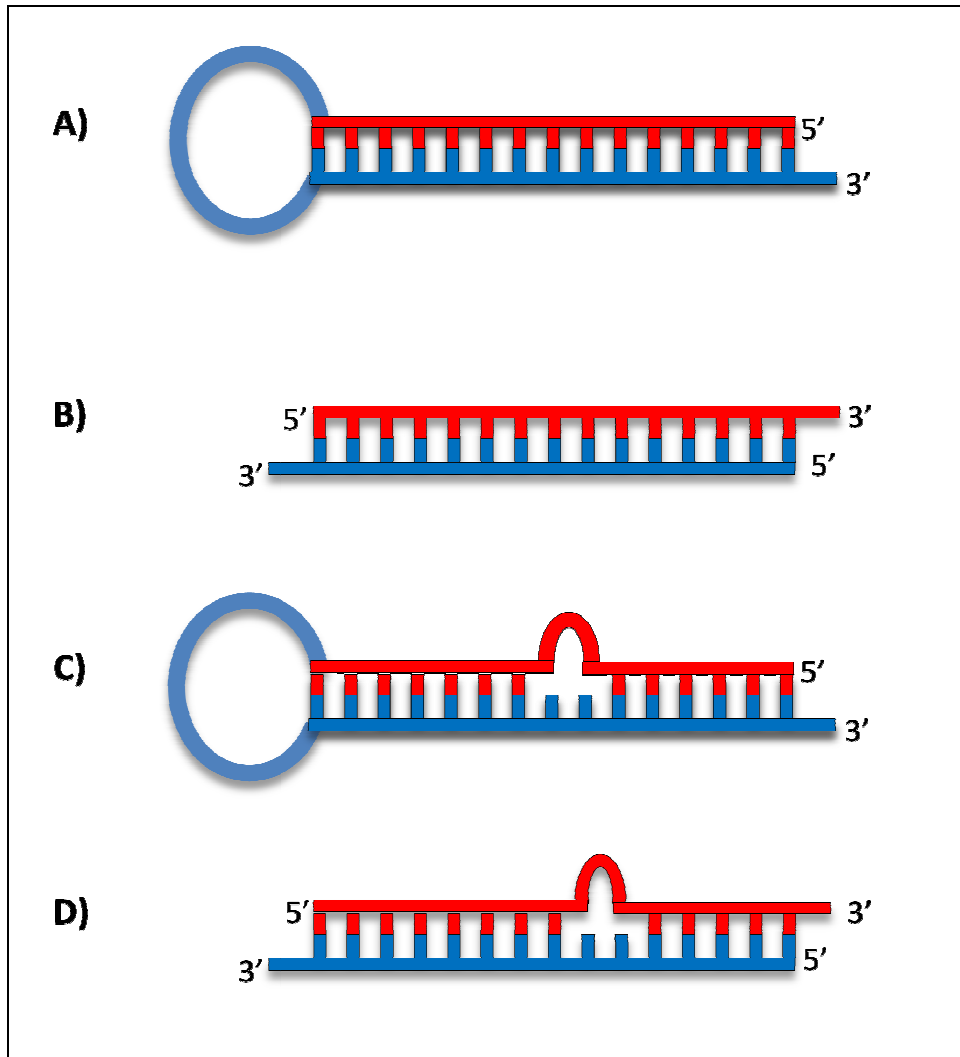
Figure 1.3 Structural differences between interfering RNA species. Processing of A) shRNA by RNase enzyme Dicer removes hairpin loop generating B) a 21-28nt siRNA molecule. Cropping of longer pri-miRNA sequences by the nuclear enzyme Drosha yields, C) pre-miRNAs, which will be further processed by the Dicer enzyme to form D) mature miRNAs.

Table 1.1 Strategies for delivery of interfering RNAs

Class	Method	Advantages	Disadvantages	Examples
Physical	Direct injection Electroporation Laser Irradiation Sonoporation Magnetic nanoparticle	Not cell type specific, Physical relocation of nucleic acid to cell, no vector, single cell transfection	Laborious, high level of skill required, costly equipment	Gene gun, amaxa nucleofector, microneedle
Chemical	Cationic Polymer Ca^{++} Phosphate Cationic Lipid	No need for vector, high- efficiency, commercially available, no size limit for cargo	Transfection efficiency can vary, cytotoxicity, some cell types hard to transfect	Lipofectamine, invivofectamine, HiPerFect, DOTAP, DEAE dextran
Biological	Virus Mediated	High-efficiency, simple to administer, may be used *in vivo*	Biosafety concern, insertional mutagenesis, immunogenicity, limited package size, costly production, fragility of viral particles	Lentivirus, Herpesvirus, Adenovirus, Adeno-associated virus, vaccinia virus, sindbis virus

Adapted from (28)

8

physically or chemically, or incorporated into viral vectors capable of nuclear expression of gene transcripts encoding siRNA precursors such as shRNAs or pre-miRNAs (28-31). Table 1.2 summarizes the compatibilities of these systems and refers to selected studies in which they have been used.

1.2 Introduction to the plasma cell

The plasma cell is a functionally active and terminally differentiated lymphocyte arising from the b-cell lineage. The b-cell repertoire within higher vertebrates contains an astounding collection of cells whose immunoglobulin (Ig) products are capable of recognizing a multitude of unique antigens. The amount of diversity seen in the Ig complement comes from the ability of the B-cell to recombine and mutate the germline genes which encode the Ig products. Plasma cells arise from a series of activation and selection events stemming from the interaction of a specialized b-cell receptor with antigen, engulfment of the receptor antigen complex, and expression of antigen proteins on major histocompatibility complexes leading to activation by helper t-cells. Under normal circumstances these activation events lead to a controlled monoclonal expansion of b-cells capable of producing Ig proteins that interact with the given antigen. This expansion of a single b-cell subgroup, paired with the almost unlimited variability of the Ig product allows plasma cells to recognize an exceedingly wide variety of antigens and makes them an integral component of the adaptive immune system.

Table 1.2 Compatibility of synthetic interfering RNAs with various delivery systems

Type of interfering RNA	Route of introduction	Cell compartment	Refs
siRNA/miRNA	Physical	cytoplasm	(30-34)
	Chemical	cytoplasm	(28)
shRNA	Physical	cytoplasm	(35)
	Chemical	Cytoplasm	(35)
	Biological	Cytoplasm/nucleus	
Pre-miRNA	Physical	Cytoplasm	
	Chemical	Cytoplasm	
	Biological	Cytoplasm/Nucleus	

Immunoglobulins

Structurally the mature Ig product of the plasma cell is a 150 kDa molecular weight molecule composed of two 330-440aa 50 kDa regions, the heavy chain (HC), and two 100-110aa 25 kDa, the Ig light chain (LC) regions. Amino acid sequencing of the Ig have yielded regions of homology in both the LC and HC chains representing the domains of each peptide class. Based on the extent of this homology these domains have been termed either the variable (V) or constant (C) domains. Thus the LC is composed of one V_L and one V_C domain, while the IgHC is composed of one V_H domain and 3-4 C_H domains based on the Ig class (36). These polypeptide chains adapt a pleated beta sheet structure of alternating hydrophobic and hydrophilic residues with the individual domains held in conformation by the hydrophobic interactions and with a conserved disulfide bond (37). The Ig molecule itself is encoded by multigene families located on separate chromosomes (37). Each of the genetic loci contains a series of gene segments encoding regions of the HC or LC proteins. Each of these gene segments are in turn flanked by specific sequence motifs that provide a recognition site for proteins encoded for by two distinct recombinase activating genes (RAG 1/2). The recombination signal sequences are a conserved palindromic heptamer and AT- rich nonamer separated by a 12 or 23 base pair sequence (38). Recognition of these sites by RAG proteins allows for the formation of novel Ig proteins based on the rearrangement and splicing of the individual V and C regions within the LC DNA and the V, C, as well as the added diversifying (D) region within the HC (38). This signal sequence also directs the rejoining of the cleaved DNA strands resulting in a directed recombination of the HC gene into the mature form which contains the V, (D), J, and C regions. This process is repeated along the LC gene locus resulting in a b-cell which is unique at three separate levels; a) selection of V, D, J, and C segments, b)

11

selection of HC and LC sub-types, and c) insertions and deletions introduced during rearrangement.

Following the expression of a functional B-cell receptor (BCR) the maturing b-cell migrates from the bone marrow to lymphoid follicles. Antigenic challenge of these follicles induces the formation of germinal centers which act as sites of selection and activation of b-cells through the binding of antigen displayed by follicular dendritic cells with the BCR. At this point the maturing Ig gene undergoes a form of secondary diversification in a unique process termed somatic hypermutation (SHM). SHM is an enzymatic process involving Activation-Induced Cytidine Deaminase (AID) which introduces point mutations within key "hotspots" of the HC and LC V regions (39). These point mutations occur by the selective conversion of cytidine to uridine within single stranded DNA loops of transcription bubbles (40). This mismatch lesion is then either carried on during replication to form an A:T substitution or is repaired by low fidelity polymerase enzymes which induce further substitutions and subversions to the genetic sequence (41).

B-cell origin and differentiation

Cells of the B-lineage arise from pluripotent hematapoetic stem cells within the fetal liver and the bone marrow in most mammals (42). Identification of these cells have been carried out by immunologic methods based on the presence of conserved surface markers such as CD43, HSA, and cKIT. Of these pluripotent cells a subset has been identified which gives rise to B and T lymphocytes as well as Natural Killer (NK) cells and are thus termed common lymphoid progenitor cells(43). It is from this group that the early phase pro-B cell population originates, characterized by its expression of the b220 isoform of CD45 as well as terminal

deoxynucleotidyl transferase (TdT) in conjunction with the lack of CD19 expression (present in all further differentiated B-cell subsets).   At this point key genetic rearrangements occur, which give rise to the recombination of the Ig heavy chain gene locus HC through the activation of genes RAG 1/2 (44). During recombination of the HC genes the protein products of the RAG-1 and RAG-2 genes perform site specific double stranded cleavages of the genomic DNA strand using a unique signal sequence motif recognized by the enzymes (38).

Because of the immense capacity of an activated b-cell to produce Ig protein the pathologic potential of unregulated expansion of a monoclonal b-cell population is compounded. Indeed, a major contributing factor to the morbidity and mortality of patients diagnosed with plasma cell dyscrasias is the aggregation and deposition of the monoclonal Ig protein within the organs, the most commonly affected being the kidneys. The chronic deposition of these proteins leads to progressive organ failure. The potential of organ involvement by circulating Ig proteins poses a unique problem for the treatment of b-cell malignancies as a detectable expansion of monoclonal b-cells is not always required for pathology to occur.

1.3 Plasma cell dyscrasias

The following section will address plasma cell dyscrasias (PCD) starting with the pre-malignant condition known as monoclonal gammopathy of undetermined significance (MGUS) and the malignant condition multiple myeloma (MM). An overview of MM will be provided which will include; diagnosis, staging, epidemiology, and a summation of lytic bone lesions. This will be followed by a discussion of pathologies arising from overproduction and deposition of immunoglobulin component proteins (i.e., LC) which, although often occurring concurrently to MM, may arise independent of a detectable malignant plasma cell compartment. The final

portion of this section will provide a brief review of some of the therapeutic options that are currently used in treatment of MM and PCD.

Plasma cell dyscrasias

Plasma cell dyscrasias (i.e., MGUS, multiple myeloma, plasmacytoma, light chain amyloidosis, etc) represent a spectrum of pre-malignant and malignant states arising from the late B-cell compartment. Dysregulation of cell processes result in the expansion of a monoclonal population of these antibody secreting cells, which home to the bone marrow microenvironment, inducing a variety of disorders ranging from the formation of lytic bone lesions, immuno-suppression, decreased hematopoesis, and organ dysfunciton. A characteristic feature of PCD is the presence of the so called M-protein, which is a measurable spike in serum and urine protein levels, occurring from the overproduction of immunoglobulin (Ig), or immunoglobulin component (i.e., LC or HC) by the monoclonal cell population. The overproduction of Ig, LC, or HC is of additional concern as the increased protein load may lead to pathologies apart from the primary neoplasia, occurring mainly by deposition and aggregation of protein in the organs and soft tissues. Renal function is of particular susceptibility in PCDs, in part due to the role of the kidney in clearing small proteins such as LCs and HCs, and to Ig independent conditions which may occur during the course of PCD.

Monoclonal gammopathy of undetermined significance

A spike in monoclonal Ig (M protein) is perhaps the most common abnormalities upon hematologic examination, occurring in 3% of persons over 50 and in up to 7% of patients

seeking a medical evaluation (45). LC M protein was first described by the English physician Henry Bence-Jones in Thomas Alexander McBean, a patient of Dr. William Macintyre, who referred to the curious properties of an "animal matter" that was present in the patients urine. Thus, the term Bence Jones Protein (BJP) was born into existence (46-48).

Spikes in M protein in the serum and urine were recognized as an indicator of a potentially malignant condition early on, and are detected by agarose gel electrophoresis followed by immunofixation to determine M protein components (49). M protein can be quantified by rate nephelometer (48). The presence of a small protein spike without evidence of MM or other PCD has also been described, known as essential hyperglobulinemia, benign monoclonal gammopathy, or the modern MGUS (50, 51). MGUS is described as a pre-malignant disorder characterized by limited plasma cell expansion without organ involvement (52). MGUS is often described as a precursor to MM or other PCDs. Like MM risk increases with age, and Approximately 1% of patients diagnosed with MGUS will proceed to MM per year (53).

Multiple Myeloma

Diagnosis of multiple myeloma

Multiple myeloma is a clonal expansion arising from the plasma cell compartment with infiltrates detectable in the bone marrow microenvironment and to a limited extent other organs (extramedullary). Patients most commonly seek medical attention due to bone pain (40-70%), weakness (20-60%), or recurrent infections (54).

Positive diagnosis of MM is based on several criteria: Presence of an elevated M protein in the sera or urine, greater than 10% monoclonal plasma cells detected in the bone marrow, and evidence of end organ damage, as indicated by elevated calcium levels, renal insufficiency, anemia, and bone lesions present on radiograph (55, 56).

The most direct consequence of expansion in monoclonal plasma cells is the presence of a monoclonal Ig protein spike (M-protein) in the serum and urine. This spike was reported to be detectable in 82% of patients by electrophoresis, and in 93% of patients by immunofixation, while a portion of patients exhibit a monoclonal PC expansion absent M protein (47). Approximately 20% of myeloma patients are found to exhibit increased sera and urine LC levels, in absence of HC protein (57). Anemia has been reported in 70% of patients, hypercalcemia in ~25% of patients, and elevated serum creatinine levels in upwards of 50% of patients (57). Lytic bone lesions and fractures are detectable in up to 80% of patients due to changes in the bone marrow microenvironment brought about by the presence of the monoclonal plasma cell population (58).

Staging in multiple myeloma

As with other malignancies, a standardized system of classification and prognosis for the severity and progression of MM is important. However, as MM consists of diffuse collections of plasmacytoid cells, it has presented special challenges for the development of systemic classification of tumor burden in the patient. As such, staging in multiple myeloma has undergone several evolutions since the initial scheme was proposed by Durie and Salmon in 1975 (59). These revised systems include; the Durie-Salmon plus, southwestern oncology

group, Mayo, and international staging systems, which were subsequently developed over the ensuing 35 years (59-62).

As mentioned, initial efforts to stage myeloma cell burden were carried out in the mid-1970's by Brian Durie and Sydney Salmon using sera and urine M-protein measured from 105 MM patients to estimate total MM cell numbers. In this, the Durie-Salmon system (DS), monoclonal cell mass was shown to correlate both singly with serum and urine M protein levels and with clinically significant criteria (hemoglobin, serum calcium, and presence of bone lesions), when taken together, could be used to generate a 3 category staging system. Each stage, representing a low, medium, or high myeloma cell mass. In addition, Durie and Salmon also identified serum creatinine as a correlate to survival, and further modified the initial three tier system to include A and B sub-categories which made the system a more robust prognostic metric for not only survival, but response to therapy as well (60). These results were confirmed by Alexanian et al. (63) in a similar study with the Southwestern Oncology Group (SWOG) which included a larger patient sample and proposed a similar staging system to that of Salmon and Durie.

Following these initial efforts several subsequent studies reevaluated the metric for tumor mass and found that serum albumin and beta-2-microglobulin (β_2M; a component of the MHC protein found on the MM cell surface, useful as an indicator of cell proliferation) were accurate predictors of overall survival (63-66). Although these observations were made as early as 1982, they weren't widely accepted until 2003 when SWOG proposed a revised 4-tiered staging system based on using β_2M and serum albumin exclusively (59). In the interim, a 1993 study by the Mayo clinic reviewed 107 patients and proposed staging of myeloma using a multivariate system measuring β_2M and serum creatinine along with thymidine kinase and C-reactive protein (CRP)

17

as measures of proliferation and IL6 production, respectively. This study also pressed for the inclusion of a plasma cell labeling index, in which plasma cells were identified by fluorescent immunohistochemical labeling for light chain production, and cell cycle determined by the incorporation of 5-bromo-deoxyuridine, indicating those in S-phase (61).

As previously mentioned, the widespread acceptance of β_2M as a metric of Myeloma cell proliferation occurred in 2003 with the publication of a review of 1,555 patients by the SWOG. In this study, again, several metrics were evaluated while β_2M and serum albumin were shown to be the most powerful indicators of survival, again, measuring proliferation and IL6 production, respectively. This study proposed a 4 tiered system, and demonstrated a close relationship in staging to that of the original DS system (59). Most recently, the findings that β_2M and serum albumin were perhaps the best (and most easily obtained) metrics for staging myeloma patients were confirmed by a multinational effort, leading to development of the International Staging System (ISS). In this 2005 study 10,750 myeloma cases were reviewed in 17 centers across North America, Europe, and Asia, which served to confirm the observations made over 20 years prior (62).

In summary, staging in MM seems to have made a single major change over the last 30 plus years, switching from a combination of M-protein, extent of bone lesions, and hemoglobin as the gold standard, to β_2M and serum albumin. The benefit of the latter seems to be the ease of sampling, while losing no advantage to the prior system.

Epidemiology of multiple myeloma

The annual incidence of newly diagnosed cases of MM is reported as 0.4-5 new cases per 100,000 people per year worldwide (67). According to the most recent annual factsheet generated by the National Cancer Institute reviewing incidence and mortality data from the surveillance epidemiology and end results (SEER) database there were, in the United States, an estimated 20,180 new cases of MM in 2010, with 11,170 males and 9,010 females constituting these cases (68). This represents an age adjusted incidence rate of 7.2 and 4.6 new cases of MM per 100,000 people per year in males and females, respectively (68). On January 1, 2008 there were reported to be 64,165 people living, with a history of MM in the United States, while an estimated 10,650 died of the disease (68). MM also ranks in the top 15 cancers in the U.S. for males as reported in a recent sex selected, age adjusted survey of SEER data (69).

Since as early as 1945 the incidence rate in MM has risen gradually. In the U.S. population as a whole, incidence rate of MM in 1949 was reported as occurring in 0.8 per 100,000 persons per year. This rose to 1.7 per 100,000 by 1963, and 3.2 per 100,000 persons by the end of the 1980's (47). A similar trend was reported in a survey of residents of Olmsted County, MN spanning from 1945-1990. In this report the initial incidence rate was significantly higher than that reported nationwide with a rate of 3.1 per 100,000 in the years spanning from 1945 to 1964 while the trend towards increasing incidence persisted to the 1990 level of 4.1 per 100,000 from 1978-1990 (70). Analysis of SEER data using the embedded faststats program confirmed this trend from 1975 until around 1992, when the reported incidence of MM seems to have plateaued (Figure 1.4).
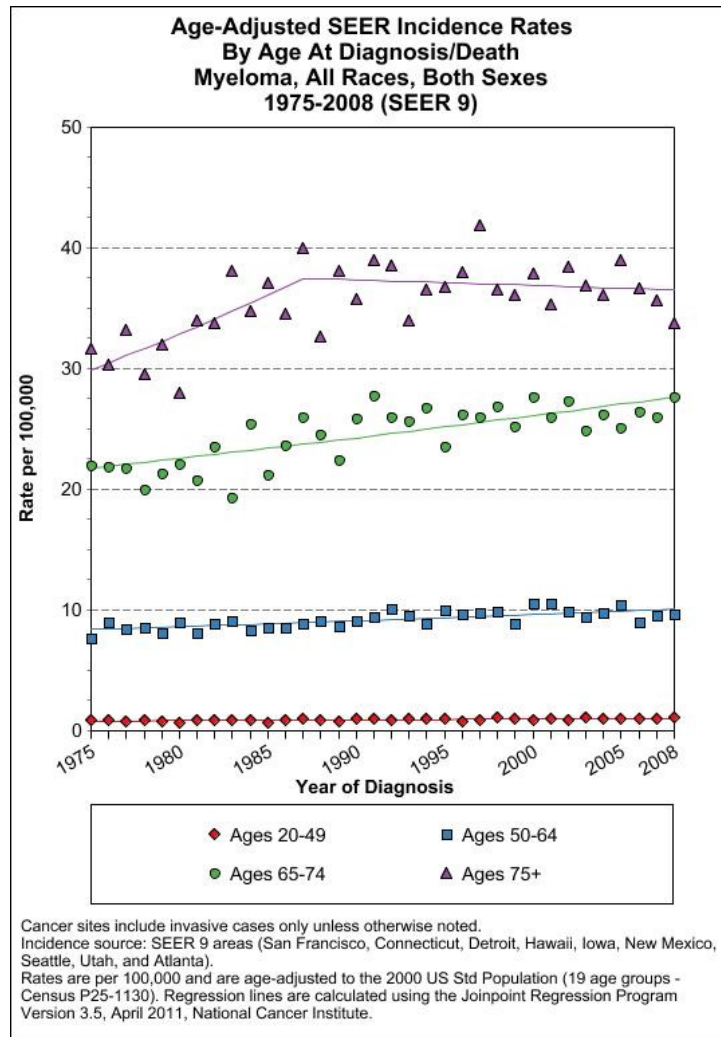
Figure 1.4 Association of age and diagnosis of MM. Data were taken from SEER Cancer Statistics, while the figure was generated using the online SEER FastStats program. (http://www.seer.cancer.gov/faststats)

Efforts have been made to determine risk factors for MM, examining the roles of age, genetic background, race, obesity, exposure to certain toxins, and exposure to ionizing radiation in MM pathogenesis. Of these, age has shown consistently to be the strongest factor in risk for MM occurrence. Taken from the 2008 SEER data, the median age of diagnosis for MM was 69 years of age (68). This trend was also reflected in a review of 1,027 newly diagnosed MM patients from the Mayo Clinic, and published in a 2003 article by Kyle et al (47). Compared with the SEER data, those collected from the Mayo study demonstrate an increased percentage of patients within comparable age groups (i.e., 34-45 v. 40-49), which may be due to the inclusion of older patients within those groups, given risk increases with age.

Aside from age, race has been implicated as the second most apparent risk factor in numerous studies of MM incidence and outcome (68, 71-73). These studies consistently indicate the risk of developing MM in blacks is twice that of whites, while Asians have the lowest incidence. While clear differences among genetic or environmental factors have yet been elucidated, these data seem to imply that one or more may exist and contribute to disease pathogenesis and progression. Factors which have been examined so far have ranged from obesity (74), socioeconomic status (75), exposure to organochlorine pesticides (76), and exposure to ionizing radiation (77). Of these, experimental groups have shown a slightly increased risk to MM, while studies of atomic bomb survivors from Hiroshima and Nagasaki have revealed conflicting reports as to a much higher incidence of MM and monoclonal gammopathy of unknown significance (MGUS) (77, 78). In addition, numerous other studies have examined tobacco use, occupation, etc. revealing no clear correlation with MM incidence. These studies have been summarized previously in several review articles and books (71).

Myeloma bone disease

The most prevalent feature of MM as a consequence of monoclonal plasma cell infiltrates are the presence of lytic bone lesions. These lesions occur most often in the spine as well as the proximal long bones manifesting as bone pain and compression fractures, and are visible by radiograph (79). Formation of these lesions is due to a decoupling of bone resorption with the process of new bone formation. Under normal circumstances the rate of bone turnover is held at a constant rate through degradation by osteoclast activity and formation of new bone by the osteoblast activity. However, the presence of myeloma infiltrates in the bone marrow microenvironment upsets this balance to favor bone resorption over bone formation. Numerous studies have demonstrated that MM cells produce a variety of factors that influence osteoclast activation, while simultaneously down-regulate osteoblast differentiation and activation (80). As a result of osteolytic activation, MM patients often present with elevated calcium levels (>2.6 mmol/L in 20-30% of patients) (81). The elevated Ca^{++} levels observed in these patients have the potential to interfere with cardiac and renal function through the inhibition of Na^{++} reabsorption, and consequential activation of the renin-aldosterone system. Hypercalcemia may also decrease glomerular filtration rate by constriction of afferent glomerular arterioles, as well as induce progressive tubular necrosis and renal acidosis.

Immunoglobulin light chains and disease pathogenesis

A major consequence of the expansion of monoclonal plasma cells is the overproduction of Ig or Ig component protein (i.e. LC or HC). In the following sections the impact of increased Ig paraprotein on renal function (and to a lesser extent other organs) will be examined. While these

pathologies may occur concurrently with MM, it is important to note that they may also occur in a pre-malignant state in which the patient may not meet criteria for diagnosis of MM (similar to MGUS), thus placing the importance on the paraprotein.

Synthesis of immunoglobulin protein is a multi-step process; the genes encoding HC and LC reside in separate chromosomal regions and are synthesized at different rates (37, 82, 83). In addition, chromosomal translocations and deletions common to myeloproliferative disorders often lead to the inactivation of HC translation and synthesis (4q:14). These factors result in disorders involving LC deposition to be over represented in comparison to those involving the HC, thus focus will be given to LC involvement with organ dysfunction. The terms M protein, Bence Jones Protein (BJP) and serum or urine free light chain (FLC) will be used interchangeably.

As previously described and increased amount of Ig or Ig component protein in the urine or serum is a common finding in PCDs. This increase in M protein can be exploited during diagnosis and staging to provide a measure of clonal expansion through the use of assays designed to detect and quantitate the κ or λ isotype of the LC component (84). A shift in the ratio of free LC to either the κ or λ subtype provides a measure to determine the LC isotype being expressed by the clonal plasma cell and aids in immunohistochemical and molecular analysis of the LC in question (85).

The function of the kidney is to remove waste products from the blood through the process of filtration, reabsorption, and secretion of many chemicals while conserving filtered electrolytes and essential metabolites. Properties of molecules important for interactions with the kidneys include; size, isoelectric point, crystal formation, and metal content (86). Renal function in

estimated to be impaired in upwards of 50% of MM patients at time of diagnosis (87), and is a

negative prognostic indicator of survival when compared to patients admitted without renal

insufficiency (47, 88, 89). Conversely, improved renal function in response to treatment is

correlated to improved outcome (488). In the broadest sense, damage to the kidneys by LC

protein is brought about by mechanical inhibition by LC aggregates of the kidney's ability to

conduct fluid within the renal spaces, and by direct cytotoxicity during the interaction between

the LC complexes and cells of the kidney (90, 91). Organizationally, LC aggregate in a variety

of ways; they may occur amorphously (myeloma kidney Figure 1.5 A), or appear organized in

fibrillar (light chain or primary amyloidosis; AL) (Figure 1.1 B) or granular (light chain

deposition disease; LCDD) (Figure 1.1 C) aggregates (refs). These features are a consequence of

the folding stability and physical features of the individual LC molecules, which in turn, are a

direct result of individual LC sequence (92, 93). These aggregates may be formed from either κ

or λ LC isotypes, whereas the distribution of the different LC species varies with type of

depositon (94, 95). In addition, aggregates may consist of various LC subtypes of either family

(i.e., $V_\lambda 1$, $V_\kappa 3$, etc.) as well as portions of the LC paraprotein (i.e. $V\text{-}J_\lambda$, C_κ, etc.), and this

composition has also been posited to control tissue distribution within an individual patient (96).

Myeloma cast nephropathy

While other factors may impact renal performance during MM or other PCD (i.e.,

hypercalcemia, infection, dehydration), a major concern for dysfunction is the production and

deposition as insoluble aggregates of monoclonal free light chain. Under normal circumstances,

0.5-1 g/d polyclonal free LC is produced, secreted into circulation, and processed by the kidneys.

A.

http://www.bindingsite.co.uk/nephrology

B.
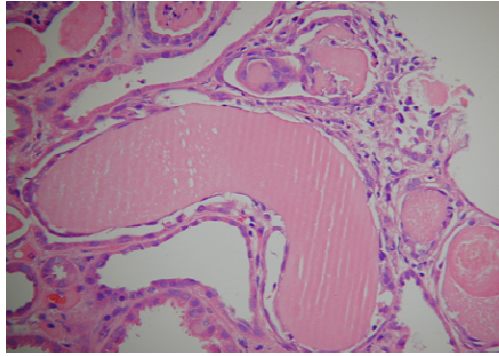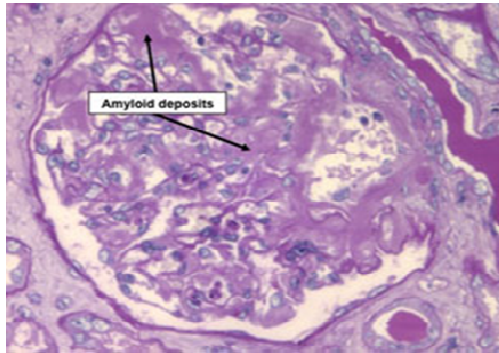
Amyloid deposits

http://stanfordhospital.org/clinicsmedServices/COE/heart/Diseases
Conditions/amyloid/al_primary_amyloidosis.html

C.

http://www.cybernephrology.ualberta.ca/cn/Schrier/Default2.htm
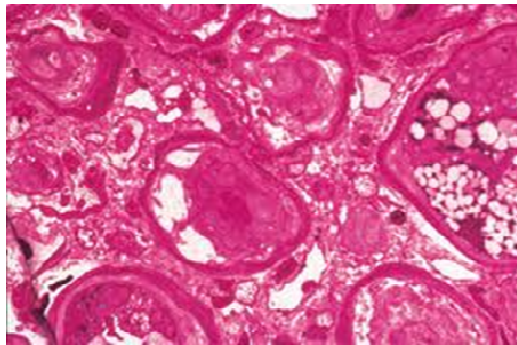
Figure 1.5 Images of LC deposits within the renal spaces. Images were taken from various sources and illustrate the variability seen with LC deposits: A.) Amorphous aggregates seen with myeloma kidney, B) Fibrillar aggregates seen with AL amyloidosis, and C) granular deposits seen with LCDD.

Provided no impairment in renal function the kidneys are capable of managing 10-30 g FLC per day (48). This free LC protein may exist either as a 22 kDa monomer or a 44 kDa dimer, both of which are small enough to pass through the glomerular basement membrane into the renal tubules. Here free LCs bind to the megalin-cubulin complex (97), are absorbed to proximal renal tubule cells by endocytosis, and catabolized to constituent amino acids by hydrolysis following binding to lysozomal compartments (98). Of the initial amount of produced LC, only ~0.4 mg/kg bw/d is secreted in the urine. During the course of MM the clonal expansion of the plasma cell results in the overproduction of Ig or Ig component protein (i.e., FLC or BJP), drastically increasing circulating LC levels, and increasing BJP to levels of 20 g/day or greater (99). Increased levels of LC within the proximal tubular space quickly exceed the ability of renal epithelial cells to clear excess LC and leading to spillage to the distal renal tubule.

Following saturation of cubulin-megalin complex, excess LC proceeds along the nephron to the distal renal tubule where it may bind with Tamm-Horsfall mucoprotein (THP). THP is a 616 aa, 70 kDa membrane-bound protein, secreted by epithelial cells within the distal luminal spaces of the thick ascending loop of Henle (100-102). Interaction between LCs and THP were found to occur between a conserved 9 aa sequence and the CDR3 region in both κ and λ LCs (100). Further, the isoelectric point (pI) is thought to contribute to the binding of LC with THP, as LCs with a pI above 5.1 (pH of renal tubule fluid) are conferred with a net positive charge which contributes to stability with the anionic THP (103, 104). These protein complexes accumulate to large, fractured, waxy casts in the lumen of distal and collecting tubules. These casts are eosinophillic, polychomatophillic, and are stained by periodic acid-schiff (105). Infiltration and interaction with cast protein by monocytes results in the formation of mononuclear and multinuclear giant cells. The immune response along with the cytotoxic effect of the LC

complexes results in diffuse damage within both distal and proximal tubules with areas of denuded basement membrane, flattened epithelial cells, and atrophied or necrotic regions (91, 105). As the process of deposition continues, fluid volume becomes increasingly reduced, further concentrating Ig precursor proteins and enhancing deposition (106). Evidence also suggests that increased NaCl levels renal tubules may increase binding rates between LCs and THP, thus potentiating accelerated cast deposition (90).

In addition, the presence of FLC may also present further challenges to renal function as there have been reports that certain LC species may exhibit a cytotoxic inhibition of sodium dependent uptake of glucose, alanine, and phosphate by brush border vesicles and proximal renal tubule cells (91, 107, 108).

Light chain deposition disease

Light chain deposition disease (LCDD) is defined as the monotypic deposition of LCs in various organs, (109). While they may occur in any organ, deposits are predominantly localized to kidney basal membranes and appear as granular electrodense material, refractory to congo red or thioflavin T, but easily stained by immunohistochemistry (95, 110). The most common finding at time of presentation is renal insufficiency, proeinuria, and, upon biopsy, nodular sclerosing glomerulopathy. This form of LC deposition is relatively rare, in one study of over 5,900 renal biopsies LCDD was identified in 6 patients (111). Of LCDD cases, approximately 50% occur in concordance with overt MM, with these cases the risk of death is 2.55 times higher than with MM alone (110, 112). In the majority of cases, deposits consist of primarily the C region of κ

LCs (68% v 32% C_λ) (95). Mechanisms of renal damage in LCDD are thought to arise from an interaction between LC and a surface receptor found on renal messangial cells (113). Interactions between LC and messangial cells result in transformation of cells to a myofibroblastic phenotype, followed by the deposition of extracellular matrix material and resulting in tubulointerstitial fibrosis (114, 115). In a multi center study Pozzi et al. reviewed 63 patients with LCDD. At the time of presentation ninety-six percent presented with renal insufficiency, and by 6 months renal function had deteriorated to the point of proteinuria in 37% of participants (95).

Therapy for LCDD is similar to that of MM. Both conventional and high dose chemotherapeutics in conjunction with ASCT are utilized to reduce the clonal B-cell population, with intent of slowing the rate of deposition, with reports of these interventions showning varying success (111, 116-118).

Light Chain Amyloidosis

Light chain or primary amyloidosis (AL) refers to the deposition of LC proteins in an ordered, fibrillar arrangement. The term amyloidosis refers to any disease caused by the deposition of amyloid fibrils. Amyloid is defined as an insoluble fibrillar protein, deposited within the extracellular matrix, *in vivo* which can be distinguished from non-amyloid deposits by fibrillar appearance upon electron microscopy, typical cross β-sheet pattern by x-ray diffraction, and a high affinity to Congo red, with resulting apple green birefringence when viewed under polarized light (119). Heretofore, there have been 25 proteins described which are known to

form amyloid fibrils under physiologic conditions and are involved in a range of disease states from type II diabetes to Creutzfeldt Jacobs disease (120). Classification of amyloidosis is based on two criteria; first, the type of amyloid is determined by the precursor protein that makes up the fibrils, and second, the extent and numbers of sites for deposition make up the criteria for systemic or localized amyloidosis (121).

AL is one of the two most common systemic amyloidoses, although on rare occasions it may be observed to have a localized site of deposition (122). While AL may be diagnosed apart from hematologic malignancy, it is known to occur in 10-15% of MM patients with a median survival of less than 2 years (123). Conversely, even fewer patients diagnosed with AL progress to develop overt lymphoproliferative disorders, likely because the short survival time from diagnosis pre-empts the rate of clonal expansion (124). AL deposits have been described in a range of tissues including; kidney, heart, liver, nerve, GI tract, lung, as well as soft tissues (125). Diagnosis of AL is reflective of this, as patients often present with vague and disparate symptoms, depending on the organ involved (126). In addition, confirmation of AL requires a positive biopsy for amyloid deposition from the organ(s) which are suspected of involvement (125).

During LC amyloid formation, the growing fibril recruits misfolded LC paraproteins and arranges them from their native conformation into a well organized β-sheet motif, stabilized by the formation of intramolecular H bonds (120). Unlike LC cast nephropathy, the LCs involved in AL are rarely intact, in the majority of amyloids only the N-terminal V and J regions are present (525). As amyloids which contain an intact C region, or are composed of C region paraprotein are so rare, it is likely that this truncation is a requirement for fibril formation and is

29

reflective of the thermodynamic instability of the VJ region (127). Although all LCs are capable of forming amyloid fibrils, those formed from λ LCs are appear at a 3:1 ratio as compared with κ LCs (122). The most common subgroups of LCs involved in AL are the $V_κ1$ and $V_λVI$ groups, which are of particular interest in AL studies for their ability to preferentially associate to amyloid fibrils (128, 129). This illustrates the importance of the primary sequence of the LC protein, which has been shown to correlate with a variety of features in AL ranging from tendency to form fibrils, sites of organ and tissue involvement, and toxicity (92, 114).

While any organ other than brain can be involved with systemic AL, the most commonly affected are the kidney and heart (129). Clinical presentation is reflective of the organ involved. Findings in patients with renal involvement are proteinuria and other symptoms of nephritic syndrome. Likewise, patients with cardiac amyloid often show an acute onset, and rapidly progressing congestive heart failure with abnormal echocardiographic findings upon clinical evauation . Patients with AL have a relatively poor prognosis, with a median survival of 1-2 years (130).

Given the grim prognosis for patients with AL, therapeutic intervention focuses on affecting either LC concentration or recruitment to fibril formation rather than directly focusing on the malignant compartment. The goal for the former "precursor/product" theory is that amyloid formation is a dynamic process of deposition and degradation, whereas concentrations of LC precursor protein act as a rate limiting step in fibrillogenesis. Indeed, scintigraphic monitoring of an AL patient with radiolabeled serum amyloid P protein (SAP) demonstrated that chemotherapeutic reduction of clonal plasma cell mass resulted in the regression of amyloid deposits within organs and tissues (131). Reduction of myeloid tumor mass in AL relies on the

same conventional and high dose chemotherapeutic agents used in MM in conjunction with ASCT when permissible (132). Other groups have evaluated the latter hypothesis of resolving amyloid deposition through inhibiting formation or stimulating degradation of amyloid fibrils. These studies have ranged from iodinated derivatives of doxyrubicin that bind amyloid fibrils to depletion of SAP to hinder fibril formation and immune molecules designed to target amyloid fibrils (133-135).

Treatment of multiple myeloma and plasma cell dyscrasia

Treatment for MM, like all PCDs, focuses mainly on the reduction of the monoclonal plasma cell population, with consideration given to addressing bone disease and renal function (which will be covered in upcoming sections). Therapies in MM and related diseases have been slow to evolve, with few major turning points in disease management. In general, agents used in the treatment of MM fall into the more broad categories of alkylating agents, inhibitors of mitosis, and corticosteroids (136). Patients diagnosed with MM undergo a series of steps for treatment. Figure 1.6 was adapted from Myeloma management guidelines and illustrates the process (135).

Listed below are several therapeutic agents used in the treatment of MM. Although the list is not exhaustive, these compounds have been used in many studies as the benchmark to which novel therapies are compared, and are representative of the way MM and PCDs in general are treated (136-138). Following this, a brief overview will be given on autologous stem cell transfer (ACST) and a few novel compounds used in maintenance therapy.

31

Melphalan

One of, if not the, oldest compounds described to treat MM is the alkylating chemotherapeutic Melphalan (139). First used in the late 1950's, Melphalan produced a response of decreased tumor mass in 35% of patients. Subsequently by 1967 the corticosteroid prednisone was also shown to effectively reduce MM cell burden, and was considered as an alternate for patients refractory to alkylating chemotherapies (140). Within 2 years combination therapy of Melphalan plus prednisone was shown to elicit responses in 70% of patients in a clinical study, subsequently adopted for treatment of MM, and remained the gold standard for over 30 years (136).

Vincristine, adriamycin, dexamethasone and high dose chemotherapeutics

By the early 1980's several new therapeutic options had become available for treating MM patients refractory to standard chemotherapy regimens, including the combinational therapy of Vincristine, Adriamycin, and Dexamethasone (VAD) (141). In addition, interest was raised in the use of high dose chemotherapies (i.e., high dose melphalan) (142, 143). Although effective, with ~25% of patients going to complete remission, these approaches induced profound myelosuppression and induced numerous unwanted side effects (465). To overcome the hematotoxic effects of treatments autologous bone marrow transplants were introduced to replenish myeloid precursor cells (143-145).

Autologous Stem Cell Transplant

From these initial attempts to replenish bone marrow precursor cells autologous stem cell transplants were born. ASCT differs from bone marrow transplants by first mobilizing and then
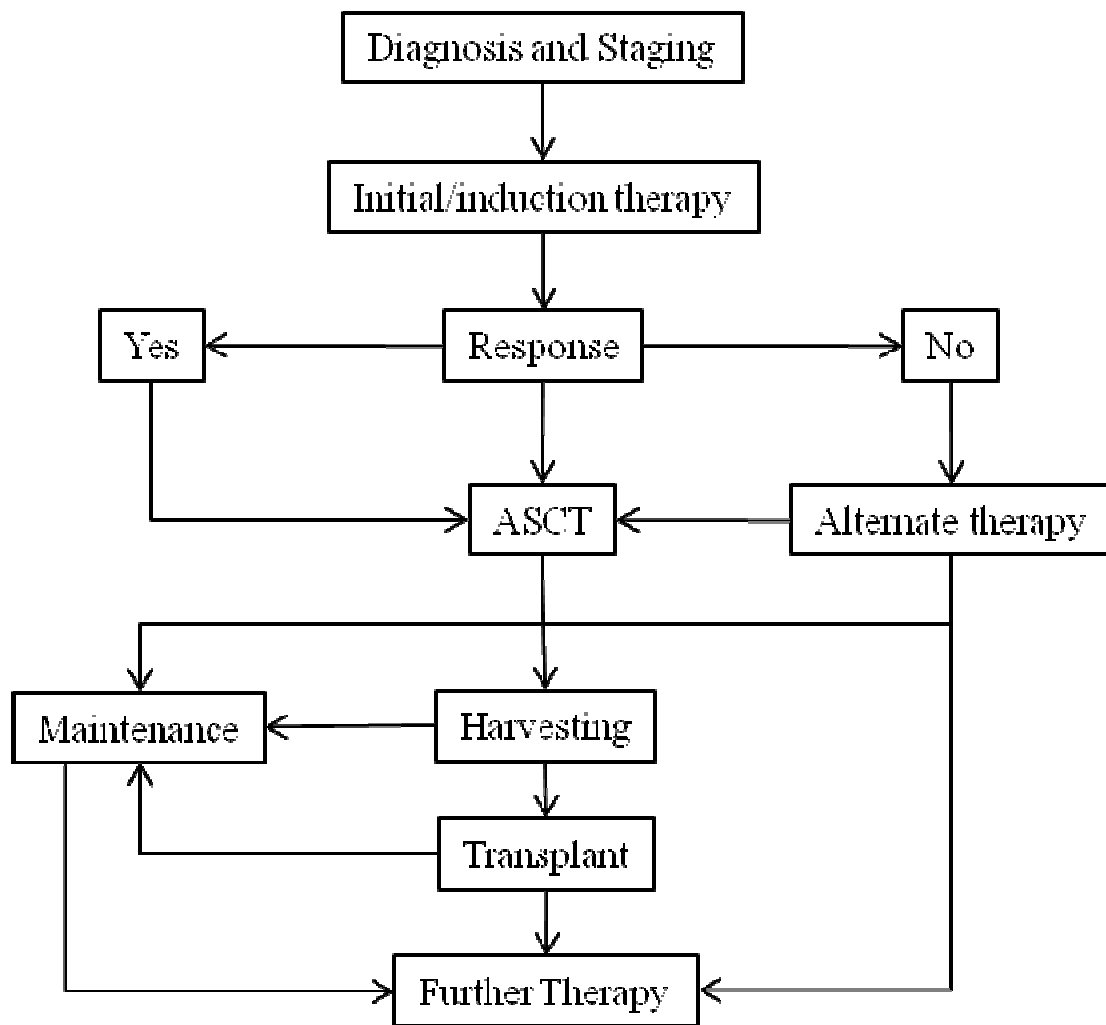
Figure 1.6 Schematic representation of the treatment protocol for patients diagnosed with PCDs. Adapted from (136)

harvesting circulating stem cells a source to replenish the myeloid compartment. In this process, patients first undergo a cytoreduction step using standard chemotherapeutics, avoiding those in the alkylator class (136). Following tumor regression, patient stem cells are mobilized either using granulocyte colony stimulating factor either in conjuction with cyclophosphamide, or alone (146). Patient blood is then harvested and white blood cells separated, while sera and red blood cells are returned to circulation (145). This technique, in conjunction with high dose chemotherapeutics, remains controversial as various studies have shown either increases in event free survival, complete or very good remission, and overall survival, while other studies have failed to show improvements over conventional therapies (136, 147-150).

Another factor with ASCT is the consideration which must be given to patient selection. The primary factors in deciding eligibility are age and renal involvement (138, 149, 150). ASCT is usually limited to patients under 65 years of age with normal renal function (149, 151), although some studies have proposed its use in patient populations of up to 75 years of age with selective conditioning reagents (152, 153).

Renal function in patients may be a more important factor in eligibility for ASCT due to the inability to tolerate toxicity induced by chemotherapeutic agents. In one Spanish study, poor renal performance was correlated with increased treatment related mortality by almost ten-fold in patients receiving high dose chemotherapy with ASCT as compared with controls (29% v. 3.3%) (154). Findings such as these have led to the conclusion that ASCT in patients with renal involvement is contraindicated, and thus limits this vulnerable group from benefits associated with transplant (136, 138).

Thalidomide

One of the more recent advances to gain widespread acceptance in MM therapy occurred in the late nineties with the drugs thalidomide. The drug was originally developed by a German pharmaceutical company by a chemist who heated the commercially available chemical phthaloylisoglutamine, generating thalidomide (57). Thalidomide was originally marketed as a sleep aid and as an over the counter cure for morning sickness in pregnant women. It was pulled from the shelves within 5 years due to prolific teratogenic effects on the developing fetus (155). Due to its ability to intercalate into DNA it was investigated in several oncology studies and found to have little effect (156). Thalidomide was used mainly in refractory or relapsed MM, demonstrating at least a partial response in 25-35% of these patients, and has recently been proposed as a frontline therapy (138, 149).

Reducing LC precursor

The notion of removing LC protein, and thus preventing deposition is not unique to AL. As early as 1965 a technique called plasmapheresis was utilized in MM and the related Waldenström's macroglobulenemia (157). By 1975 the role of BJPs in myeloma kidney were more clearly understood, and a case study citing improved renal function in an MM patient was published (106, 158). Subsequently, approaches such as this have been examined in various PCDs, typically when renal function has been compromised (95, 159-161). While the effect of this technique on survival in all PCDs remains unclear, a 2003 paper by Lachmann et al. demonstrated a positive effect on survival in patients with AL treated with chemotherapy and who demonstrated a drop in circulating FLC levels (162).

Reducing LC precursor: A molecular approach

Over the course of PCD progression the production and increasing concentration of circulating FLC can have a profound impact on therapeutic option and patient outcome, through aggregation and deposition in vital organs and tissues. Treatment with chemotherapy is effective in some, but not all cases, and the use of conventional alkylating or ACST in conjunction with high dose chemotherapeutics may be limited due to organ involvement. Renal toxicity is of particular importance in selection of therapies as high treatment related mortality is associated with impaired kidney performance due to BJP deposition. Further, reliance on high dose therapies might not be appropriate in conditions such as AL, when an overt malignancy is not present. Recent advances in the understanding of the process of protein synthesis have revealed a previously unknown process, namely RNAi (4), which has been posited as a novel therapeutic in a variety of disease states (163, 164). While the efficacy of this approach remains to be seen, owing to issues with delivery and off target gene silencing (25), RNAi offers a promising new approach to reducing LC burden in patients with PCD.

Chapter 2

Project Rationale and Summary

Plasma cell dyscrasias (PCD) occur in a spectrum of disease states (multiple myeloma, light chain deposition disease, and light chain amyloidosis) whose differential diagnosis and outcome are determined both by the malignancy and the toxic sequalae, which are often related to the production and deposition of immunoglobulin light chain (LC). Overproduction of LC protein and their deposition as insoluble aggregates has been indicated as a critical factor in progressive organ dysfunction and eventual failure, and the presence of deposits in PCD is indicative of poor prognosis. Reduced circulating LC levels in response to chemotherapeutic intervention, or by direct removal of LC with methods such as plasmapheresis results in a recovery of function within affected organs, and improved prognosis. In a number of patients, myelo-ablative chemotherapy in conjunction with repopulation of the immune compartment by autologous stem cell transplant has shown dramatic improvement and disease remission accompanied with event free survival. However, selection to undergo this treatment is stringent, and based, in part, on renal function, which is often impaired in PCDs due to the presence of overwhelming LC aggregates. Each of these examples serves to illustrate the negative impact that increased circulating LC levels may have on patients with PCDs.

While chemotherapeutic intervention is effective, and warranted in patients with aggressively expanding plasmacytoid cell populations, it is often harsh and not well tolerated, especially in patients with complicating factors such as increased age, or concurrent organ dysfunction. The increased cost to health associated with chemotherapeutics might negate the perceived benefits in patients where disease progression resulted mainly from the uncontrolled

production of LC proteins (i.e., LCDD, AL). Thus, it would be rational to devise a treatment strategy capable of reducing LC production specifically and directly, rather than indirectly through the non-targeted destruction of rapidly dividing cells as with most chemotherapy agents. Indeed, this approach has been pursued elsewhere, most recently in the form of monoclonal antibodies which target various forms of LC deposits (135) although there has been at least one study which has attempted to reduce the production of LC by interrupting the translation of messenger RNA to protein using an approach known as antisense deoxyoligonucleotide interference.

Recent advances in the understanding of the way cells manage the expression of self and non-self proteins by post-transcriptional regulation have revealed several forms of small interfering RNAs (siRNA), which act as initiators for the targeted "silencing" of individual proteins. This process, known as RNA interference (RNAi), is carried out by a conserved family of related proteins sharing common RNA-binding and RNase motifs, and which are found in all eukaryotic cells. Exploitation of this natural protein-reducing system offers distinct advantages over earlier forms of gene silencing techniques (165). SiRNAs have been used in a variety of cell systems to generate both transient and sustained models of gene knockdown that have been applied in studies of gene function and target discovery for pharmaceutical development (31). Further, their application as therapeutic molecules has been proposed for a variety of disease states (166-168).

The goals of the present study were to determine if interfering RNA molecules could be adapted to reduce LC production by human plasmacytoid cells, and whether these systems may be applicable to *in vivo* in addition to *in vitro* models of PCD. To test these hypotheses the following specific aims were outlined:

Specific Aims

1) **Demonstrate gene knock down in cell cultures following exposure to synthetic siRNAs.**

   Human myeloma lines will be selected and screened for production of LC products.

   Synthetic siRNA molecules will be designed to target the V, J, or C regions of LC mRNAs.

   Cell supernatants will be monitored for secreted LC products by ELISA, while cell

   associated LC protein will be measured by flow cytometry. Finally, levels of LC mRNA will

   be assessed by real time PCR.

2) **Design short-hairpin RNA expressing viral vector construct which are capable of**

   transducing human myeloma line and inducing sustained knockdown of LC protein.

   Synthetic siRNA molecules shown effective in transiently reducing LC protein production in

   human myeloma lines will be adapted to include a loop structure which upon transcription

   generated a folded stem-loop structure that was capable of entering the RNAi pathway.

   These shRNA encoding constructs will be ligated into lentiviral expression vectors under

   control of a U6 RNA pol III promoter. Expression plasmids contain an enhanced green

   fluorescent protein (EGFP) reporter gene under control of a cytolomegalovirus (CMV

   promoter). Lentiviral expression plasmids will be screened for shRNA insert by DNA

   sequencing and transiently transfected to HEK 293 cells. Following confirmation of EGFP

   expression lentiviral vectors will be sent to the Viral Vector Core Facility at the University of

   Tennessee Health Science Center in Memphis, TN for packaging to infective, replication

   incompetent lentiviral particles. Lentiviral particles will be used to infect the human

   myeloma line 8226, and mouse myeloma line SP2/O-λ6. Cell populations receiving virus

   will be assayed for transduction by identification of cells expressing EGFP by flow

cytometry. Cells shown positive for EGFP expression will be used to generate clonal lines and analyzed for LC production by ELISA and real time PCR.

3) **Test the efficacy of shRNA driven gene knockdown using *in vivo* model systems of PCD.**
Immunocompromised mice (Rag1 -/-, SCID beige) will be recruited as hosts for generation of xenograft tumors. The first series of tumors will be generated from either parental 8226 cells or clones which have been transduced with either an empty or shRNA expressing construct. Tumors will be administered either intraperitoneally or by sub-cutaneous injection within the inguinal region. Mice will be held for up to 28 days and monitored for presence of human LC protein in either sera or urine.

Subcutaneous xenograft tumors will be generated in a second group of mice by injection of untreated 8226 cells to the inguinal area. Tumors will be allowed to grow while LC products will be measured from the sera or urine. Mice will receive lentiviral particles with or without shRNA expression cassettes at the site of lesions as intra-tumoral injections. Mouse sera and urine will again be collected at 7 and 14 days following administration of virus. Assay of sera and urine for human LC products will be conducted by ELISA, while tumor tissue will be analyzed for LC mRNA levels by real time PCR. Cultured tumor samples will be analyzed for LC and mRNA protein expression, while heart, lung, kidney, spleen, and tumor samples were analyzed for presence of LC by immunohistochemistry.

Chapter 3

Materials and Methods

The following sections review general methodologies used in these studies. All materials were acquired from sources mentioned below unless specified elsewhere.

3.1 Cell lines and culture conditions

Unless otherwise specified all cells were maintained in Dulbecco's modified Eagles medium formula 12 (DMEM F-12; Lonza, Wakersville, MD) supplemented with 5% fetal bovine serum and 1% penicillin/streptomycin (P/S) with or without 50 µg/mL gentamycin. Cells were maintained in a humidified incubator at 37°C in a 5% CO_2 atmosphere.

The cell line SP2/O-λ6 was provided by Dr. Alan Solomon (Human Immunology and Cancer Program, University of Tennessee Medical Center, Knoxville). These cells were generated by transfecting, by electroporation, the mouse myeloma line SP2/O with an expression construct encoding the full length patient derived amyloidogenic λ6 LC protein Wil ($V_\lambda 6$, $J_\lambda 2$, $C_\lambda 2$) (169). In this system, expression of LC Wil is regulated by the cytolomegalovirus (CMV) promoter along with the sequence under control of the cytomegalovirus promoter and mouse µ enhancer (Figure 3.1).

Human myeloma lines RPMI 8226 (CCL-155) U266 (TIB-196) were purchased from American Type Culture Collection (ATCC, Manassas, VA). RPMI 8226 has been previously reported to secrete a full length λ2 LC (170).

41
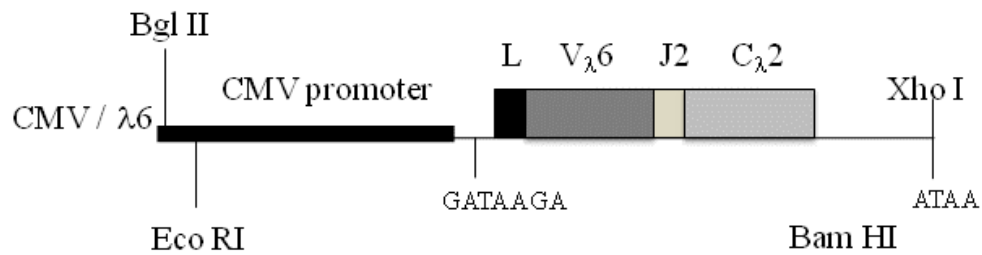
Figure 4.1 Schematic Representation of construct encoding patient derived amyloidogenic λ6 LC found in transgenic cell line SP2/O-λ6. The mouse myeloma cell line SP2/O was stably transfected with an expression construct encoding the human λ6 LC Wil by electroporation. LC transcription is controlled by the presence of the cytolomegalovirus RNApol III (CMV) promoter. Expression of LC Wil is strengthened by presence of the mouse mu enhancer. This map illustrates the presence of the full length LC protein including the leader (L), variable (V), joining (J2) and constant ($C_\lambda 2$) regions.

The IgG κ1producing human myeloma line, Bur, was provided by the HICP and was shown by immunofixation assay to express a full length IgG associated with a κ1 LC (Section 6 Figure 6.2).

The human embryonic kidney line HEK 293 was acquired from ATCC (ATCC # CRL-1573) and maintained as above. Cells were maintained by removing media and incubating for 5 min in presence of buffered trypsin, followed by sharply striking side of container. Trypsin was neutralized by the addition of 5 x volume of complete media. Cells were transferred to 15 ml conical tubes (BD Falcon) and collected by centrifugation at 600 x g for 5 min.

3.2 Cell counting and viability assays

Trypan blue dye exclusion assay

Basic cell counts and viability assays were performed by using trypan blue dye-exclusion assay and Neubauer hemacytometer . At time of count, cell suspensions (usually 20 µl) were collected and added to 1.5 ml eppendorf tube (Fisher Scientific) containing trypan blue dye (Sigma-Aldrich) at a 1:1 ratio. Cells were incubated at room temperature for at least 4 min and transferred to hemacytometer for counting.

Cell Titer Blue

In cases where quantification of multiple samples was needed the CellTiter Blue fluorescence viability assay (Promega) was used. Briefly, cells were agitated and 100 µl of culture was removed to one well of a black, clear bottom, low-binding polystyrene 96-well microplate (Corning). Standard curves were generated by 1:1 serial dilution of a known quantity of the cells being studied starting with 10^6 cells per well, while blank wells received 100 µl of culture media alone. Each well received 20 µl of CellTiter Blue reagent and plates were incubated for 2-4 h at

$37°C$ in a humidified incubator under 5% CO_2. Fluorescent activity was measured at $530_{ex}/645_{em}$ on Synergy HT plate reader (Bio-Tek, Winooski, VT), and viable cell numbers estimated from the standard curve.

3.3 Animal models and procedures

Mice

Female immunocompromised RAG1-/- knockout mice (595; provided by HICP) and severe compromised immune deficient x beige mouse line (SCID/beige; Charles Rivers Laboratory, Raleigh, NC) were housed in the animal facility at the University of Tennessee Medical Center, Knoxville. Animals were maintained under a 12 h light/dark cycle and received standard rodent chow and water *ad libitum*. When required, mice were lightly anesthetized using isoflurane. Euthanasia was carried out by isoflurane overdose. All procedures were approved by the University of Tennessee Institutional Animal Care and Use Committee (IACUC) under Protocol number 730.

Xenograft tumors

RAG1-/- or SCID/beige mice were lightly anesthetized and received up to 10^7 8226 cells as either intra-peritoneal (i.p.) or sub-cutaneous injection (s.c.; at shoulder region of right flank or within left inguinal region). Cells were counted and washed 3x in sterile, ice-cold PBS, and immediately prior to injection, resuspended in 200 µl PBS for i.p. injection or 50 µl PBS + 50 µl Matrigel basement membrane matrix (BD BioSciences San Jose, CA) for s.c. delivery. In both cases, cells were maintained on ice and administered using 1 cc tuberculin syringe, fitted with a ½ inch 27 ½ gauge needle.

Mice receiving cells s.c. were monitored for tumor development visually and by weekly palpation at site of injection. Samples of sera or urine from mice receiving i.p. injections were monitored for presence of human LC using ELISA [Section 3.9].

Blood collection

Whole blood was collected from mice via the retro-orbital sinus by first lightly anesthetizing mice with isoflurane followed by blood collection using FisherBrand silicate glass capillary tubes (Fisher Scientific). Samples (50-250 µl) were collected in 1.5 ml microcentrifuge tubes and allowed to sit for 1 h at RT or overnight at 4° to allow clotting to occur. Sera were isolated by centrifugation at 13, 000 x g on a Biofuge*Pico* tabletop centrifuge (Thermo Scientific, Ashville, NC) for 10 min, followed by careful aspiration to a clean tube. Samples were stored at -80° until used.

Urine Collection

Urine was collected from mice by placing a 3 x 6 inch piece of Parafilm underneath a grated surface. Mice were allowed to grip bars and were scruffed, typically resulting in voiding of the bladder. Urine was collected from Parafilm to clean 1.5 ml microcentrifuge tubes and stored at -20° until time of analysis.

3.4 Nucleic acid isolation and concentration

RNA extraction

Total RNA was isolated from cultured cells and animal tissues using RNeasy plus mini kit (Qiagen, Valencia, CA). For cell lines, $2x10^5$-10^6 cultured cells were harvested by centrifugation

at 3,500 rpm (700 × g) for 5 min in 1.5 ml Eppendorf tubes on a Biofuge*Pico* tabletop centrifuge

(Thermo Scientific, Ashville, NC). Cells were then lysed in 350 µl RLT Plus buffer, followed by

passage through QiaShredder spin column (Qiagen) and centrifugation at 10,000 x g for 2 min.

Flow-through was transferred to gDNA eliminator column (kit), and the sample centrifuged at

10,000 × g) for 30 sec. Finally, 1 volume of 80% ethanol/H_2O was added to samples. Mixtures

were transferred to RNeasy spin column, centrifuged for 30 s at 10,000 x g, and supernatants

discarded. Bound RNA was washed once using 700 µl RW1buffer (kit) followed by 2 washes

with 500 µl RLT buffer (kit). Residual buffer was removed by centrifugation and the RNA eluted

to clean tubes by elution in 60 µl RNase/DNase-free water (kit). RNA yield was determined by

diluting samples 1:10 in 100 µl distilled water, followed by measuring the A_{260}/A_{280} on an

Ultrospec Pro 3300 UV/visible spectrophotometer (GE Healthcare Life Sciences, Piscataway, NJ),

RNA concentration was estimated by:

$$[RNA] = 40 \; X \; A260 \; x \; Dilution \; factor$$

While purity was estimated according to the following equation:

$$purity = \frac{A260}{A280}$$

Plasmid Purification

Transfection-grade plasmid DNA was prepared using Plasmid Midi Kit (Qiagen). Bacteria from

overnight cultures (25 or 100 ml) were pelleted by centrifugation for 15 min at 6000 x g and 4° C

using a Sorvall RC2 centrifuge (ThermoScientific). Supernatant was removed by decantation and

bacterial cells disrupted using the supplied alkaline lysis reagents. First, cells were resuspended in

4 ml of Buffer P1, supplemented with 100 µg/ml RNase A. Buffer P2 (Na/OH lysis buffer) was

added to cell suspensions (4 ml) followed by 5 min incubation at room temperature. The lysis

reaction was neutralized by addition of 4 ml of buffer P3 (pre-chilled to 4° C) and samples were

placed on ice for 15 min. Precipitates were removed either by centrifugation at 6,000 x g for 10

min at 4° C and decanting supernatant through cotton gauze, or by passage through QIAfilter

cartridge (kit). Supernatants were passed through a pre-equilibrated QIAtip-100 column (kit) by

gravity flow to bind plasmid DNA. Columns were washed 2x with 10 ml buffer QC (gravity flow;

kit) and DNA eluted to a clean Oak Ridge centrifuge tube using 5 ml buffer QF (kit). Nucleic

acids were precipitated by addition of 3.5 ml isopropanol followed by holding at 4° C for 30 min.

After centrifugation at 15,000 x g for 30 min at 4° C, supernatants were decanted, and pellets air

dried for 10 min at room temperature. DNA was resuspended in 400 µl DNase free water and

concentrated by ethanol precipitation.

Ethanol Precipitation of DNA

For 400 µl of sample in DNase free water, salt content was adjusted to 75 mM with addition of 15

µl of 5 M NaCl followed by the addition of 2.5 volumes of pure ethanol. Samples were incubated

overnight at -80° or for 15-20 min on dry ice. DNA precipitate was separated from solution by

centrifugation at 13,000 x g for 20 min at 4° C on a BioFuge*Fresca* refrigerated centrifuge

(Thermo Scientific). Pellets were resuspended in 20-50 µl DNase free water.

3.5 First-strand cDNA synthesis and amplification

Reverse Transcriptase reaction

For each sample first-strand complimentary DNA (cDNA) was generated using SuperScript III

Reverse Transcriptase (Invitrogen). For each 20 µl of reaction, total RNA (200ng-1µg) was added

to 0.5 ml snap-top tubes along with 1 µl of 50 µM oligo(dT)$_{20}$ (Sigma Aldrich, St Louis, MO), 1 µl

10 mM dNTP mix (Fisher Scientific), and water to a final volume of 13 µl. Tubes were heated to

65° C for 5 min to disrupt secondary structure, and rapidly cooled on ice for 1 min. To this, 4 µl of

5x first strand buffer (kit) was added along with 1 µl 0.1 M DTT, 1 µl RNasin RNase inhibitor, and

1 µl Superscript III enzyme (kit). Reactions were incubated at 55° C for 1h, and heat inactivated

by increasing temperature to 70° C for 15 min.

Polymerase Chain Reaction (PCR)

PCR was performed using either Taq DNA polymerase or Phusion DNA polymerase and

proofreading enzyme (New England Biolabs, Ipswich, MA). For Taq based PCR, 2x buffer was

prepared (100 µl) by the addition of 20 µl 10x Eppendorf PCR buffer (Sigma Aldrich), 40 µl

Eppendorf PCR enhancer (Sigma Aldrich), 1.6 µl 25 mM dNTP mix, and 38.4 µl water. PCR

reactions were typically carried out in 16 µl volumes containing 8 µl 2x mix, 0.5 µl forward primer

(20mM; Sigma Alrdich), 0.5 µl reverse primer (20mM; Sigma Aldrich), 1-2 µl of template DNA,

Taq polymerase at a ratio of 1:50 (enzyme: reaction volume), and water was added to final volume.

Similarly, Phusion based PCR reactions (20 µl) were prepared with 10 µl Phusion HT

buffer (New England Biolabs), 0.5 µl forward primer (20 mM), 0.5 µl reverse primer (20 mM), 1-2

µl template DNA, 1:50 Phusion enzyme, and water to final volume.

Real-time, Quantitative PCR (qPCR)

Quantitative PCR was conducted using iQ SYBR Green SuperMix (BioRad, Hercules, CA).

Briefly, each 20 µl reaction contained 10 µl 2x iQ SYBR Green SuperMix, 1 µl forward and

reverse primer mix (20 µM each) - the cDNAs were diluted to 1:10 or 1:100 in DNase free water

and 1 µl added to each reaction. Primers for LC genes were designed to amplify ~100 bp

fragments from target genes using Primer-BLAST primer design tool (591), while validated

primers to human or mouse GAPDH, β-actin, or aldylase served as reference genes (RealTime

Primers, LLC., Elkins Park, PA). Amplification efficiencies were determined for each primer set

by analysis of serial dilution curves and were shown to be between 95-105% (592). Reactions

were performed using an iCycler thermocycler base (BioRad) while fluorescence intensity was

monitored in reaction wells with an iQ5 optical system (BioRad). Fluorescence data were

analyzed using the integrated iQ5 control software and relative gene expression levels between

treated and control cells were calculated using the $2^{-\Delta\Delta CT}$ (Livak) method (592).

In all cases, PCR conditions were optimized for each primer set and template and will be

reported when appropriate.

3.6 Isolation and sequencing of PCR products

Agarose gel electrophoresis

Following amplification, PCR amplicons were separated based on size by agarose gel

electrophoresis, stained with ethidium bromide, and visualized using a UV light box. Solid

agarose was prepared as 2% stock solutions (w/v) by adding 2 mg SeaKem low melting point

agarose per 100 ml Tris acetate-EDTA (TAE) solution. Agarose was melted by autoclaving for

one cycle, stocks were aliquoted and stored in closed glass jars. Gels were prepared by melting

agarose stocks in a microwave oven and diluting agarose to 1.5% with additional TAE. Gels were

poured and allowed to cool. PCR reactions were mixed with DNA loading buffer and 10-15 µl of

samples were added to individual lanes. Hyperladder HI molecular weight marker (Bioline, Inc.,

Tauton MA) was used to estimate product size. Gels were typically electrophoresed for 70 min at

110 volts, or until loading bands had migrated further than 75% of the gel. Gels were then soaked

for 10 min in an ethidium bromide bath and visualized by UV trans-illuminator. Images were

captured on Canon PowerShot G5 digital camera (Canon USA, Lake Success, NY).

Isolation of PCR products

Following separation by agarose gel electrophoresis, bands corresponding to predicted PCR

product size were excised and purified using the Wizard SV PCR and Gel cleanup kit (Promega).

Gel slices were first dissolved in membrane binding solution (w/v; kit) by incubating for 5-10 min

at 60° C, until gel slice was no longer visible. Solutions were transferred to Wizard SV silica mini-

columns and allowed to incubate for 1 min at room temperature. DNA was bound to columns by

pulling solution through column membranes by centrifuging at $13,000 \times g$ for 1 min on a

Biofuge*Pico* tabletop centrifuge. DNA was washed 2x using 200 µl column wash solution, flow

through was discarded after each wash. DNA was then eluted into fresh tubes using 400 µl of

DNase free water (2 elutions of 200 µl each) which had been pre-heated to 60° C. DNA was

concentrated by ethanol precipitation as outlined above (Section 3.4). Concentrations and purity

were estimated by reading absorbance at A_{260} and purity by the ratio of A_{260}/A_{230}.

DNA Sequencing

All gene sequencing was carried out by the University of Tennessee Molecular Biology Resource

Facility (UTMBRF) at the University of Tennessee, Knoxville. LC gene sequences were

compared with published or previously determined sequences using sequence tools found on Basic

Local Alignment Search Tool (BLAST) website (http://blast.ncbi.nlm.nih.gov/). LC sequences

were also compared against databases at international ImMunoGeneTics (IMGT) information

system (http://www.imgt.org) to determine Ig germline origin.

3.7 Nucleic Acids

Synthetic siRNAs Synthesis

Small interfering RNA duplexes were designed from data acquired by LC gene sequencing. To

reduce chances of off target effects, each siRNA (both sense and anti-sense strand) were used to

generate searches of the BLAST database for non-LC gene products that possessed significant

nucleotide sequence homology. Selected sequences were submitted to Sigma-Aldrich for

synthesis. RNAs arrived as lyophilized single strand species and were reconstituted to 20 μM

solutions in siRNA suspension buffer (Sigma Aldrich). Secondary structures were removed by

heating RNA solutions to 95°C for 1 min. Nucleic acids were combined in equimolar amounts in

1.5 mL microcentrifuge tubes followed by incubation for 1 h at 55° C to allow duplexes to form.

AllStars non-silencing siRNA duplexes were purchased from Qiagen with or without Alexa488

fluorescent labels and served as non-silencing controls. SiRNA duplexes were stored at -20° C

until the day of experiments.

Short Hairpin RNA Construct Synthesis

Expression constructs were designed which, when transcribed, generated 50-60 nt RNA sequences,

which fold to form a stem loop structure consisting of a 21 bp stem duplex with an intervening 6 or

9 nt single stranded loop region. Custom DNA oligonucleotides (forward and reverse) encoding

these sequences were synthesized by Sigma Aldrich and arrived as separate lyophilized

precipitates. Forward and reverse strands were resuspended to 20 μM using DNase free water.

For annealing, 5 µl of both forward and reverse oligonucleotides were added to a 1.5 ml microcentrifuge tube and heated to ~95° C in a glass beaker containing 500 mL boiling water. Oligonucleotides were incubated for 4 min and the beaker was removed from heat source and annealing occurred as the water to slowly returned to room temperature.

3.8 Lentiviral expression plasmids

PLKO.1

The replication incompetent lentiviral expression plasmid pLKO.1-TRC cloning vector (# 8543) was acquired from AddGene plasmid repository (www.addgene.org) (171) and arrived as bacterial stab cultures (E. *coli*, Stbl3 competent cells; Invitrogen). Upon arrival bacteria were transferred to Luria Bertani media (LB) agarose plates containing 50 µg /ml Carbenecillin. Cultures were grown overnight, the following day solitary colonies were selected and transferred to 1 L flasks containing 250 ml LB media. Cultures were grown overnight and plasmid recovered by midi-prep as above (Section 3.4).

pLB

The replication incompetent lentiviral expression plasmid pLB was acquired from Addgene (plasmid # 11619) (172) as bacterial stock and was propagated as above (Section 3.8). As with pLKO.1 plasmids were recovered from cultures by midi-prep.

3.9 Microscopy and Flow Cytometry

Immunohistochemical and immunofluorescence microscopy

Tissues and cells were observed using a Leica DMRB epifluorescent microscope, and digital images captured by using a SPOT-RT cooled CCD color camera and accompanying SPOT Advanced, v. 3.5.2 imaging software (Diagnostic Instruments, Inc., Sterling heights, MI). The microscope was fitted with a DAPI/blue fluorescent protein filter (excitation 360/40 nm, emission 460/50 nm, with 400 nm bandwidth), and a FITC/GFP filter (excitation 560/40 nm, emission 535/40 nm). For cells with multiple fluorescent labels SPOT Advanced software was used to correct brightness and background for individual channels and generate image overlays.

Flow Cytometry

Transfection efficiencies, EGFP expression, and immunoglobulin light chain expression were monitored using a FACScan flow cytometer (Becton Dickson, San Jose CA). For each, channel FL-1 (488 nm excitation, 530 emission) was used to monitor either Alexa488, EGFP, or FITC fluorescence. In the case of immunoglobulin expression Alexa630 conjugated antibodies were also used. The intensity of red fluorescence was captured on channel FL-2 (630 nm emission) For each experiment at least 5,000 events were collected and data analyzed using Cell Quest software v. 1.2 or Cyflogic v.1.2.1.

3.9 Enzyme Linked Immunosorbent Assays (ELISA)

General ELISA Development and Absorbance

For all ELISAs used in these studies Horseradish Peroxidase conjugated antibodies were used in conjunction with 2,2'-azino-bis(3-ethylbenzthiazoline-6-sulphonic acid (ABTS) + 0.06% H_2O_2 for detection of bound antigen. For each assay, immunoreactivity was visualized by measuring the absorbance at 405 nm using a BioTek Synergy HT Luminescence Reader (BioTek Instruments, Winooski, VT).

Detection of λ_6 LC

Culture supernatants were collected at 24, 48, or 72 h post-transfection after cell separation by centrifugation at $400 \times$ g for 5 min. For the SP2/O-λ6 cell line supernatants were diluted 1:10 in PBS + 1% bovine serum albumin (BSA; w/v) + 0.1% Tween 20 (Sigma-Aldrich) (PBST +BSA). High-binding affinity ELISA/RIA plates (Fisher Scientific) were coated overnight at 4°C with 100 µl of 3.75 µg/ml mouse anti-human Vλ6 monoclonal antibody (173), rinsed and blocked for 1 h at 37°C with PBS + 1% BSA. Diluted supernatants were applied to the plate for 1 h at 37°C. A standard curve was prepared by serial dilution of purified recombinant λ6Wil VJ(127) over the range from 400 µg/ml to 0.3 µg/ml. Plates were rinsed and 100 µl of rabbit anti-human λ6 LC antibody (127) in PBS containing 1% BSA, 0.5% filtered goat serum (Sigma-Aldrich), 0.5% filtered mouse serum (Sigma-Aldrich), 0.5% MOPC31c (Sigma-Aldrich), 0.1% tween20 (Sigma-Aldrich). Following incubation at 37° C for 1 h plates were rinsed and bound antibody detected by addition of HRP-conjugated goat anti-rabbit Ab (Jackson Immunoresearch, West Grove, PA). Following 1 h incubation at 37° C the plates were developed using ABTS + 0.06% H_2O_2 and visualized as above.

Detection of Total λ LC

<div align="center">

Total λ ELISA A

</div>

Culture supernatants were diluted 1:100 in PBST before analysis. AO193 Rabbit anti-human total λ (11µg/ml; DAKO, Carpinteria, CA) served as the capture antiserum and monoclonal mouse anti-human total λ light chain antibody (1 µg/ml; Dako) as the detection reagent. Bound antibody was detected by the addition of HRP-conjugated goat anti-mouse Ig (Jackson Immunoresearch). Plates were coated overnight at 4° C and blocked for 1h at 37° C on the day of assay. All antibodies and antigens were allowed to bind for 1 h at 37° C with intermittent washes using PBST.

<div align="center">

Total λ ELISA B

</div>

Plates were coated either overnight at 4° C or for 2 h at RT with 100 µl of 10 µg/ml 18-9G11 mouse monoclonal anti-human total λ LC antibody. Wells were blocked for 1 h at RT by addition of 200 µl PBS containing 1% BSA. The patient-derived BJP Cot was used to generate a standard curve, starting with 30 ng protein and proceeding with a 1:1 serial dilution in duplicate wells along the first columns of the plate. Culture supernatants were diluted 1:100 in PBST+BSA, while mouse sera and urine were diluted 1:10 in PBST+BSA. Each well received 100 µl of dilute sample, and were incubated for 1h at RT. Plates were washed 3x in PBST followed by the addition of 100 µl ABD Star130 HRP-conjugated anti-human total λ LC polyclonal IgG (AbD Serotec, Raleigh, NC). Following final 1 h incubation, plates were again washed and developed and absorbance read at 405 nm.

Total κ ELISA

The polyclonal rabbit anti-human total κ antibody AO191 (Dako) was coated (100 µl; 10 µg/ml) to each well of a high binding affinity 96-well ELISA/RIA plate overnight at 4° C. On the day of experiments, plates were blocked for 1 h at 37° C with 200 µl PBS + 1% BSA. Standard curves were prepared using purified, patient derived Bur BJP starting with 200 ng protein followed by a 1:1 serial dilution in PBST + 1% BSA. Bur supernatants were diluted 1:100 in PBST + BSA and 100 µl of sample were added to individual wells. Plates were incubated for 1 h at 37° C and washed 3x with TBST. Bound antigen was detected using a 1:2000 dilution of Star127P HRP-conjugated goat anti-human total k LC polyclonal IgG (AbD SeroTec). Plates were developed using ABTS and absorbance read at 405 nm.

Chapter 4

Small interfering RNA design and transfection

4.1 Rationale

As discussed previously, the introduction of small double-stranded RNA molecules to eukaryotic

cells will induce the targeted reduction of specific gene products (174). Utilizing these so-called

siRNAs, the RISC is capable of locating and degrading mRNA strands which show

complimentarity to the siRNA guide strand (16). Several factors may influence the efficiency of

this process, however, and must be addressed in order to optimize experimental outcomes.

Perhaps the two most important of these is the proper design of siRNA sequences, and the

delivery of synthetic RNAs to the cytoplasm of the target cell (35).

In addressing the former, several authors have demonstrated the robust specificity of RNAi in

experiments that accomplished a significant reduction in the mutant allele of a targeted protein,

with little or no effect on wild type levels (125, 167, 175, 176). Additionally, better

understanding of the RNAi machinery has led to improved models of siRNA design; for

example, designing duplex strands that mimic products of the RNase enzyme Dicer, thereby

increasing the efficiency by which siRNAs are taken into the RNAi pathway, or by altering the

thermodynamic stability of the guide strand at the 5' end, ensuring proper strand selection and

thereby reducing the likelihood of off-target effects (177, 178).

Delivery of siRNAs to cell in higher eukaryotes also presents a unique challenge, as cellular

uptake of naked dsRNA molecules was shown to be inefficient *in vitro* and even more so *in vivo*

(45). As a result, a variety of compounds have been developed to enhance cellular delivery of

siRNAs (and nucleic acids in general). Reagents and methods developed for transfection vary,

from the use of cationic polymers and lipids to conjugation of siRNA molecules with magnetic nanoparticles for transient transfections, or the incorporation of constructs encoding a desired siRNA into a viral expression plasmid for stable incorporation (28, 171, 179, 180). While many of these systems remain experimental, varieties of compounds are commercially available and are compatible with numerous cell types.

The following sections will review the steps taken to identify products of the LC gene and in designing siRNA molecules which were later shown effective in reducing LC production in the mouse and human myeloma cell lines. This section will also review the process by which appropriate transfection reagents were selected for each cell line and the steps taken to optimize transfection efficiency and reduce cytotoxicity.

4.2 Methods

Cells

The first step taken in designing siRNAs to target LC genes was the isolation and characterizations of the LC protein. For this, the transgenic mouse myeloma line SP2/O-λ6 and human myeloma lines, RPMI 8226 and Bur were selected. The mouse line SP2/O-λ6 was developed by the Human Immunology and Cancer Program, and contains a construct expressing a patient-derived amyloidogenic λ6 LC under control of a CMV promoter which is reinforced by the presence of a mouse mu enhancer sequence (Figure 3.1). The human myeloma line RPMI 8226 has been shown to secrete measurable quantities of a full length λ2 LC containing V-, J-, and C-regions (214). Additionally, the patient-derived human myeloma line Bur was provided by the HICP and has been shown to produce a full IgG protein with an associated κ1 LC. In

each case, cells were cultured under standard conditions (Section 3.1). Cell number and viability were assessed as previously described (Section 3.2).

Identification LC gene products

For each cell line, the full sequence of LC gene was determined by first isolating total RNA lysates prepared from 10^6 cells. RNA was reverse-transcribed to cDNA as in Section 3.3. Primers corresponding to LC Wil (Fwd 5'- CGCGCATGGCCAATTTTTTACT-3', Rev 5'- AGGAATTCAACCTAGGACGGTCAACTTGGT-3') and Bur (Fwd 5'- GGCTCCCAGG TGCCAAATGTGA-3', Rev 5'- ACAGATGGAGCAGCCACAGTTC-3') were used to amplify the L, V, J regions of each LC. PCR products were purified and submitted to the DNA sequencing laboratory in the Molecular Biology Resource Facility at The University of Tennessee, Knoxville using primers LC Wil and Bur. For 8226 cells, the LC sequence was acquired from NCBI Nucleotide database (http://www.ncbi.nlm.nih.gov/nuccore/ ; GenBank ID: U07992.1).

Design of siRNA

For each siRNA, 21-bp RNA duplexes containing 3' 2 nt overhangs were designed based on the determined sequence of the expressed LC gene. The protein and isotype-specific nucleotide sequences were compared to others contained in human and mouse mRNA libraries using the Nucleotide BLAST suite (http://blast.ncbi.nlm.nih.gov/). Duplexes that possessed significant homology >85% base pair identity to non-LC genes were eliminated, while those corresponding specifically to LCs were synthesized (Sigma-Aldrich).

Transfection conditions

Transfection media were acquired from several vendors and administered according to manufacturer's instructions. A summary of each protocol is shown in Table 4.1. In each case, cells were incubated for 1-3 days and uptake of fluorescent control siRNA was assessed by fluorescence microscopy and/or flow cytometry. Cell viability was also monitored by trypan blue exclusion assay and cell counting by using a hemacytometer.

Optimization of transfection conditions

To determine optimal transfection conditions for cells, serial dilutions of Alexa488 labeled siRNAs were incubated with increasing ratios of delivery reagent. Following transfection, cells were incubated for 24-72 h under standard conditions. Cells were recovered and viability assessed by trypan blue dye exclusion and hemacytometry or by CellTiter Blue assay. Replicate samples were harvested and analyzed for uptake of Alexa488 labeled siRNA by flow cytometry. For each treatment group, the healthy cell population was identified by drawing regions in the flow cytometer data using untreated populations of 8226 cells. Marker regions were drawn on FL-1 to exclude negative cells.

4.4 Results

Total RNA extraction and conversion to cDNA was carried out as described in Sections 3.3-3.5. PCR primers were designed to amplify LC mRNAs and bands corresponding to ~300 bp were excised and isolated as described in Section 3.5. Results from the UTMBRF were entered into the ExPASY Translate program and are shown in Figure 4.1.

Table 4.1 Summary of transfection reagents and protocols

Reagent	Manufacturer	Protocol summary	Notes
DharmaFect reagents 1-4	Dharmacon/ Thermo Scientific	For 96-well format: 1 µM siRNA mixed 1:1 (moles RNA/ µl Transfection reagent) in serum/antibiotic free (s/a-) media, allowed to incubate 5 min. Mixture diluted to 100 ml and added to $2x10^4$ cells.	Small amount of siRNA used. Protocol optimized for adherent cell types. Incompatible with sera/antibiotic containing media.
Lipofectamine	Invitrogen	For 24-well format: 0.2 µg siRNA diluted to 25 µl in s/a- media. Mixture incubated for 30 min at RT and diluted to 200 µL. $2x10^4$ Cells washed and transferred to 200 µl s/a- media in 24 well plate and siRNA/transfection solution added slowly. Cells incubated 6 h under normal conditions, collected and media replaced with 0.6 ml fresh complete DMEM F-12.	Protocol optimized for adherent cells. Incompatible with sera or antibiotic containing media during transfection. Media change at 6 h cumbersome in experiments with large number of reps.
Lipofectamine 2000 (L2K)	Invitrogen	For 24-well format: Prior to treatment, $2 x 10^5$ cells added to each well in 500- µl media. SiRNAs diluted in 50 µl s/a- media, 1 µl diluted likewise, sera and transfectant combined, incubated 5 min at RT, siRNA complexes added to wells.	Compatible with sera. Relatively small amount of siRNA required. No need to change buffer following transfection.
RNAifect	Qiagen	For 96-well format: SiRNA (1 µg) was added to 100 µl complete media along with 3 µl RNAifect. Solutions were incubated at RT for 20 min, meanwhile $2x10^4$ cells were collected and media removed. Cells were resuspended in 100 µl siRNA solutions and transferred to individual wells of plate.	Protocol optimized to adherent cells, but adaptable to suspension. Compatible with serum and antibiotics during transfection.
Hiperfect	Qiagen	For 24-well format: 1 µg siRNA was added to a tube containing 100 µl s/a- media, to this 3 µl hiperfect was added and solutions incubated for 15 min at RT. Concurrently, $2x10^5$ cells were harvested by centrifugation and transferred to individual wells in 100 µl complete media. SiRNA solution added to wells and incubated for 6 h followed by addition of 400 µl complete media.	Simple protocol, compatible with suspension cells. No negative effects of serum or antibiotics during procedure.

A

```
1          11         21         31         41
NFLLTQPHSV SESPGKTVTI SCTRSSGSIA NNYVHWYQQR PGSSPTTVIF
                                 V1 WII →                V2 WII
51         61         71         81         91
EDDHRPSGVP DRFSGSVDTS SNSASLTISG LKTEDEADYY CQSYDHNNQV
→
101        111        121        131        141
FGGGTKLTVL GQPKAAPSVT LFPPSSEELQ ANKATLVCLI SDFYPGAVTV
         J1 WII                            C1
151        161        171        181        191
AWKAPSSPVK AGVETTTPSK QSNNKYAASS YLSLTPEQWK SHKSYSCQVT
                    C2
201        211
HEGSTVEKTV APTECS
```

B

```
1          11         21         31         41
ELSVLTQPAS VNGSPGQLII ISCTGPSSDI GDYQYISWYQ QHPGKAPKLI
                                 V1 8226
51         61         71         81         91
IYDVDKRPSG VSNRFSGSKS GNTASLTISG LQAEDEADYY CSSYRGSALF
101        111        121        131        141
EVVFGGGTKV TVLRQPKAAP SVTLFPPSSE ELQANKATLV CLISDFYPGA
                                          C1
151        161        171        181        191
VTVAWKADSS PVKAGVETTT PSKQSNNKYA ASSYLSLTPE QWKSHRSYSC
                    C2
201        211
QVTHEGSTVE KTVAPAECS
                 C3 8226
```

C

```
1          11         21         31         41
FWLPGAKCDI QMTQSPSSLS ASVGDRVTIT CRASQGIYNY LAWFQQKPGK
         V1 Bur
51         61         71         81         91
APKSLIHAAS SLQSGVPSKF SGSGSGTDFT LTISNLQPED FATYYCQQFY
                                          C4 κ
101
SYPLTFGGGPR T
```

Figure 4.1 Sequence of LC gene products and segments targeted by siRNAs. Sequences for LC gene products from cell lines A) SP2/O-λ6, B) 8226, and C) Bur were acquired from PCR products submitted to UTMBRF. Results were translated to AA sequences. Underlined areas represent sites to which indicated siRNA sequences correspond.

Based on these data short ~21 bp RNA duplexes were designed corresponding to regions of hyper-variability (i.e., junctions between complimentarity defining regions and framework regions; CDR/FRs, V- J- recombination site). These regions were chosen as they are sites of greatest somatic mutation and therefore have the highest degree of sequence differences from the germline gene as well as other LCs of the same isotype.

Alternately, siRNAs were designed to areas of the LC C-domain to act as tools for isotype-specific gene silencing (i.e. κ, λ LCs), these sequences were generated by comparing regions among the various κ or λ germline genes and selecting those which share homology with their respective counterparts. SiRNA sequences are shown in Table 4.2 while their locations along the LC gene products are noted as underlined areas in Figure 4.1.

Selection and optimization of transfection system

Given the variety of transfection systems available, it was important to determine which method of delivery would yield the best results for each myeloma line. It was decided to limit transfection reagents to cationic lipid based systems, as they are the most commonly used reagents in the literature and are readily available from a number of sources. To avoid complicating the results of experiments with artifacts generated by different transfectant formulations it was also desirable to identify transfection media that were compatible with all cell lines. To achieve this, media from several commercial vendors were acquired and used to transfect Alexa488-labeled "AllStars", non-silencing control siRNA (Qiagen), while unlabeled Allstars, and separately, untreated cells served as controls. A summary of the results for each reagent and cell line is shown in Table 4.3.

Table 4.2 Sequence of siRNA oligonucleotides

Oligonucleotide	Length (bp)	Sequence
SP2/O-1 [a]		
Wil C1	21	AACAACUAUGUUCACUGGUAC CAUUGUUGAUACAAGUGACCA
Wil C2	21	AAGUUGACCGUCCUGGGUCAG GAUUCAACUGGCAGGACCCAG
Wil J1	21	AAGUUGACCGUCCUGGGUCAG GAUUCAACUGGCAGGACCCAG
RPMI8226 [b]		
8226 V1	21	GUGACAUUGGUGACUAUCAUU UUCACUGUAACCACUGAUAGU
8226 V2	21	CCUGCAGAAUGUUCUUAGUUU UUGGACGUCUUACAAGAAUCA
SP2/O-1 *RPMI8226* [c]		
C1	21	GUCUCCAUAAGUGACUUCUAUU UUCAGAGGUAUUCACUGAAGAU
C2	21	CCAAACAAAGCAACAACAAUU UUGGUUUGUUUCGUUGUUGUU
Bur [d]		
Bur V1	21	UAUUAACAUUUACGGGACUGAUU UUAUAAUUGUAAAUGCCCUGACU
κ C1	21	AGUCAACCCGGGUUGUACAACUU UUUCAGUUGGCGGGAAGAUGUUG

[a]Sequence bridges the FR1/CDR1, FR2/CDR2, or J/C region of IgLC protein Wil.
[b]Against CDR1,2 site of Vλ regions of RPMI8226 cells. [c]Against shared homology
sequences in constant domain of λ IgLC. [d]Sequence to V region of LC Bur or to C
region of κ LCs

Table 4.3 Results of transfection reagent selection trials

Cell line	Reagent	Uptake of siRNA	Method of detection	Cytotoxicity
SP2/O-λ6	Dharmafect (1-4)	ND	FM	ND
	Lipofectamine	ND	FM	ND
	Lipofectamine 2000	Yes	FM, FC	ND
	RNAifect	Yes	FM, FC	Only at higher ratios of reagent:siRNA
	HiperFect	Yes	FM, FC	ND
RPMI 8226	Dharmafect	NT	NT	NT
	Lipofectamine	NT	NT	NT
	Lipofectaimine 2000	Yes	FM, FC	ND
	RNAifect	Very low	FM, FC	Yes
	Hiperfect	Yes	FM, FC	ND
Bur	Dharmafect	NT	NT	NT
	Lipofectamine	NT	NT	NT
	Lipofectamine 2000	NT	NT	NT
	RNAifect	NT	NT	NT
	HiperFect	Yes	FC	ND

Legend: ND = Not detected, NT = Not tested, FM = Fluorescent microscopy, FC = Flow Cytometry

Of the reagents tested, 3 were effective at delivering their siRNA payload to the mouse line SP2/O-λ6, and of these, RNAifect was initially selected for use; however, it was shown later to be cytotoxic to the human line 8226 and its use was discontinued. This led to our use of HiperFect and Lipofectamine 2000 as effective, non-toxic, transfection reagents.

Both HiperFect and Lipofectamine 2000 were capable of delivering labeled siRNAs to either SP2/O-λ6 or RPMI 8226 myeloma lines over a range of concentrations (Figures 4.2 and 4.3). While Lipofectamine 2000 was successful at transfecting 8226 and SP2/O-λ6 cells over a wide range of siRNA concentrations cell counts taken following treatments were lower than expected for a 48 culture of 8226 cells given that 2×10^5 cells were plated initially (Table 4.4). Forward (FSC) and side scatter (SSC) from flow cytometry studies also revealed an increased number of events falling away from the gated population, demonstrating decreased size and increased complexity, a possible indicator of increased cell death.

Treatment of cells with HiperFect resulted in an increased uptake of Alexa488 labeled siRNAs as compared with controls as measured by Flow cytometry (Figure 4.3). Cell counts revealed that cell growth and viability were dependant on the ratio of siRNA to reagent, with siRNAs delivered at a ratio of 1:3 (siRNA:reagent) being well tolerated, while delivery with the higher 1:6 ratio reducing cell viability (Table 4.4). These results were mirrored in data collected from flow cytometry experiments, where cells receiving higher ratios of reagent were observed to have altered FSC/SSC profiles, indicating increased cell death (Figure 4.3). Figure 4.4 illustrates a typical fluorescent image and flow cytometry histogram observed following transfection with 1 μg Alexa488 labeled siRNA with HiperFect reagent using the 1:3 ratio at both 24 and 48 h (the final conditions selected for experiments).
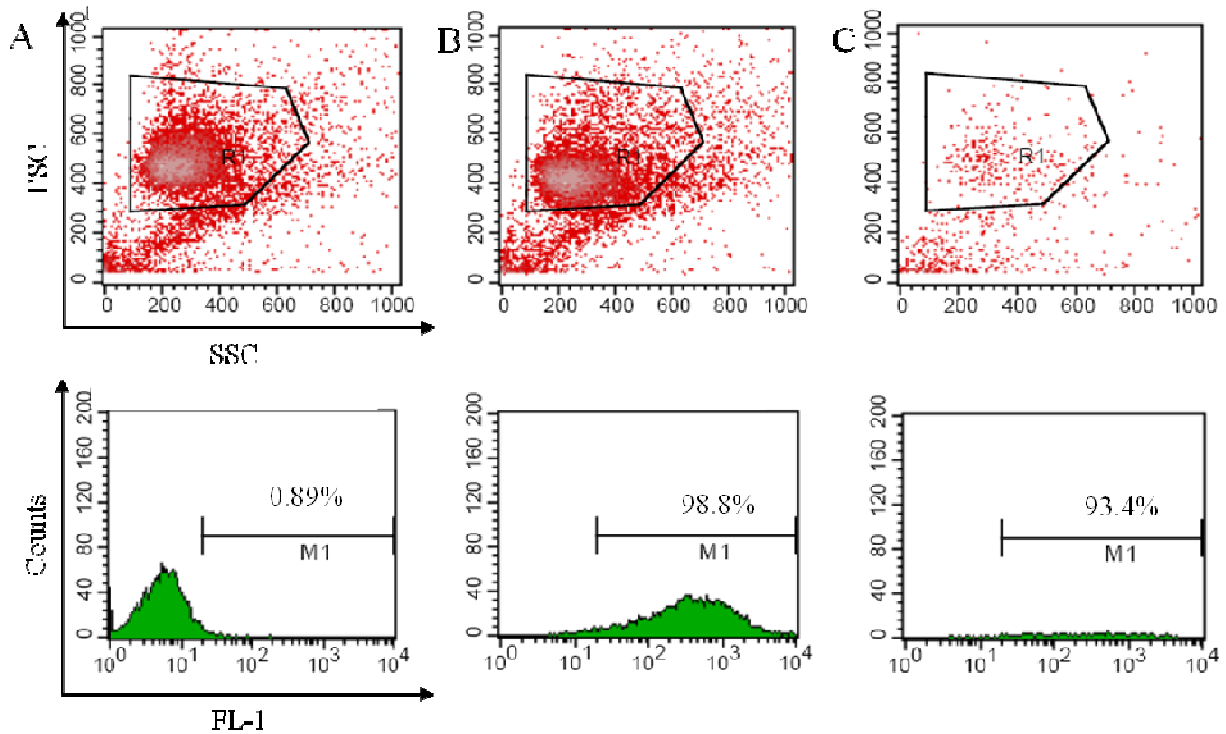
Figure 4.2 Alexa488 Labeled SiRNA Uptake in RPMI 8226 cells During Lipofectamine 2000 Optimizations. Forward scatter (FSC) and Side scatter (SSC) plots of A) untreated 8226 cells with FL-1 (green fluorescence) histogram shown underneath following 48 h incubation. Marker region M1 was drawn around untreated cells and was used to estimate percent of cells considered positive. B) 8226 cells treated with 1.5 µg Alexa488 labeled AllStars control siRNA with 1.5 µl Lipofectamine 2000 resulted in uptake of labeled siRNA, however cells begin to show signs of cytotoxicity as noted by spread in FSC and SSC. C) Exposure of 8226 cells to 1 µg siRNA and 0.5 µl Lipofectamine 2000 resulted in loss of cell population.
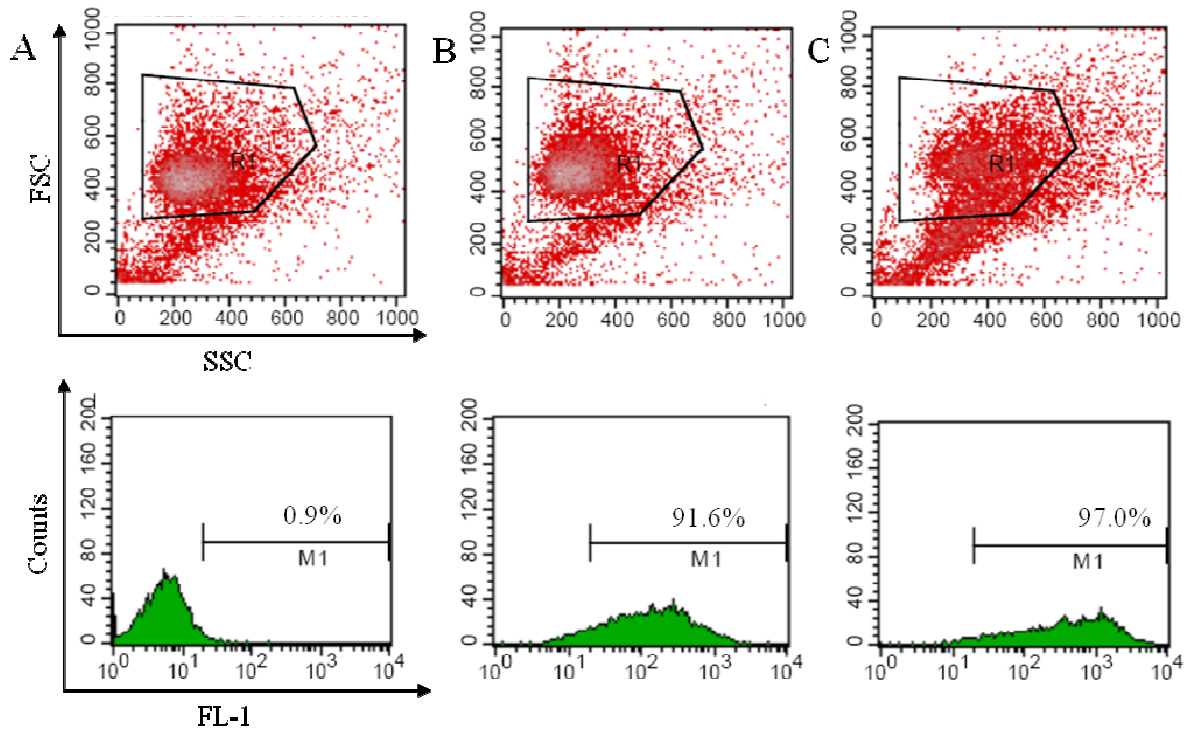
Figure 4.3 Alexa488 Labeled SiRNA Uptake in RPMI 8226 cells During HiperFect Optimizations. Forward scatter (FSC) and Side scatter (SSC) plots of A) untreated 8226 cells with FL-1 (green fluorescence) histogram shown underneath following 48 h incubation. Marker region M1 was drawn around untreated cells and was used to estimate percent of cells considered positive. B) 8226 cells treated with 0.75 µg Alexa488 labeled AllStars control siRNA with 2.25 µl HiperFect (1:3) resulted in uptake of labeled siRNA. C) Exposure of 8226 cells to 0.75 µg siRNA and 4.5 µl HiperFect (1:6) resulted in increased cell death.

Table 4.4 Optimization of Hiperfect and Lipofectamine 2000 in RPMI 8226 cells (48h)

Reagent	siRNA (µg)	Volume reagent	Ratio	% positive	Total cells/well	% viable
Lipofectamine 2000	1.5	0.5	3:1	NA	63,000	86
		1	3:2	98	110,000	90
		1.5	1:1	79	193,000	79
	1	0.5	2:1	94	64,000	85
		1	1:1	96	147,000	93
		1.5	1:1.5	86	142,000	77
	0	0.5	NA	7	165,600	81
		1	NA	1	182,400	84
		1.5	NA	1	420,800	88
HiperFect	1.5	4.5	1:3	95	297,000	88
		9	1:6	98	205,000	47
	0.75	2.25	1:3	91	313,000	87
		5.5	1:6	97	175,000	44
	0.375	1.125	1:3	79	344,000	96
		2.25	1:6	93	181,000	74
	0	3	NA	1	195,000	88
		6	NA	1	259,000	92

Legend: NA= Not Applicable
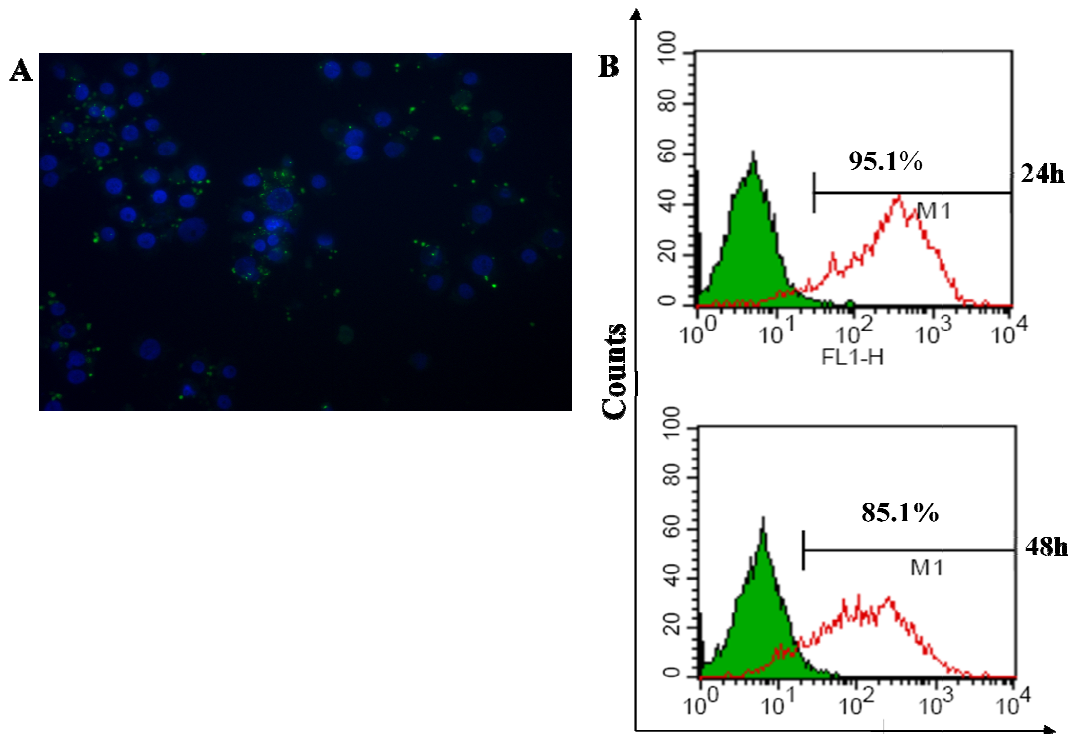
Figure 4.4 Transfection of RPMI 8226 Cells With Alexa488 Labeled Control SiRNA Using HiperFect Transfection Reagent. A) RPMI 8226 cells were treated with 1 μg Alexa488 labeled AllStars non-silencing control siRNA with 3 μl HiperFect reagent and harvested at 24 h. Cells were cytospun to glass slides, fixed, permeablized and treated with Hoescht stain (blue) for visualization of nucleus. B) RPMI 8226 cells were treated with either 1 μg Alexa488 labeled or unlabeled AllStars non-silencing control siRNA along with 3 μl HiperFect. Cells were incubated for 24-48 h and uptake of labeled Alexa488 assessed by flow cytometry. Populations of 8226 cells were gated and histograms generated using channel FL-1. Green histograms represent cell population treated with unlabeled siRNAs while open histograms represent cells receiving labeled siRNAs. Region M-1 was drawn on the negative control cells and percentages are the percent of cells considered positive for Alexa488 uptake.

4.4 Discussion

Two major challenges in designing RNAi based experiments are the development of siRNA

oligonucleotides and the selection of an appropriately safe and effective method of transfection.

Individual LCs expressed by different plasma cells may differ significantly from the germline,

owing to hypermutation events that occur during the maturation of individual plasma cells.

While this presents an added level of challenge to designing interfering RNAs to a LC of

interest, it also provides a unique opportunity to selectively target a pathologic LC for silencing,

while in theory, avoiding collateral damage to the remaining immune repertoire. As illustrated

here, obtaining an siRNA sequence specific for an individual LC is possible, and these sequences

may be used to design functional siRNA duplexes.

Transfection of myeloma cell lines with siRNAs also requires planning, and testing of numerous

products as different lines exhibit varying levels of tolerance to given products. For example, the

earliest studies conducted for this dissertation utilized the mouse myeloma line SP2/O-λ6

exclusively and the transfection reagent RNAifect offered an efficient and non-toxic means of

transfection. However, with the inclusion of the human myeloma line 8226, RNAifect was

shown to be ineffective and cytotoxic.   Further screenings identified the reagents

Lipofectamine2000 and HiperFect, both of which were well tolerated and resulted in efficient

transfection rates. However, exposure of the 8226 line to Lipfectamine 2000 resulted in lower

cell numbers than expected as compared with controls and with HiperFect treated counterparts.

Exposure of 8226 cells to HiperFect also had the potential to induce cell death when used at

jphihigher transfectant: siRNAs ratios (i.e., 1:6 siRNA: reagent); however these complications

were avoided easily enough by adhering to the 1:3 ratio of siRNA: reagent.

These results provide evidence that it is possible to identify LC gene products from different myeloma lines and use this data to rationally design siRNA sequences from of these isolates. Further, that efficient delivery of siRNAs to human and mouse myeloma lines is possible using neutral lipid based reagents, and that this delivery can be accomplished without inducing cell death.

Chapter 5

Inhibition of Pathologic Immunoglobulin Light Chain Production by Small Interfering RNA Molecules

5.1 Abstract

A main contributing factor to the morbidity and mortality of patients with plasma cell dyscrasias results from the pathologic deposition of monoclonal Ig light chains, i.e., BJPs within organs and soft tissues. As an alternative to plasma cell chemotherapy to reduce BJP synthesis and thus prevent aggregate formation we have investigated another means to achieve this objective, namely, RNAi.

Experimentally, we have stably transfected the SP2/O mouse myeloma cells with a construct containing the V, J, and C region of a λ BJP (Wil) under the control of a CMV promoter and have shown that they constitutively express measurable quantities of mRNA and protein Wil. Concurrently, we have also recruited the human myeloma cell line RPMI8226 to this study as a robust and clinically relevant model cell line. Treatment of these cells with synthetic, small double stranded RNA based on the Wil protein sequence or RPMI8226 IgLC protein sequence reduced both target mRNA levels by 24h and protein production by 50% in each cell line over the 72 h experimental period as compared with controls. These data provide conclusive evidence that RNAi can effectively reduce BJP production *in vitro* and provide the base for testing the clinical potential of this strategy using a relevant *in vivo* murine model of plasma cell dyscrasia.

5.2 Introduction

Under normal circumstances the polyclonal expansion of B-cell clones is a critical feature in the adaptive immune response to pathogens. Plasma cell dyscrasias however, are characterized by the proliferation of monoclonal B-cells that secrete an Ig or free HC, or LC protein which often aggregates and deposits, in vital tissues and organs (181-183). This results in a loss of compliance within tissues and progressive organ failure which contributes significantly to the morbidity and mortality of patients. Deposition of free LC, manifests as amorphous aggregates, crystals, or structured fibrils most commonly in the kidneys, heart, liver, or nerve fibers. Manifestations of plasma cell dyscrasias in which the LC aggregation and deposition dominates the pathology include: cast nephropathy or "myeloma kidney" in multiple myeloma (99); intracellular crystals in patients with Fanconi syndrome (184, 185); LCDD (186), and; fibrillar matrices in AL amyloidosis (122).

Current treatment of plasma cell dyscrasia relies on ablative chemotherapeutic approaches with alkylating agents and high dose steroids to reduce the monoclonal B-cell component sometimes followed by autologous stem cell transplant if warranted (146, 187). Often the use of non-steroidal anti-inflammatory drugs and chemotherapeutic agents can exacerbate the acute tubular necrosis that is observed in patients with plasma cell dyscrasia (188). Furthermore, although strict criteria are applied when determining eligibility for autologous stem cell transplant, this treatment is associated with a high incidence of mortality (159). Supportive therapy for patients often includes increased hydration to assist with clearance of LC from the kidneys as well as dialysis and plasmapheresis to further reduce serum monoclonal LC protein levels (52, 99). Recent reports have shown an improved outcome in myeloma patients with LC cast nephropathy was observed by reducing serum free LC by plasma exchange (189).

74

Previously, it has been shown using a human myeloma cell line, that targeted depletion of LC synthesis *in vitro* could be achieved using post-transcriptional gene silencing (190). Although initially demonstrated using antisense olignucleotides, the same effect has never been demonstrated using small interfering RNA technology, which has superseded antisense technology. RNAi exploits an evolutionarily conserved mechanism of post-transcriptional gene silencing (4). The presence of double stranded RNA molecules within the cytoplasm of eukaryotic cells triggers an enzymatic cascade resulting in the specific degradation of target mRNA, thus inhibiting the production of the encoded protein (13, 191). RNAi has been shown to be a robust and specific tool to selectively "silence" protein synthesis in a variety of cell types (192, 193). Furthermore, RNAi has been shown effective in reducing target protein concentrations in animal models of disease (194-196). Currently RNAi-based therapies are being evaluated in humans for the treatment of macular degeneration and respiratory syncytial virus infection (197, 198).

Building on these observation, herein we describe the treatment of three cell lines; SP2/O-λ6, a mouse myeloma cell line stably transfected and expressing the human λ_6 Bence Jones protein (BJP) Wil, the plasma cell line RPMI 8226 (human λ_2) and Bur (human IgG κ_1) with synthetic siRNA molecules that target the V, J and C domains of the LC proteins. SiRNA delivered by lipid based transfection media was shown to be non-toxic and efficiently reduced target LC mRNA as well as intracellular and secreted protein levels by up to 50% as compared with controls.

5.3 Materials and Methods

Cell lines

Mouse myeloma (SP2/O-λ6) cells expressing the human λ_6 Wil BJP and the patient derived myeloma line Bur were provided by Dr. Alan Solomon (University of Tennessee Medical Center, Knoxville). SP2/O-λ6 cells were stably transfected by electroporation with a construct containing the λ6 Wil VJC sequence under control of the cytomegalovirus promoter and mouse mu enhancer sequence (Chapter 3, Figure 3.1). Sequence identity of the Wil insert was confirmed by DNA sequencing. The human myeloma cell line RPMI 8226 was purchased from American Type Culture Collection (ATCC). Cell lines were cultured as described in Section 3.1.

Small-interfering RNA (siRNA)

SiRNA duplexes corresponding to nucleotide sequences within the variable domain of λ6Wil and RPMI 8226 were purchased from Sigma Aldrich. In addition, siRNA oligonucleotides were designed to regions of conserved homology within the C domain of λ LCs (Sigma-Aldrich). All sequences were verified and checked for homology with non-LC proteins using BLAST (http://blast.ncbi.nlm.nih.gov/Blast.cgi) and are shown in Chapter 4, Table 4.2. AllStars non-silencing siRNA (Qiagen) served as a negative control.

Cell Culture and Viability

On day of experiments, cell numbers and viability were determined by trypan blue dye exclusion assay and counting on hemacytometer. Cells were washed by centrifugation and resuspended in 100 µl phenol red-free DMEM F-12 (Sigma Aldrich) containing 5% FBS and P/S.

A volume containing 2×10^5 cells was added to each well of a 24-well microplate to which was added 1.5 μg siRNA complexed with 4.5 μl HiPerFect siRNA transfection reagent (Qiagen) in 100 μl phenol red free DMEM F-12 lacking serum or antibiotics. As a control, cells were treated with AllStars siRNA formulated with HiPerFect as above. Cells were incubated at 37°C for 24, 48, or 72 h. At each timepoint cell viability was assessed using the Cell Titer Blue assay (Promega) according to manufacturer's instructions.

Transfection Efficiency

Cellular uptake of siRNA was measured by flow cytometry using a FACScan flow cytometer (BD Immunocytometry systems) and employing CellQuest Pro software. Optimal transfection conditions were determined for each cell line by titrating the concentration of AllStars siRNA labeled with Alexa488 (Qiagen) and HiperFect transfection reagent (Qiagen), non-labeled AllStars siRNA (Qiagen) served as a control. Alexa488-labeled AllStars treated cells were incorporated during each experiment to monitor transfection efficiency.   Steps taken in determining these conditions are outlined in Chapter 4.

RNA Isolation and Analysis

Following treatment with siRNA as previously described total RNA was isolated from either SP2/O-λ6 or RPMI 8226 cells using RNAeasy Plus RNA isolation kit (Qiagen) according to manufacturer's instructions and the integrity of product was assessed by agarose gel electrophoresis. RNA concentration was determined by UV spectroscopy at 260nm and 280nm.

Reverse Transcriptase Real Time PCR

Analysis of LC gene expression was carried out by RT qPCR (Chapter3.5) using the following primers (Sigma-Genosys): Wil (forward) 5´ -ACGGTAACCATCTCCTGCA-3´, (reverse) 5´-AGGGTCTGTGGTCATCCTC-3´, 121-bp product; RPMI 8226 LC (forward) 5´-CAAAGCCCCCAAACTCATAA-3´, (reverse) 5´-AACACCACCTCGAAAAGTGC-3´, 180-bp product. Primers to human and mouse glyceraldehyde-3-phosphate dehydrogenase (GAPDH; Real Time Primers LLC) were used to amplify the calibrator gene; human GAPDH (forward) 5´-GAGTCAACGCGGATTTGGTCGT-3´, (reverse) 5´-TTGATTTTGGAGGGATCTCG-3´, 238-bp product; murine GAPDH (forward) 5´-CTGGAGAAACCTGCCAAGTA-3´, (reverse) 5´-TGTTGCTGTAGCCGTATTCA-3´, 223-bp product. For each primer set amplification efficiency was shown to be ~100%. Relative LC mRNA levels for cells in each experimental siRNA treatment group were calculated using the $2^{\Delta\Delta C_T}$ method and reported using cells receiving AllStars siRNA as the reference group.

ELISA of Secreted LC

Culture supernatants were collected at 24, 48, or 72 h post-transfection after cell separation by centrifugation at 400 × g for 5 min. For the SP2/O-λ6 cell line supernatants were diluted 1:10 in PBS + 1% bovine serum albumin (BSA; w/v) + 0.1% Tween 20 (Sigma-Aldrich) and analyzed using l6 LC ELISA (Chapter 3.9). A standard curve was prepared by serial dilution of purified recombinant λ6Wil VJ(127) over the range from 0.3 µg/ml to 400 µg/ml.

For LC 8226, supernatants were diluted 1:100 in PBST before analysis using total λ LC ELISA A (Chapter 3.9). In this case the patient derived λ2 LC Rhea was used to generated a standard curve which ranged from 300 ng/mL to 40 µg/ml.

Detection of LC Bur was accomplished using the total κ ELISA (Chapter 3.9). Standard curves were prepared using purified, patient derived Bur BJP starting with 200 ng protein followed by a 1:1 serial dilution in PBST + 1% BSA. Bur supernatants were diluted 1:100 in PBST + BSA and 100 μl of sample were added to individual wells.

Flow Cytometry of Cellular LC

The concentration of cellular LC was measured by flow cytometry (199). RPMI 8226 cells treated with experimental or control siRNA were cultured and transfected as previously described. At 24, 48, or 72 h cells were isolated by centrifugation at $500 \times g$, the supernatant removed, and the cells washed in PBS + 1% BSA. Cells were treated with fixative and permeablization buffer (BD Cytofix/Cytoperm; BD Biosciences) according to manufacutrer's instructions, blocked for 20 minutes in Cytoperm solution (BD Biosciences) containing 1% BSA. Cells were then resuspended in CytoPerm solution containing 11 μg/ml FITC labeled rabbit anti-human total λ antisera (DAKO) or unlabeled rabbit anti-human total λ antisera (DAKO), which served as a control. After a 1 h incubation at RT cells were washed 3× in PBS and resuspended in 0.5 ml PBS for analysis by flow cytometry (FACScan; BD Biosciences).

Statistical Analysis

ELISA results were normalized and expressed as percent control siRNA treated cells. For each set, data were pooled and analyzed for significance by One-Way ANOVA using Dunnett's Multiple Comparisons test (GraphPad Prism; GraphPad Software Inc.).

5.4 Results

Transfection efficiency

Optimal transfection conditions for both SP2/O-λ6 and 8226 cells were determined by flow

cytometry. For each experiment, incorporation of Alexa488-labeled AllStars siRNA and trypan

blue was used to document transfection efficiency and monitor cytotoxicity, respectively. In the

case of SP2/O-λ6, ~97% of the cells were transfected by 24 h, and at 48 h and 72 h this value

decreased to ~59% and ~40%, respectively (Figure 5.1). 8226 cells were similarly transfected at

24 h, but remained ~95% labeled at 72 h (Figure 5.1). The mean fluorescence intensity of the

transfected cell populations decreased in both cell lines over the 72- h period of study, due most

likely to the dilution of the fluorescent oligonucleotide in the dividing cells (this was more

evident in SP2O-λ6 cells, due to their more rapid, doubling time, i.e., ~12 h).

Effect of siRNA treatment on LC mRNA levels

Using appropriate primers, the PCR reaction products from SP2/O-λ6 and 8226 cells had the

expected bands at ~115bp and ~180 bp, respectively, as evidenced by agarose gel

electrophoresis; no secondary low molecular weight products were observed (data not shown).

At 24 h SP2O-λ6 cells exposed to V1, V2, and J1 Wil elicited a 23, 32 and 20% reduction in LC

mRNA levels, as compared to the sham-treated cells, whereas treatment with C1 λ and C2 λ

induced a 39 and 35% reduction. By 48 h, cells exposed to V1, V2, and J1 Wil siRNA had 24,

40, and 34% reductions in mRNA levels, as compared with cells treated with sham siRNA. The

values after treatment with C1λ and C2 λ remained similar to those at 24h. At 72 h post-

transfection, the results were erratic, presumably due to cell doubling and cell death; however, in
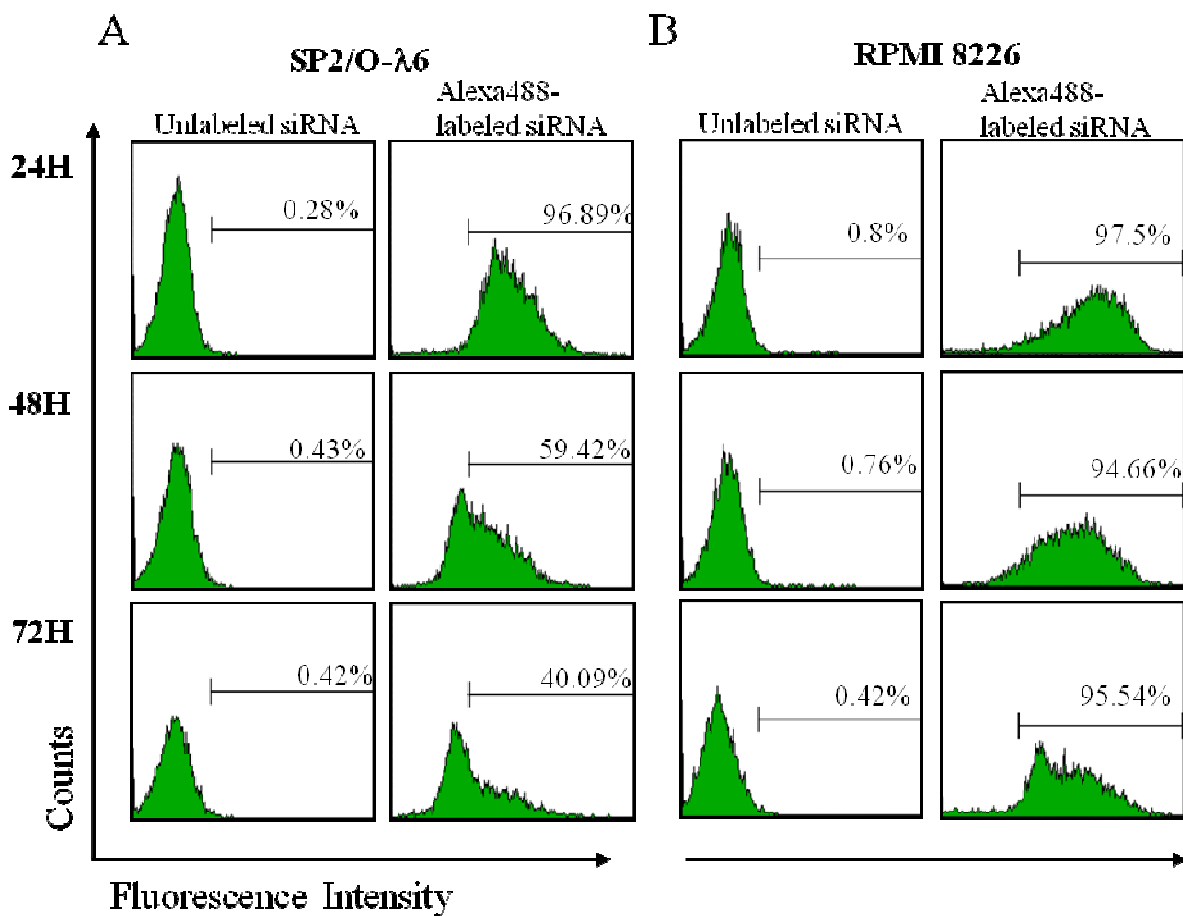
Figure 5.1 SP2/O-λ6 and RPMI8226 cells demonstrated positive uptake of siRNA. *A,* SP2/O-λ6 and *B,* RPMI8226 were transfected alexa488-labeled or unlabeled AllStars siRNA and analyzed by flow cytometry at 24, 48, or 72 h. Regional markers were set based on cells transfected with non-labeled AllStars siRNA. Numbers represent the percentage of positively transfected cells. For all data, percentages indicated are from a representative experimental group.

general, the levels were equivalent to those of untreated cells with exception of V2 Wil and C2 λ in the SP2/O-λ6 line which remained 21 and 30%, respectively, below levels found in the controls (Figure 5.2).

Treatment of RPMI 8226 cells with V1 8226 and C3 8226 decreased target LC mRNA by 61 and 43%. A lesser degree of suppression was observed after treatment with C1 λ and C2 λ (32 and 39% respectively). However, by 48h mRNA levels in cells exposed to C1 λ siRNA was reduced by 51%. In contrast, in cells treated with V1 8226, C2 λ and C3 8226 there was a less (32-35%) reduction at 48h. By 72h, the exposure of cells to V1 8226, C1 λ, and C2 λ siRNAs these values reverted to near control levels, whereas mRNA levels in C3 8226 treated cells remained suppressed (Figure 5.3).

Effect of siRNAs on LC production.

 1 x 10^6 of untreated SP2/O-λ6 cells generated ~180 ng of λ6 LC Wil per day. Treatment with siRNA had no effect on cell viability or number throughout the 72 h experimental period, as evidenced in the Cell Titer Blue viability assay (Fig. 5.3). When these cells were treated with siRNAs targeting the V, J, or C regions, the amount of secreted LC in the culture supernatants at all three time points was significantly reduced ($p<0.05$) (Figure 5.4), whereas exposure to siRNA specific to LC 8226 had no effect (data not shown). This response was most pronounced at 72 h post-transfection, where V- and J-region-specific siRNAs produced an ~50% decrease in λ6 LC Wil secretion relative to sham-treated cells (C-region siRNA treatment reduced secretion by 40%).
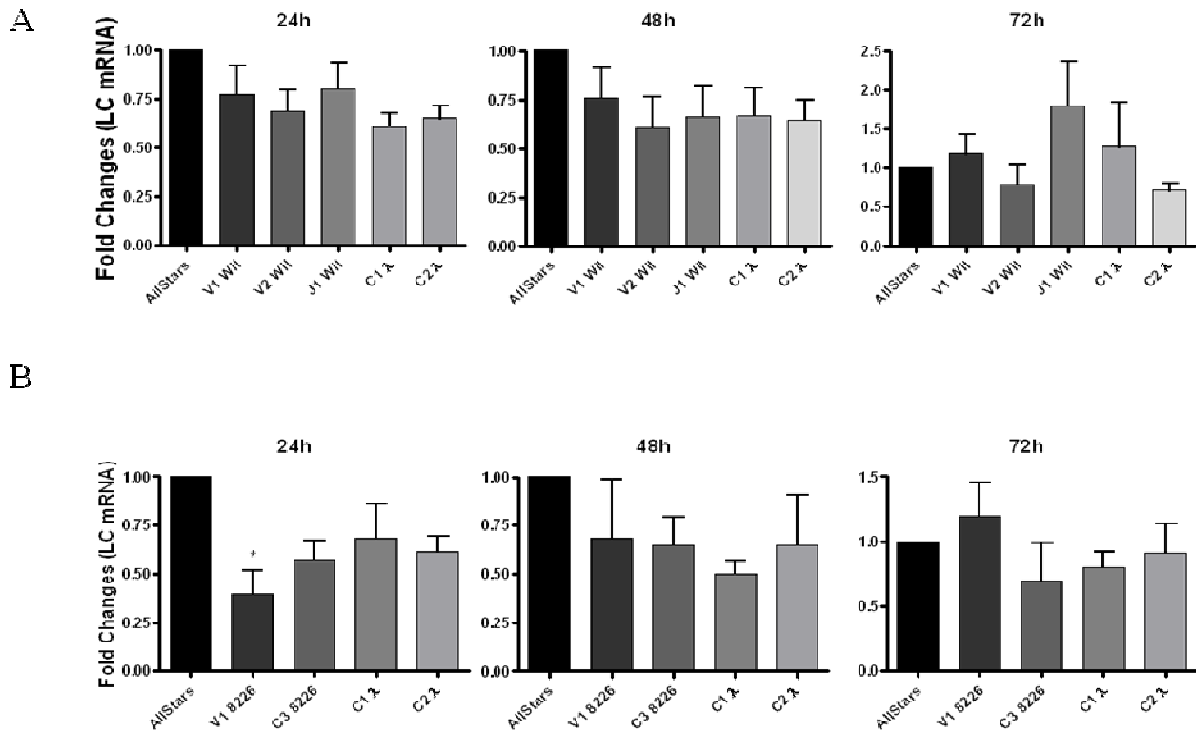
Figure 5.2 Transfection with experimental siRNAs reduced LC mRNA in human and mouse myeloma cells. *A,* SP2/O-λ6 cells were treated with siRNA directed to either the V or J region of IgLC Wil or with siRNA targeting C domain of λ LCs. Gene expression level of LC Wil was quantitated by real-time PCR using murine GAPDH as a reference gene. PCR was performed in triplicate, columns show expression relative to sham siRNA treated cells as mean ± SEM of 3 representative experiments. *B,* RPMI8226 cells were treated with siRNA directed to either the V region of the   RPMI8226 LC or with siRNA targeting C domain of λ LCs and were analyzed as above. Data were normalized to human GAPDH. PCR was performed in triplicate, columns show expression relative to 8226 LC mRNA from sham siRNA treated cells.
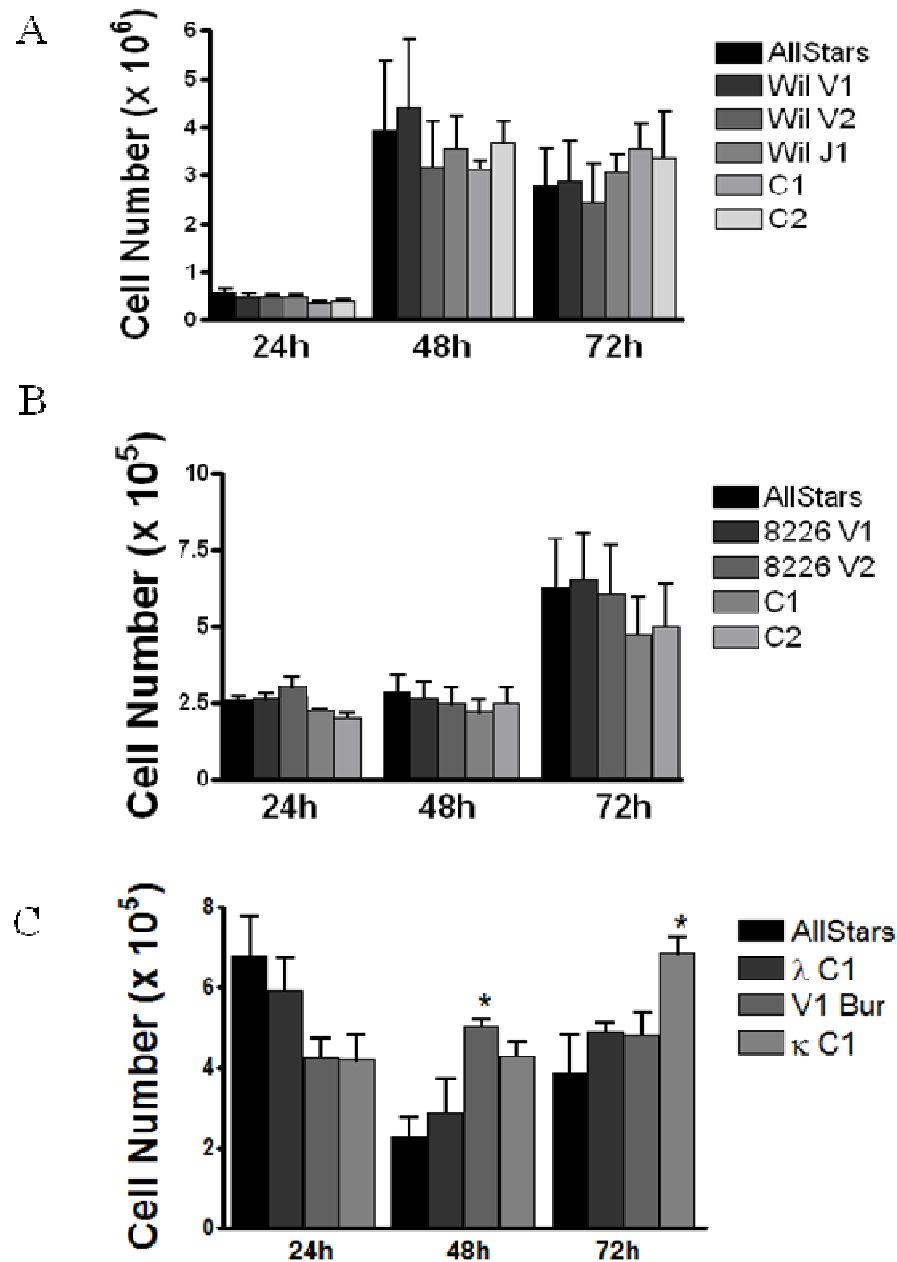
Figure 5.3 Treatment with siRNA had little effect on cell viability. A) Following transfection with siRNA 100 μL of SP2/O-λ6 culture was sampled and viability assessed by CellTiter Blue assay. Cell numbers were estimated using serially diluted SP2/O-λ6 cells. Data were pooled among 5 experimental replicates and analyzed by one-way ANOVA. B) RPMI 8226 cells were sampled and viability assessed as above. C) Likewise, viability for cell line Bur was assessed. Data were pooled among 6 experimental replicates and analyzed by one-way ANOVA (mean ± SEM; * denotes $p < 0.05$)
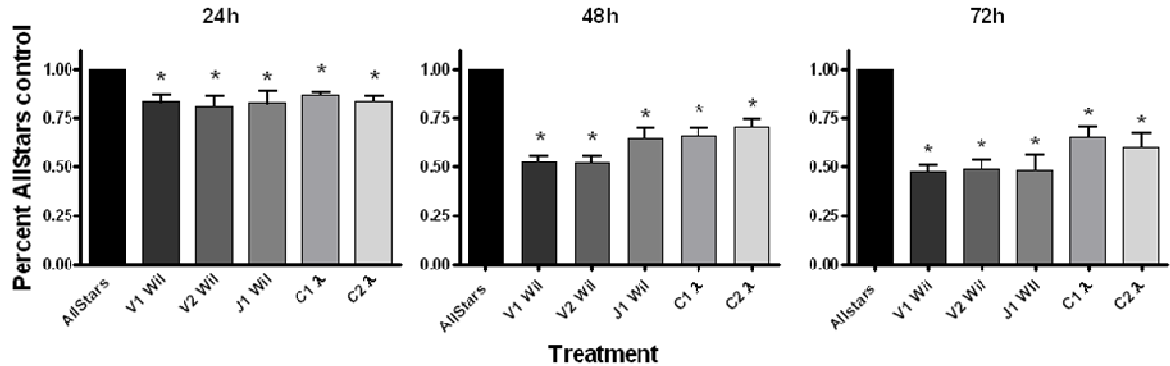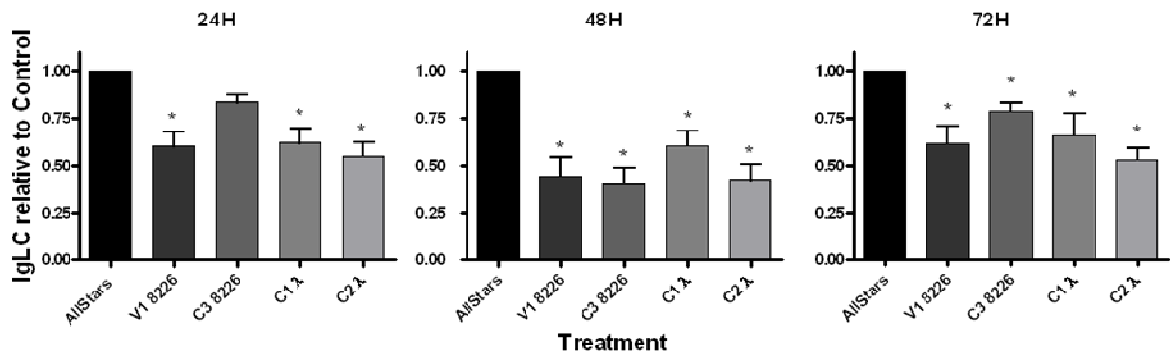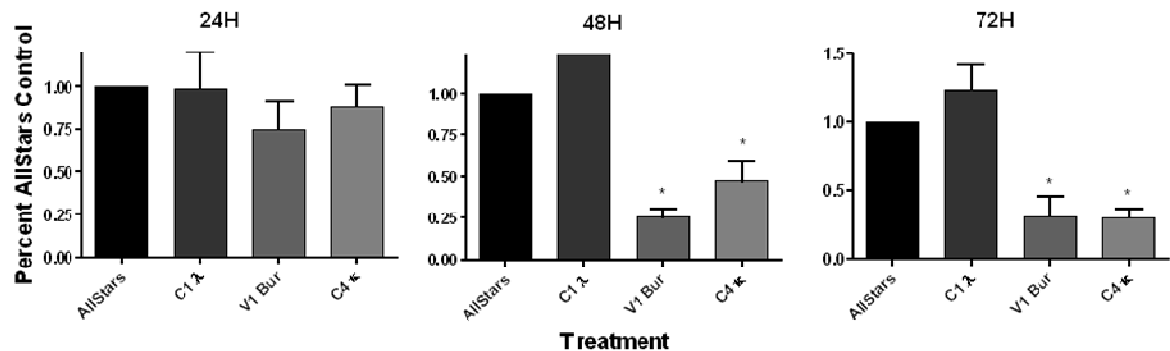
Figure 5.4 Cell culture supernatant IgLC concentration was reduced following treatment with experimental siRNA. A) SP2/O-λ6, B) RPMI 8226, or C) Bur myeloma cells were cultured for 24, 48 or 72 hrs along with indicated siRNA oligonucleotides. At given timepoints supernatant was collected, cleared by centrifugation, and analyzed by ELISA. For each experimental replicate, supernatant LC was reported as the ratio of LC concentration from cells receiving experimental siRNA to cells receiving AllStars siRNA. For each group ratios were pooled and analyzed by one-way ANOVA (n = 6; mean ±SEM; *, $p < 0.05$). *B,* RPMI8226 cells were cultured and analyzed as above (n = 6; mean ±SEM; *, $p < 0.05$).

In the case of RPMI 8226, 1×10^6 untreated cells produced ~13.4 µg of LC per day. Treatment with the siRNAs had no effect on cell viability or number (Figure 5.4). At 24 h post-transfection, exposure to V1 8226, C1, and C2 siRNA constructs significantly reduced ($p < 0.05$) LC secretion by 40, 39, and 61% respectively as compared with untreated controls. Treatment with AllStars non-silencing control siRNA had no effect on LC concentration (Fig. 5.4). At 48 h, LC secretion decreased by 54 and 60% respectively. The C1 and C2 siRNA constructs also significantly reduced (p < 0.05) protein production by 40 and 65%, respectively, and this effect was still apparent at 72 h. In contrast, treatment of 8226 cells with siRNA specific to LC Wil had no effect on LC production at any timepoint (data not shown).

Exposure to siRNAs targeting cell line Bur were also successful in reducing secreted LC, however, unlike with the other myeloma lines, this reduction was only seen after 48 h and remained strongly evident at 72 h (Figure 5.4). Additionally, these data illustrate the specificity of siRNAs as exposure of cell line Bur to siRNA molecules targeting C1 λ had no effect on LC production as compared with controls. Interestingly, cells exposed to either κ targeting siRNA were found to have significantly higher cell numbers at 48 and 72 h as compared with non-silencing controls, however it is not clear why this may have occurred (Figure 5.3)

Reduction in cytoplasmic LC production by siRNA-treated 8226 cells was also documented by flow cytometry (Figure 5.5). To determine treatment effect on cellular LC content, a gate region was drawn that excluded control siRNA-treated cells (cells within this gated region were considered negative for cellular LC staining). The geometric mean of each population also was used to estimate relative fluorescent intensity between cells exposed to experimental and control siRNAs. Data collected from the gated region at 24 and 48h revealed
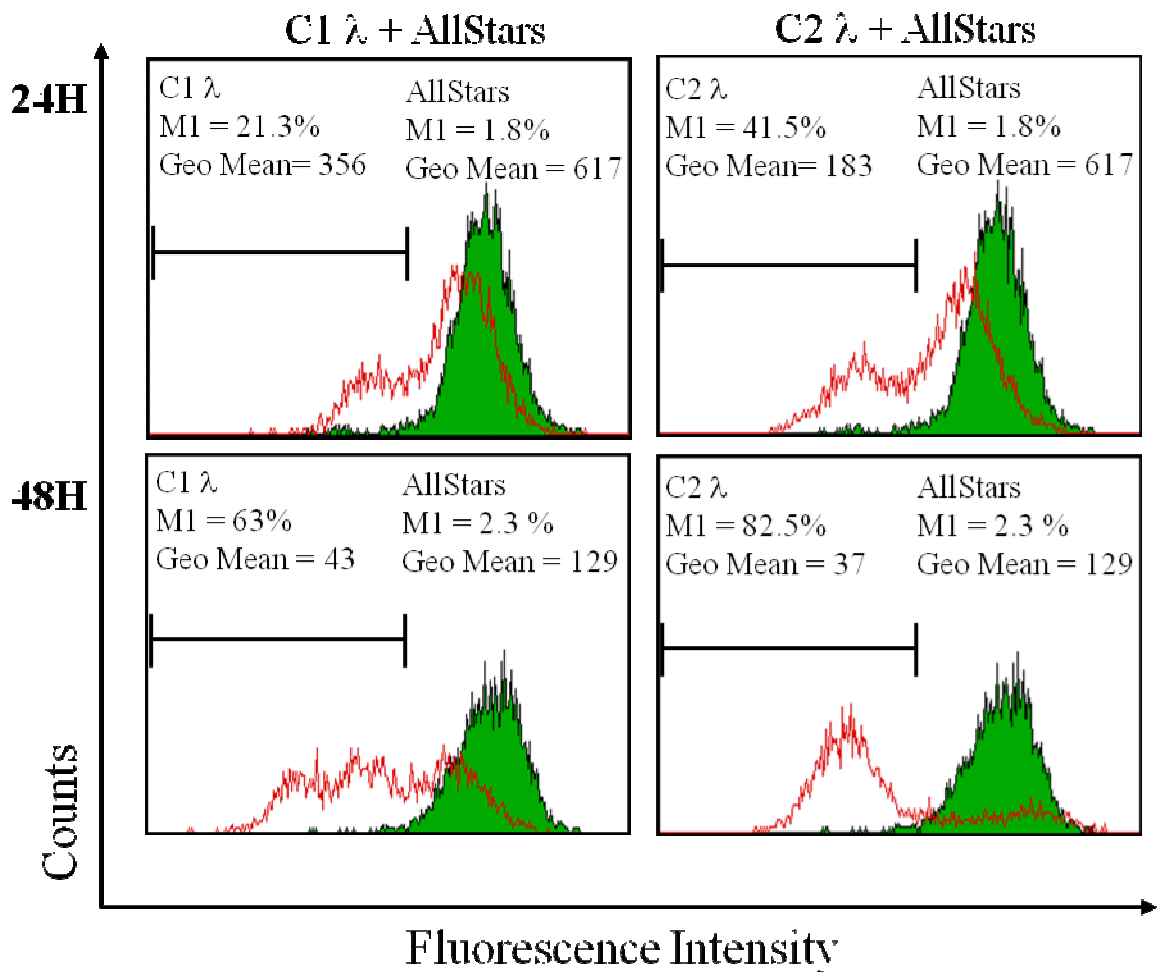
Figure 5.5 A sub-population of cells containing lower cellular IgLC concentration emerged following transfection with experimental siRNA. RPMI8226 cells were transfected with C1 λ, C2, λ or AllStars control siRNA. At the indicated times cells were stained with FITC conjugated rabbit anti-human total λ Ab and analyzed by flow cytometry. Regional markers excluding sham treated cells were set for FL-1. For each panel, the geometric mean of the gated cell population and the percent of cells falling within the marker region are reported. Open histograms represent cells treated with C1 or C2 siRNA and closed histograms represent sham treated cells. Histograms are taken from an example flow cytometry experiment.

that 21.3 and 63% of C1 λ treated cells fell within the region considered negative, as compared with controls where 1.8 and 2.3% of the population fell within the marker region. Comparison of geometric means revealed that exposure to C1 λ siRNA elicited at 24 and 48 h, respectively, 58 and 33% reduction in fluorescence intensity, as compared with controls (Figure 5.5). C2 λ siRNA effected an even greater reduction in cellular LC concentration at 24h, resulting in a 70% loss of fluorescence as estimated by comparison of geometric means of control cells. By 24 h, 42% of the population fell within the gated negative region as compared with controls where only 2% fell within the marker region. This effect was more pronounced at 48h where there was a 70% loss of fluorescence. In addition, 83% of the population of C2 λ treated cells fell within the negative gated region, as compared with controls where only 2% were gated.

6.5 Discussion

A major contributing factor to the morbidity and mortality of plasma cell dyscrasias is the overproduction of immunoglobulin free LC proteins and their subsequent aggregation and deposition in tissues and organs. Current standard of care calls for dose-intensive chemotherapeutic intervention to reduce the monoclonal B cell population and thereby effect a decrease in circulating LC protein concentration. A recent retrospective survey of patients diagnosed with myeloma and LC cast nephropathy indicated that a reduction of circulating free LC levels of ~50% correlated with an improved clinical outcome in patients who responded to treatments as compared with non-responders (189). It is also reasonable to assume that reduction in free LC concentration in patients with AL will reduce the growth of the pathologic fibrils, to the benefit of the patient. Thus, methods that decrease free LC production are potentially clinically beneficial and highly desirable.

Previously, antisense deoxyoligonucleotides were shown capable of achieving a modest reduction in the secretion of free LC by human myeloma cells *in vitro* and in human myeloma cell line xenograft tumor models (190). Recently, interfering RNA has superseded antisense technology in regards to efficiency(200), and specificity (175, 201) as the method of choice for post-transcriptional "silencing" of protein expression (165, 200, 202, 203). Although there have been incidences of cytotoxicity and non-specific activation of the host innate immune system following RNAi treatment in animals (204, 205) these effects can be avoided, or at least lessened, with proper siRNA sequence design and careful selection of delivery system(206-208). We have evaluated the ability siRNA treatment to reduce secreted LC concentration using 2 cell lines. SP2/O-λ6 cells that secrete Vλ6Wil BJp were chosen as we have recently developed a transgenic mouse stably expressing the λ6Wil BJp into which these studies could translate (JW and AS, unpublished data). However, this system is somewhat artificial we included also the well-characterized human myeloma cell line RPMI 8226, while cell line Bur served to test RNAi on a cell line expressing the κ LC isotype. Treatment of each of these cell lines with experimental siRNAs targeting nucleotide sequences within the V, J, and C regions resulted in significant decreases in the secreted LC protein concentration and mRNA levels as compared to cells transfected with benign siRNA. Interestringly, the C1 and C2 siRNA constructs depleted LC secretion by the RPMI 8226 much more effectively than the λ6Wil LC-producing SP2/O-λ6 cell line. Since these siRNAs were designed with the goal of targeting highly conserved, and therefore universal, regions within the C domain of all λ LC subgroups is somewhat counterintuitive that C region siRNAs would be more efficacious for one cell type as compared with another. This decrease may be due to differences in the secondary structure of the SP2/O-λ6 (Cλ2) and RPMI 8226 (Cλ3) mRNA molecules affecting the annealing efficiency as has been

posited elsewhere (209). Cell counts and viability assays demonstrated no significant difference in cell number following transfection with siRNA using a lipid based reagent. Studies *in vivo* using similar lipid transfection systems have produced little or no toxicity in animal models (168, 190, 210, 211).

Immunostaining of fixed and permeabilized RPMI 8226 cells that had been treated with C1, C2, or AllStars siRNA revealed a substantial population of cells at 24 h (21-63%) and 48 h (41-82%) with reduced intracellular LC. This sub-population was not observed in untreated cells or those transfected with AllStars control siRNA. Intracellular LC reached a minimal point at 48 h, as evidenced by the 82% decrease in positively stained cells. This is likely due to the fact that siRNA treatment is most effective during the initial 48 h post transfection in addition to the secretion of intracellular LC pool into the culture supernatant over this time. The combination of these 2 effects - blockage of LC gene translation and loss of cytoplasmic protein by secretion - likely resulted in the population of LC-negative cells. At 72 h post-transfection however, the effect of the siRNA treatment was diminished significantly by inactivation and dilution of the reagent following cell division, thereby allowing the intracellular pool of LC protein to replenish. This is supported by the fact that the doubling time for the RPMI 8226 cell line was ~72 h, as evidenced in the flow cytometric analysis of cells transfected with Alexa488-labeled AllStars siRNA.

Since RNA interference operates in a specific fashion by degrading mature mRNA sequences post-transcriptionally we expected that a reduction in LC protein would be accompanied by a reduction in target mRNA levels. Indeed, when treated with siRNA molecules targeting the LC V, J, or C regions both SP2/O-λ6 and RPMI 8226 cell lines exhibited a

reduction in target mRNA levels as compared with their respective control siRNA treated counterparts.

Because aggregation and deposition of the free LC component secreted by neoplastic plasma cells contributes to the poor prognostic outcome of patients diagnosed with LC diseases treatment using RNA interference offers a novel method of therapeutic intervention for a patient population with historically limited options. The results presented herein demonstrate the high degree of efficiency by which siRNA reduces intracellular and secreted LC protein. In both the SP2/O-λ6 and RPMI 8226 cell lines reduction in secreted LC reached >50% of normal, which is within a range that is considered to be clinically beneficial. Thus, RNAi offers a targeted approach to reducing LC secretion in plasma cell dyscrasias and with careful design and implementation may circumvent undesirable non-specific responses. These findings support the hypothesis that RNAi therapy could provide a valuable tool for the treatment of patients with plasma cell dyscrasia, as an adjuvant to traditional chemotherapies.

Chapter 6

Design and Synthesis of ShRNA Bearing Lentivirus Constructs

6.1 Rationale

Delivery of exogenous interfering RNAs to myeloma cells was effective in reducing the production of pathologic LC protein (Chapter 5). However this reduction was transient, likely resulting from the dilution of internalized siRNAs with each cell division and degradation of the siRNA molecules. It has been reported that delivery of shRNAs expression constructs by viral particles results in a sustained reduction of target proteins (31, 35, 212). In particular, viral vectors derived from the lentivirus family have been shown effective in transducing slowly dividing cell types including human myeloma lines (171, 213). Separation and truncation of key elements of lentivirus genes have produced self inactivating vectors which retain the ability to integrate to the host genome and produced a sustainable expression of gene products (390). Further, vesicular stomatitis virus g-protein (VSVG)-pseudotyped lentiviral vectors have demonstrated the potential to infect bone marrow stem cells *in vivo* (214).

While these studies indicate that it is possible to transduce myeloma cells with shRNA expression systems by using lentiviral particle delivery systems it remained to be seen whether the level of silencing generated by these interfering RNAs would be robust enough to reduce a pathologic LC produced in high quantities by plasmacytoid cells. To address this, siRNAs previously shown effective in reducing LC production in the transgenic mouse myeloma line SP2/O-λ6 and the human myeloma line RPMI 8226 were modified by first linearizing the guide and passenger strands followed by addition of an intervening sequence of nucleotides, which when transcribed, through complimentarity of the two siRNA strands would self-anneal to form

the characteristic stem-loop structure of a shRNA molecule (215). These shRNA cassettes were then ligated into a self inactivating lentivirus expression plasmids and functional lentiviral particles generated. Mouse or human myeloma lines were then exposed to the particles and the transfection efficiency and stability determined. This Chapter describes the steps taken in designing and generating these particles (see the schematic provided in Figure 6.1).

6.2 Materials and Methods

Propagation of Vector pLB

The self inactivating (SIN) lentiviral expression plasmid pLB cloning vector was acquired from AddGene plasmid repository (www.addgene.org; vector11619) (Figure 6.2 A). Viral plasmids were handled and purified as previously described (Chapter 3.4).

Propagation of Vector PLKO.1

The SIN lentiviral expression plasmid 8543 (pLKO.1) was acquired from Addgene as bacterial stock and was propagated as above (Figure 6.2 B). As with pLB plasmids were recovered from cultures by midi-prep and ethanol precipitation (Chapter 3.4).

Design of shRNAs

Short hairpin RNAs (shRNA) were designed based on small interfering RNA (siRNA) sequences targeting the V region of λ6 LC Wil (Wil V1) and LC 8226 (8226 V1) (Table 4.1). For plasmid pLB, these were modified according to the following format: 5'T (sense oligo)-TTCAAGAGA-(antisense oligo) TTTTTTC 3' to generate both the 5' and 3'restriction enzyme sites as well as to produce a stem-loop structure during synthesis (Table 6.1).

93
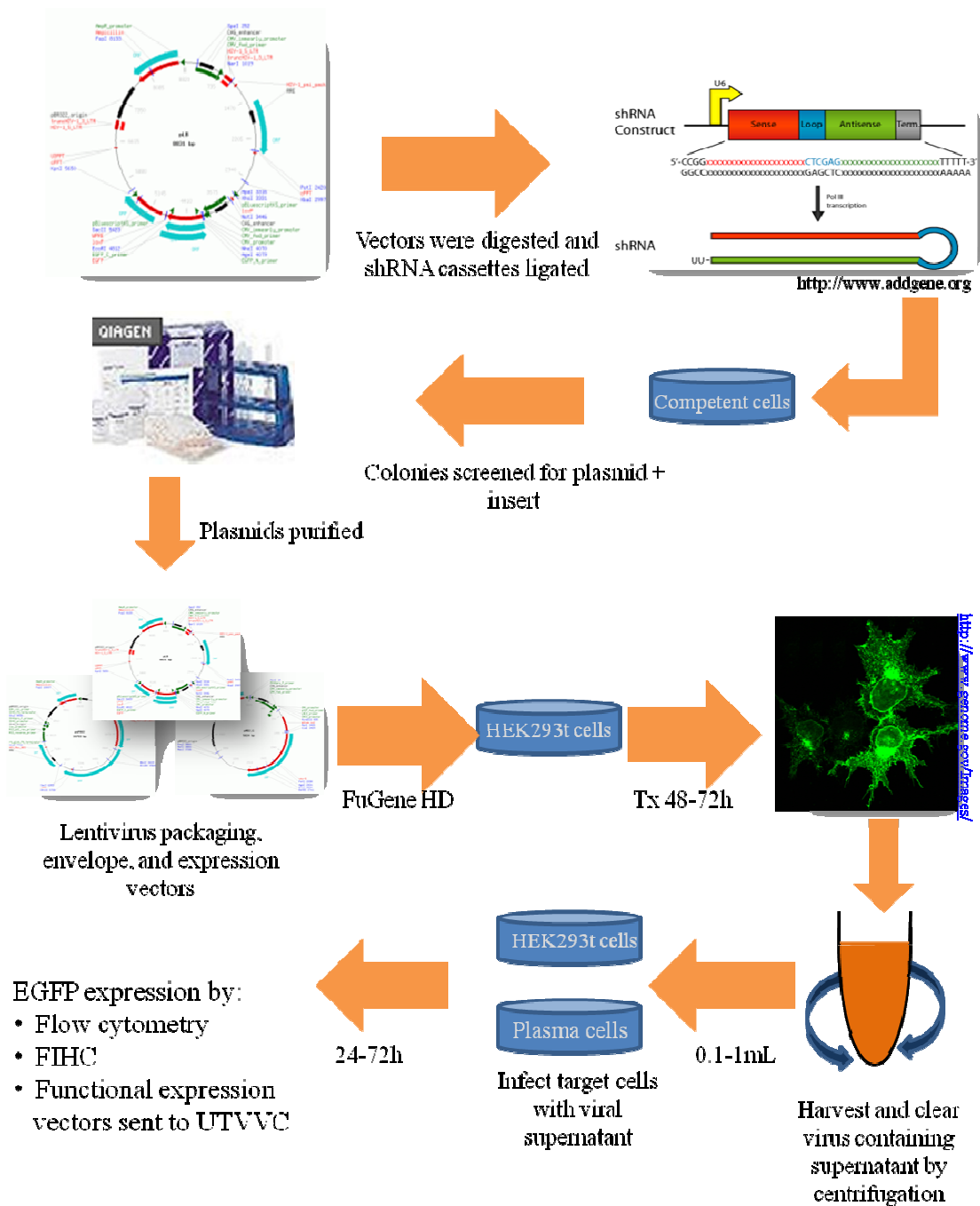
Figure 6.1 Schematic of the experimental design for generation shRNA-expressing Lentiviral Vectors. Lentiviral plasmid expression vectors were acquired and assembled with genes encoding shRNA sequences. Expression vectors were cloned into bacterial colonies and amplified. Following colony screening, plasmids were tested for functionality and ability to be packaged to lentiviral vector particles before being packaged to high-viral titer stock solutions.

Figure 6.2 Maps of Lentivirus Expression Plasmids pLB and pLKO.1. Vectors A) pLB and B) pLKO.1 were acquired from Addgene. Maps depict plasmid size and locations of functional genetic elements.

Table 6.1 Sequence of shRNA inserts

Vector	Dir	5' siRNA sense loop siRNA antisense 3'
pLB		
Wil V1	Fwd	t-**GCCAACAACTATGTTCACT-**ttcaagaga-**GTGAACATAGTTGTTGGC-**tttttttc
	Rev	tcgaaaaaaa-**GCCAACTATGTTCA-**tctctgaa-**GTGAACATAGTTGTTG-**a
8226 V1	Fwd	t-**GTGACATTGGTGACTATC-**ttcaagaga-**CACTGTAACCACTGATAG-**tttttttc
	Rev	tcgaaaaaaa-**CTATCAGTGGTTACAGTG-**tctctgaa-**GATTGTCACCAATGTCAC-**a
Bur V1	Fwd	t-**AGTCAGGGCATTTACAATTA-**ttcaagaga-**TAATTGTAAATGCCCTGAC-**tttttttc
	Rev	tcgaaaaaaa-**GTCAGGGCATTTACAATTAT-**tctctgaa-**TAATTGTAAATGCCTGAC-**a
pLKO.1		
Wil V1	Fwd	ccgg-**AACAACTATGTTCACT-**ctcgag-**GTGAACATAGTTGTTGGC-**tttttg
	Rev	aattcaaaaa-**GCCAACTATGTTCA-**gagctc-**GTGAACATAGTTGTTG-**ccgg
8226 V1	Fwd	ccgg-**GTGACATTGGTGACTATC-**ctcgag-**CACTGTAACCACTGATAG-**tttttg
	Rev	aattcaaaaa- **CTATCAGTGGTTACAGTG-**gagctc-**GATTGTCACCAATGTCAC-**ccgg

Legend: Bold Text represents siRNA portion of insert

For plasmid pLKO.1, sequences were modified to include 5' CCGG-(sense oligo)-CTCGAG-(antisense oligo)-TTTTTG 3' (Table 6.1), to generate a loop region and restriction sites. DNA oligonucleotides were ordered from Sigma Aldrich and were phosphorylated using T4 polynucleotide kinase (New England Biolabs, Ipswich, MA). Oligonucleotides were resuspended at 20 µM in TE buffer and annealed by first heating to 90°C for 4 min, followed by cooling slowly to room temperature over several hours.

Digestion of Expression Vectors

<u>Vector pLB</u>

The lentivirus expression vector pLB (6 µg) was digested for 2 h at 37° in a 50 µl reaction containing 1 µl each XhoI and HpaI restriction enzymes (New England Biolabs) and 5 µl 10X NEbuffer 4 (New England Biolabs). Linearized fragment was isolated by agarose gel electrophoresis and Wizard PCR clean-up kit (Promega, Madison, WI). For each reaction, 25 pmol of vector was removed and treated with Antarctic phosphatase (New England Biolabs) according to manufacturer's instructions.

<u>Vector pLKO.1</u>

Vector pLKO.1 (6 µg) was resuspended in 5 µl 10x NEbuffer 1 (New England Biolabs) along with 1 µl of AgeI and 1 µL of EcoRI restriction enzymes. Water was added to each reaction to a final volume of 50 µl and tubes were incubated for 2h at 37°C. Following the reaction, linearized fragments were isolated and purified as above.

Ligation of shRNA constructs

For each plasmid, 2 µl annealed shRNA oligonucleotides were added to a reaction containing 1 µl DNA ligase (New England Biolabs), 5 µL 10x T4 Ligase buffer (New England Biolabs), and 20 ng digested pLB or pLKO.1 vector. Ligation reactions were carried out overnight at 16° C.

Transformation of competent cells

XL-1 Blue supercompetent cells were prepared according to manufacturer's instructions and were treated with ligated pLB or pLKO.1 vector at increasing ratios (from 1:1 to 1:6). Cells were incubated on ice for 30 min and heat shocked at 42°C for 45 sec before being returned to ice for 1 min. Starter cultures were prepared by incubating cells at 37°C with constant shaking before being plated overnight on LB agarose supplemented with 50 µg/ml carbenicillin (Sigma Aldrich) as a selection agent. Colonies were selected and again grown overnight in 5 ml LB media supplemented with 50 mg/ml carbenicillin.

Colony Screening for Ligated insert

<u>Screening of Crude Lysate by Restriction Enzyme Digest</u>

For each culture, 1ml bacteria were harvested by centrifugation at 13,000 x g using a Biofuge Pico tabletop centrifuge for 5 min. Cells were resuspended in 300 µl of a STET solution (8% sucrose, 0.5% tritonx100, 50 mM EDTA, and 50 mM tris HCl), held on ice for 10 min, and boiled at > 90°C for 90 sec. Bacterial debris was removed following centrifugation at 14,000 rpm 13,000 x g for 30 min by aspirating supernatants into clean tubes. Nucleic acids were precipitated by the addition of 1 volume isopropanol and 30 min incubation at -20°C. DNA was pelleted by centrifugation at 14,000 rpm at 4° C on a Biofuge Fresca tabletop centrifuge for 20

min and resuspended in 50 µl Tris EDTA buffer (TE; 10 mM tris, 1 mM EDTA). For vector

pLB, 45 ml of DNA was added to a clean tube along with 5 µl NEbuffer 4 and 1 µl each

XhoI/HPAI (expected product size 60 bp) or NotI/Xba (~500 bp). Likewise for vector pLKO.1,

45 µl DNA was adjusted with 5 µl 10x Nebuffer 1 and 1 µl each AgeI/EcoRI added to each tube.

Restriction enzyme reactions were allowed to proceed for 2 h at 37°C and 10 µl product

separated by gel electrophoresis.

<u>Screening of lysates by PCR and Sequencing</u>

For samples that were suspected to contain ligated plasmid, 2 µl of DNA from each colony was

amplified by PCR using vector-specific primers that flanked the insertion site for the shRNA

construct. For vector pLB fwd primer, 5' TAGTAACTATAGAGGCTTA-ATGTGCG-3' and

reverse 5'TGGGCTATGAACTAATGACCCCGTA-3' were used which would generate an

expected product 0f 394 bp for an empty vector and 454 bp for a vector containing an shRNA

insert. For vector pLKO.1, forward 5'CAAGGCTGTTAGAGAGATAA-TTGGA-3' and

reverse 5'TATTCTTTCCCCTGCACTGT-3' were used and were expected to generate a 350 bp

product for empty vectors or 410 bp products for those containing shRNA inserts. Amplification

was carried out using the Phusion DNA polymerase enzyme (New England Biolabs) in 20 µl

volumes following manufacturer's instructions. Amplification was achieved using the PCR

protocol described in Chapter 3.5. PCR products (10 µLwere separated by agarose gel

electrophoresis. Products were purified using Wizard kits and presence of shRNA inserts

confirmed by DNA sequencing (UT MBRF).

Vector Purification

Vectors were purified from 125 ml of bacterial culture using polyethylene glycol (PEG)/ chloroform precipitation. Bacteria were grown overnight and collected the following day by centrifugation at 1,000 x g for 5 min. Supernatants were removed, pellets dried for 3 min, and the bacteria lysed by addition of alkaline lysis solutions taken from the Qiagen plasmid midiprep kit. Following lysis, the solutions were centrifuged at 10,000 x g for 20 minutes at 4°C, and supernatants containing plasmid DNA were removed and placed in a clean tube. DNA was precipitated by adding ammonium acetate to a final concentration of 2M, followed by 2 volumes of 100% ethanol. Tubes were placed on dry ice for 10 min and DNA was isolated as a pellet by centrifugation at 14,000 x g for 20 min at 4°C. DNA was transferred to a clean 1.5 ml microcentrifuge tube in 0.4 ml buffer TE to which an equal volume of saturated phenol - chloroform; isoamyl alcohol solution (25:24:1) - was added. Solutions were mixed and allowed to settle briefly before centrifugation at 13,000 x g on Biofuge *Pico* tabletop centrifuge for 2 min. Aqueous layers were removed and placed in clean tubes. Extractions were repeated twice. DNA was precipitated by the addition of 0.8 ml PEG solution (30% PEG 8000, 1.6M NaCl) to each tube and incubation overnight at -20°C before collection by centrifugation at 14,000 x g for 20 min at 4°C.

Transient transfection of cells with lentivirus expression vectors

HEK 293t and RPMI 8226 cells were acquired from the ATCC (Manassas, VA) and grown in DMEM F-12 containing 10% or 5% FBS, respectively, along with antibiotics. Cells were housed in a 37°C humidified chamber containing 5% CO_2. For each line, either empty or shRNA expressing pLB vector was combined with FuGeneHD transfection reagent (Roche).

The optimal ratio of DNA-to-transfection reagent was determined for each line according to manufacturer's instruction.

Generation of lentiviral particles

HEK 293t cells were grown in DMEM F-12 containing 10% FBS and antibiotics. Cells were housed in a 37°C humidified chamber containing 5% CO_2. For transfection experiments, cells were grown to ~80% confluence in 6 mm dishes or 24 well plates. On the day of transfection, media was exchanged to serum containing DMEM F-12 without antibiotics. ShRNA containing pLB expression vectors (1 µg) along with PMD2.G (0.5 µg; Addgene vector number 12259) and psPAX (0.5 µg; Addgene vector number 12260) were introduced to HEK 293t cells using Fugene HD transfection reagent (Roche) at a ratio of 2:6 (µg total DNA: µl FuGene HD). Cells were examined for EGFP expression under an inverted fluorescence microscope following 24 h incubation. At 48 and 72 h cell supernatants were harvested and filtered through 0.45 µm nylon filters and stored at -80°C.

Transduction of cells with low titer virus

HEK 293t cells were plated and grown to ~80% confluence in 10 mm dishes using DMEM F-12 with serum and antibiotics. On the day of transduction media was removed and cells washed in serum and antibiotic free DMEM F-12. 1 -1.9 ml Antibiotic free DMEM F-12 containing 10% FBS along with 10 µg/ml polybrene (Millipore) was then added to each plate. 0.1-1 ml viral supernatant was then added to each plate, bringing the final volume to 2 ml. Cells were incubated with virus for 6 h before supernatants removed and were replaced with fresh media.

At 24-72 h Cells were removed from plates by trypsinization and EGFP expression was measured by flow cytometry and fluorescence microscopy.

Similarly, RPMI 8226 and SP2/O-λ6 cells were exposed to increasing (0.1-1 ml) amounts of viral supernatant in presence of polybrene (10 μg/ml). Cells were incubated for 6 h in presence of virus before centrifugation and removal to fresh media.

6.3 Results

Recovered plasmids were visualized by gel electrophoresis and ethidium bromide staining; plasmid pLB is shown (Figure 6.3 A). For each plasmid, several glycerol stocks were prepared and were stored at -80° C. As needed, stocks were expanded and plasmid DNA purified using the Qiagen plasmid midiprep kit. Following annealing reactions shRNA inserts were visualized by gel electrophoresis and presence of double stranded oligonucleotides are evidenced by appearance of a ~120 bp band (Figure 6.3 B).

Following ligation reactions, plasmid preps were analyzed by gel electrophoresis. For plasmid pLB, several colonies were identified which contained bands of 450 bp in size, indicating non-ligated plasmids while others contained bands of ~500 bp indicating a ligated plasmid. Likewise, digestion of colonies generated from pLKO.1 with NotI/EcoRI restriction enzymes produced bands which were shifted by ~ 60 bp with shRNA inserts (Figure 6.4 A). These steps were repeated for each plasmid/insert combination, an example for both pLB 8226V1 and pLKO.1 Wil V1 are shown (Figure 6.4 A, B).
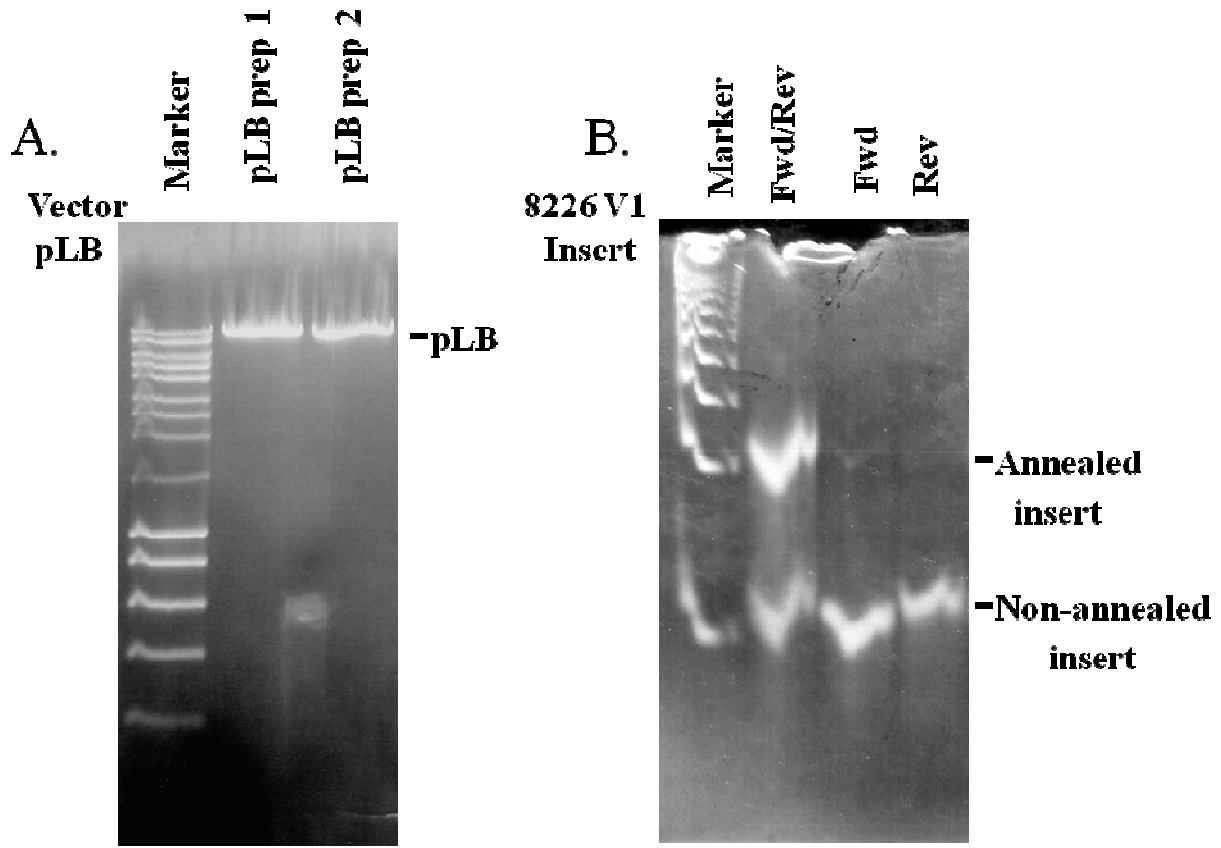
Figure 6.3. Lentiviral Vector pLB and Annealed 8226 V1 Insert. **A)** Bacterial stocks of transformed with plasmid pLB were grown overnight. The following day cells were lysed, plasmid DNA extracted, and linearized by restriction enzyme digest using HpaI and NotI. Products visualized by agarose gel electrophoresis and ethidium bromide staining, Hyperladder I was used as molecular marker. B) Plasmid inserts encoding shRNA sequences were annealed and visualized on agarose gel. Lanes demonstrate annealed forward and reverse oligonucleotides (120 bp), forward alone or reverse alone (60 bp). Hyperladder II was used as a molecular marker.
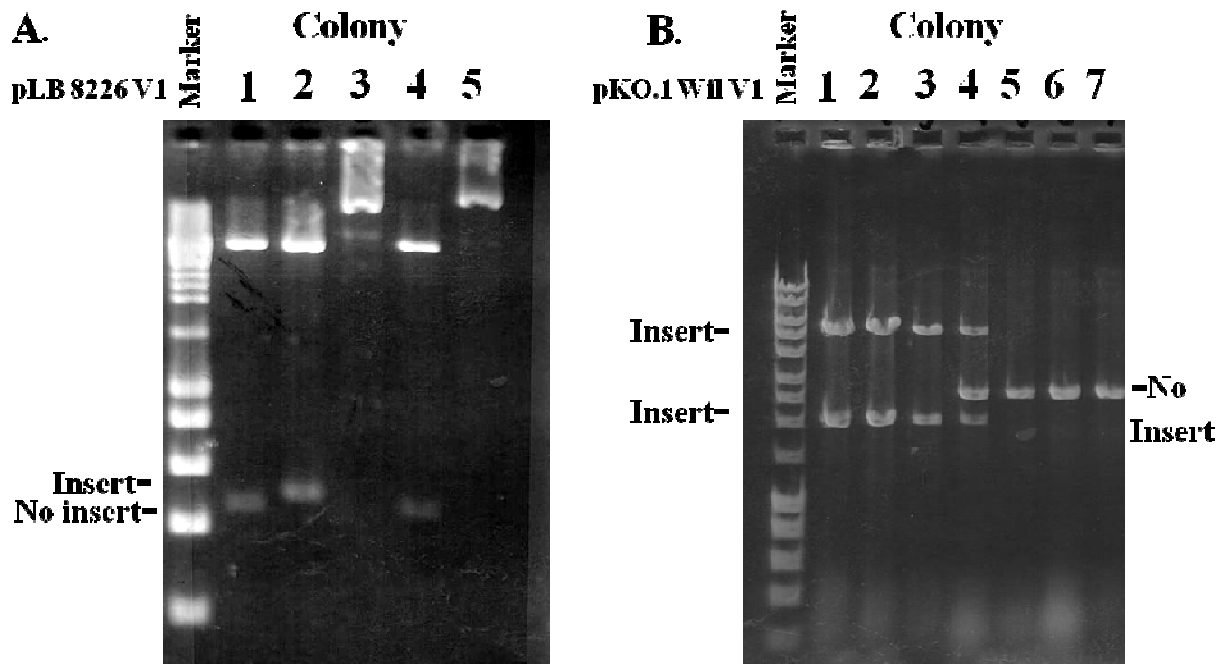
Figure 6.4 Restriction Enzyme Digests of Ligated Expression Vectors. A) Annealed insert encoding shRNA 8226 V1 was ligated to expression plasmid pLB. Plasmids were used to transform XL-1 Blue *E.coli*. Bacteria were grown on selective agar plates and selected colonies expanded to 5 ml starter cultures. Crude lysates were prepared and digested with NotI/Xba, producing a 450 bp band for plasmids without shRNA inserts or a 500 bp band for those with inserts. B) Likewise, plasmid plko1 Wil V1 was prepared and digested with NcoI/EcoRI. Since the EcoRI site was degraded during initial digestions it was expected that a single cut would occur without presence of the insert producing a single 8 kb band. Restoration of the EcoRI site allows a double digest to occur producing a 2 kb and 6 kb fragment.

Results of digest were confirmed by PCR amplification of plasmid DNA. In the case of pLB two sets of primers were designed; one to flank the regions surrounding the shRNA insert (product sizes of 400 or 460 bp without or with inserts, respectively), and another in which the forward and reverse primers were located internally of the shRNA expression insert. Products were separated by gel electrophoresis and visualized by staining with ethidium bromide.

As shown, primers flanking the insertion site as well as those used in combination with primers targeting sequences along the 8226 V1 insert along plasmid pLB amplified a target of the expected size for presence of the 8226 V1 insert (Figure 6.5 A). No product was observed when both forward and reverse primers targeting insert 8226 V1 were used (Figure 6.5 A). Amplification of plasmid PLKO.1 with primers located upstream of the shRNA insertion site in combination with those internal to Wil V1 revealed several colonies which contained ligated expression plasmid.   In each case, bands were submitted to UTMBRF for sequencing Purified plasmids were acquired using phenol chloroform extraction method and purity and yield were assessed by reading absorbance values for A_{260}/A_{280} and functionality tested by transfecting HEK 293, RPMI 8226 or SP2/O-λ6 cells using FuGene HD (not shown).

Plasmids pLB, pLB 8226 V1, and pLB Wil V1 were shown capable of producing infective viral particles by co-transfection with plasmids encoding packaging signals and coat protein genes to HEK 293t cells. Following a 3 day window for virus production, supernatants from these cells were removed and added to cultures of either naïve 293t cells, 8226 cells, or SP2/O-λ6 cells. Infectivity of viral particles was assessed by EGFP expression using fluorescence microscopy (Figure 6.6). While low in number, 293t cells were observed which demonstrated EGFP expression from cultures receiving 8226 V1, Wil V1, and empty vector viral particles.
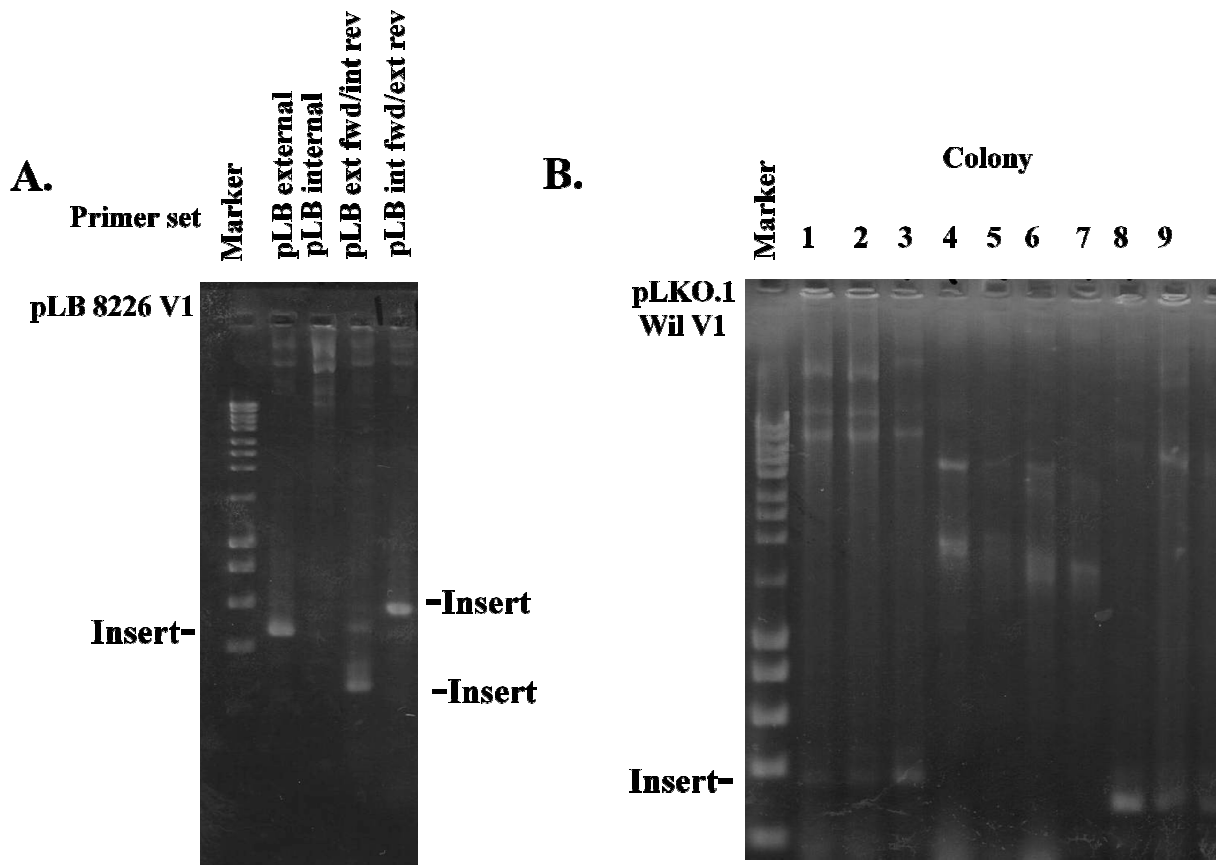
Figure 6.5 Purified Plasmid DNA was Screened for Presence of ShRNA Expression Constructs by PCR. A) Primers were designed to amplify regions of pLB plasmid which flank shRNA inserts (pLB external) or which require presence of insert encoding 8226 V1 shRNA for the reaction to occur (pLB internal, or internal/external). B) Similarly, plasmid DNA for pLKO.1 Wil V1 was screened using a forward primer to Wil V1 construct and a reverse primer for pLKO.1. In plasmids containing the inserts a 250 bp band was produced.
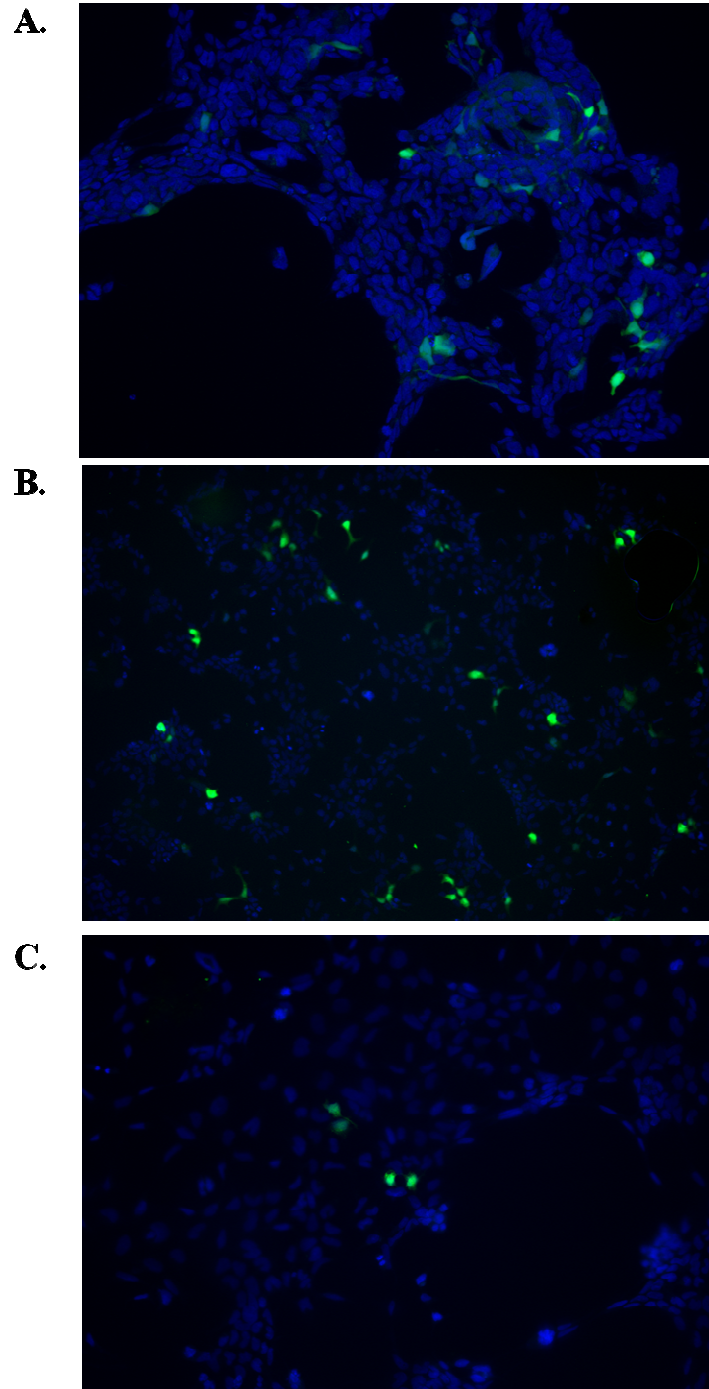
Figure 6.6 Transduction of HEK 293t Cells with Lentivirus Supernatants Results in Expression of EGFP. Supernatants (2 mL) from co-transfected HEK 293 cells along with 10 µg/ml polybrene were used to infect naïve HEK 293 cells with lentiviral particles expressing A) empty pLB vector B) pLB 8226 V1 or C) pLB Wil V1 shRNAs

A lack of fluorescence was observed in cytospin preparations of either myeloma cell line. Plasmids used in preparing viral particles were sent to the UT Viral Vector Core Facility for generation of high titer viral vectors.

6.4 Discussion

While both vectors pLKO.1 and pLB were amenable to the generation of lentiviral vectors, it was decided to utilize vector pLB for these studies due to the presence of a CMV driven EGFP reporter protein, allowing for easy identification of transduced cells by flow cytometry, fluorescence microscopy, or immunohistochemical detection of EGFP. Digestion and ligation of vectors to shRNA constructs provided an ample number of transformed colonies from which to generate starting materials. Purification of plasmids from these bacteria proved difficult, however, and was unsuccessful using a variety of plasmid mini-, and midi-prep kits. Of these methods, a straightforward phenol chloroform reaction provided the best results and was adopted over the previously used Qiagen midi-prep kit for purification of plasmid DNA.

Plasmid functionality was tested in two ways; first, by transfection of HEK293t cells with pLB based plasmids to show EGFP expression and by co-transfections to generated infective lentiviral particles. Transfection of kidney cells with either shRNA-expressing or empty expression plasmid of the kidney line HEK293t was successful in generating a large population of cells which were positive for EGFP, although similar treatment of myeloma lines failed to replicate this response. The ability of each of the pLB constructs to produce viral particles was successful, and demonstrated that these particles could infect naïve HEK293t cells. While not as striking, a few SP2/O-λ6 and RPMI 8226 cells were seen to express EGFP following exposure to

virus. The relatively lower efficiency of transduction was thought to be a consequence of using low titer amounts of virus, although reasons for this were not examined further.

These studies provide evidence that a functional lentiviral particle which encodes a construct for the expression of an anti LC shRNA molecule can be generated. Further, these materials were used by the UT Viral Vector Core Facility to generate a high titer (1 x 10^9 infectious units/ ml) production run of lentiviral particles containing empty pLB expression vector or pLB vectors expressing 8226 V1 or Wil V1 shRNAs.

Chapter 7

Transduction of myeloma cell lines with shRNA expressing lentiviral particles

7.1 Introduction

Previous work has shown that production of toxic LC species can be reduced by delivery of synthetic siRNA molecules to human and mouse myeloma lines (Chapter 6). Exposure of cultured cells to siRNAs directed against their LC product in the presence of lipid based transfection reagents resulted in decreased LC mRNA and protein, without reducing cell number or viability (Chapter 6). These responses were transient, however, and lipid based media are not easily adaptable for administration *in vivo*. To address this, an alternate means of delivering silencing RNAs was explored. Short-hairpin RNAs (shRNA) that mimic the naturally occurring RNA substrates (i.e., endogenous siRNAs, pre-miRNAs) for the enzyme Dicer are effective in reducing protein production (For review see Chapter 1.1). These shRNAs are synthesized as a single-stranded RNA transcript which self-anneals to form the characteristic stem-loop structure of shRNAs and include 3'-2 nt overhanging regions (for illustration see Chapter 1, Figure 1.3). As these molecules do not require post-transcriptional modifications by the cell to function they are amenable to incorporation into plasmids such as those found in retro- or lentiviral expression systems (171). Packaging of these expression constructs into non-replicative viral particles affords an effective means of delivery to eukaryotic cells both *in vitro* and, to a limited extent, *in vivo*. Exposure of cells to these particles which encode targeted shRNAs resulted in a stable reduction of target gene products (171, 216).

Stable transduction of myeloma lines has been demonstrated using lentiviral expression systems in several studies although none have targeted products of LC genes specifically (213, 217, 218). Based on our earlier data demonstrating transient knockdown of LC genes by siRNAs (Chapter 5) we posit that lentiviral mediated delivery of a shRNA-expressing plasmid to myeloma lines will reduce target LC production, and that this approach may offer the advantage of more robust, stable, and long-term knockdown of LC gene products as compared with gene silencing using synthetic siRNAs.

To test this hypothesis, the siRNA sequences Wil V1 and 8226 V1 (previously shown effective in reducing LC production – Fig 5.5) were adapted for expression as shRNAs. These constructs were then cloned into lentiviral expression plasmids containing an EGFP reporter construct. Plasmids were first shown capable of expressing EGFP in the human embryonic kidney line HEK293 and were later packaged by the Viral Vector Core Facility into replication incompetent self inactivating (SIN) lentiviral particles.

Exposure of the human myeloma line RPMI 8226 to increasing amounts of either 8226 V1 shRNA-expressing or empty vector lentiviral particles resulted in a mixed population of transduced cells as measured by EGFP expression and the presence of green fluorescence in the cells. Several clones were generated from these initial transduction which were shown to be >95% positive for EGFP expression. Measurement of LC secretions from supernatants of clonal populations demonstrated reduced levels of LC mRNA and protein as compared with untreated 8226 and empty vector control treated cells.

7.2 Methods

Cells

SP2/O-λ6 and RPMI 8226 cells were maintained as described in Chapter 3.1. During sub-cloning by limiting dilution cell line RPMI 8226 was maintained in an enriched DMEM-F12 based media which was supplemented with 20% filter-sterilized RPMI 8226 conditioned media (harvested from "heavy" 8226 culture after centrifugation) as well as 15% FBS, 0.2 μg/ml human insulin, and antibiotics (penicillin, streptomycin, gentamicin).

Lentiviral Vectors

The SIN lentiviral expression plasmid pLB was acquired from AddGene plasmid repository (vector11619) (593). Plasmids were subjected to digestion by the restriction enzymes NotI and XhoI. DNA sequences encoding shRNAs directed against the λ2 LC 8226 or the λ6 LC Wil were ligated to linearized expression plasmid (Chapter 3.7). ShRNA-encoding expression plasmids were purified using Qiagen plasmid Midi-Prep kit (Chapter 3.4) and supplied with the pLB (without inserts) to the UT Viral Vector Core Facility (University of Tennessee Health Science Center, Memphis, TN) for packaging as VSVG-pseudotyped lentiviral vectors in viral particles. Preparations of virus were returned for analysis with titers of 1 x 10^9 infectious units (IFU) per mL (219).

Transduction of myeloma cell lines

Cells were counted by hemacytometer and collected by centrifugation (600 x g for 5 min). Cells were added to each well of a 24-well microplate at a concentration of 1 x 10^6, for low multiplicity of infection (MOI) exposure, or 1 x 10^5 cells per well for high MOI exposure in 1 ml

antibiotic-free DMEM F-12 containing 5% fetal bovine serum and 10 µg/ml polybrene. Viral particles ranging from 0.05×10^6 - 1×10^7 IFU were added to each well and cells were incubated for 6 h at 37°C under 5% CO_2. Cells were collected by centrifugation at 500 x g for 5 min and washed 3x in fresh DMEM F-12. Cells were resuspended in growth media and returned to incubator for 24-72h.

Generation of clonal myeloma populations by limiting dilution.

8226 cells were infected with either 8226 V1 shRNA-expressing virus or those containing the empty pLB vector as a control. Cell cultures shown positive for EGFP expression by fluorescent microscopy were counted by hemacytometer and collected by centrifugation (600 x g for 5 min). For limiting dilution cloning, a sample of 1×10^5 8226 cells was resuspended in 1 mL fresh DMEM F12 containing 5% FBS and penicillin/streptomycin, or 15% FBS, 0.2 mg/ml human insulin, and 20% conditioned media. In each case, 200 µl of 8226 cells in suspension was added to each well of the first column of a tissue culture-treated 96-well microplate (BD Falcon). A 1:1 serial dilution (100 µl cells) was then diluted across each plate. Cells were housed in a humidified incubator at 37°C under 5% CO_2 for 4-6 weeks. Wells were observed for colony formation, and screened for EGFP expression by fluorescent microscopy. Colonies found to be positive for EGFP fluorescence were further re-cloned or expanded by growth in 24 well plates, then 6 well plates.

Flow Cytometry

Cells transduced with pLB vectors were analyzed for expression of EGFP by flow cytometry. Cells were counted, collected by centrifugation, and washed 3x in PBS containing 1% bovine

serum albumin. Cells were then resuspended in PBS/BSA and cell size, complexity, and fluorescence were analyzed on FACScan flow cytometer (BD Biosciences).

To detect LC expression, cells were harvested and washed as above, then fixed for 20 min using BDcytofix solution followed by permeablization using BDcytoperm buffer (Beckton Dickson). Human λ LC was detected using an Alexa594-conjugated rabbit anti-total human lambda polyclonal IgG (Invitrogen). Antibody was diluted 1:2000 in BDcytoperm and incubated with cells for 1h at room temperature. Cells were washed 3x as above and analyzed by FACS. Regions of interest were drawn around populations of untreated cells, and no fewer than 5,000 events were collected for analysis.

Analysis of LC expression by ELISA

Secreted λ LC was detected from cell supernatants using either Total human λ ELISA A or total human λ ELISA B as indicated. For detailed descriptions please see Chapter 3.9.

Real Time PCR

Levels of LC mRNA were assessed using real time PCR analysis of cDNA acquired by reverse transcriptase of total RNA extracted from 8226 cells following the protocol found in Chapter 3.5.

Statistical Analysis

Data concerning LC production from ELISAs were pooled, entered into GraphPad Prism version 4 (GraphPad Software, Inc.) and analyzed for statistical significance by One-Way ANOVA. Dunnett's Multiple Comparisons test was used to determine which groups were significantly different as compared to controls.

7.3 Results

Transduction of cell line 8226

By 24 h, exposure of 8226 cells to increasing titers (MOI 0.5, 1, 2.5, 5, 10) of lentiviral vectors encoding shRNA 8226 V1 yielded a corresponding increase in the proportion of cells expressing EGFP as measured by flow cytometry (Figure 7.1). Following initial evaluation, transduced cells were expanded to 10 ml tissue culture flasks and maintained under standard conditions. Cells were re-evaluated repeatedly up to14 d by flow cytometry and showed slight variances in the population of positive cells as compared with analysis at 24 h. While EGFP positive cells were still observed in cultures exposed to 0.5-5 MOI lentivirus a slight decreases the proportion of EGFP expressing cells was seen, while those transduced at an MOI of 10 demonstrated an increased number of positive cells as compared with samples taken at 24 h (Figure 7.2).

At 7 and 21 days post-transduction, 24 h cell culture supernatants from 8226 cells were collected and analyzed for secreted LC by ELISA. Analysis of cell supernatants on day 7 demonstrated a trend toward reduced LC secretion in cells exposed to shRNA expressing lentiviral vectors as compared with untreated 8226 cells. In supernatants from cells exposed to MOI values of 0.5, 1.25, and 2.5, secreted LC was found at 89, 79, and 62% of that seen in untreated control cells. Supernatants from cells exposed to MOI 5 or 10 contained LC levels 74% and 83% of untreated control cells. As cultures were sparse on d 7, only single replicates of wells were prepared so no statistical analysis was performed (Figure 7.3 A).

When experiments were repeated on d 21 a similar trend was observed with supernatants from cells exposed to MOI 0.5, 1.25, and 2.5 pLB 8226 V1 lentiviral vectors with 73%, 75%, and 89% levels of LC protein as compared to that found in untreated 8226 cells, while those exposed to
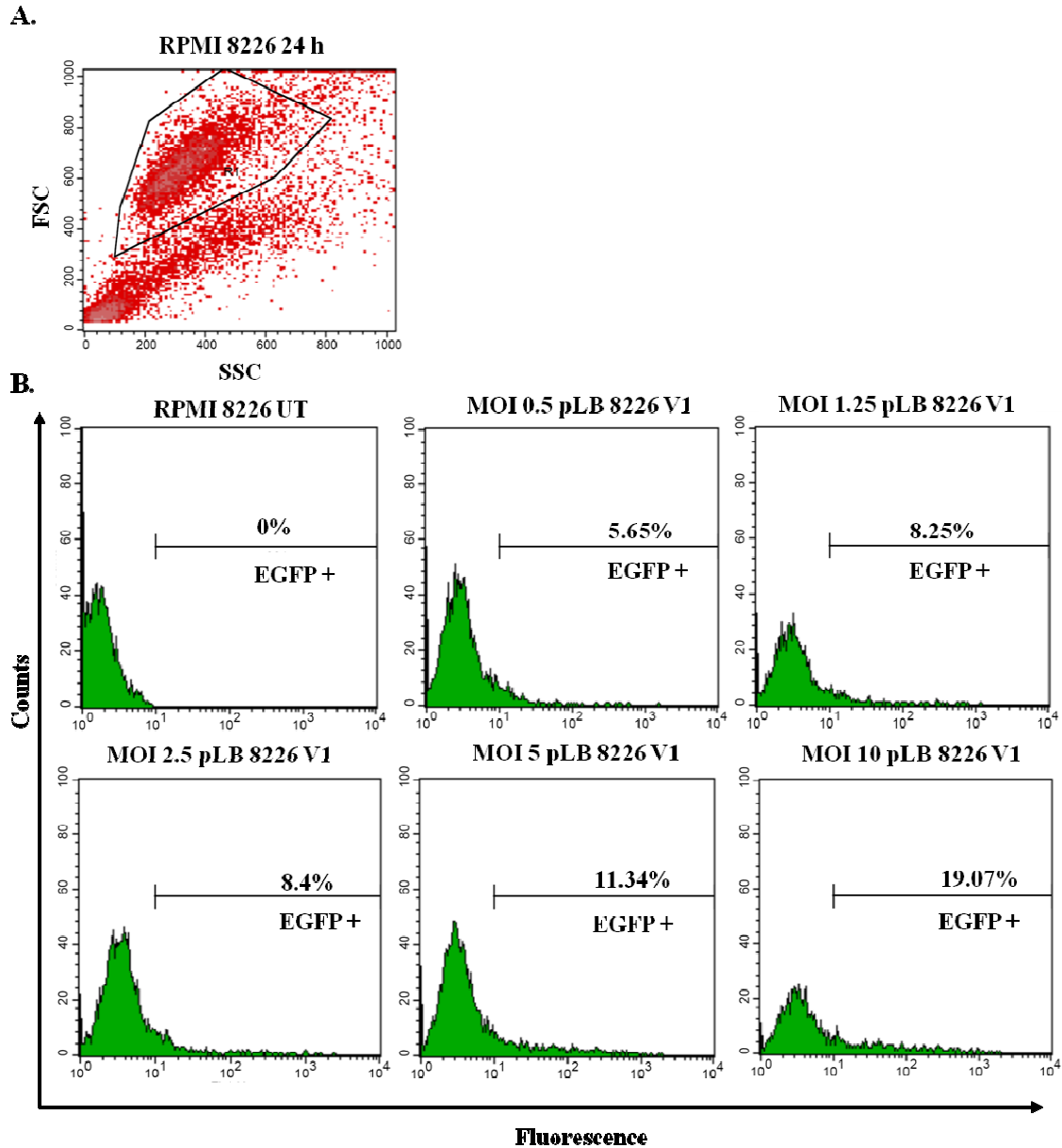
Figure 7.1. Evaluation of enhanced green fluorescent protein at 24 h following exposure to pLB 8226V1 expressing lentiviral particles. RPMI 8226 cells were plated at 1×10^6 cells per well along with increasing amounts of viral titer in presence of polybrene. 6 h following transduction cells were washed and cultured overnight before samples were analyzed for EGFP by flow cytometry. A) Forward (FSC) and side scatter (SSC) analysis of untreated 8226 cells were used to generate regions of interest. B) Markers were drawn to exclude negative cells on channel FL-1 allowing for selection of cells positive for EGFP expression. Viral titer is noted at top of histogram while percentage represents the proportion of positive cells in each culture.
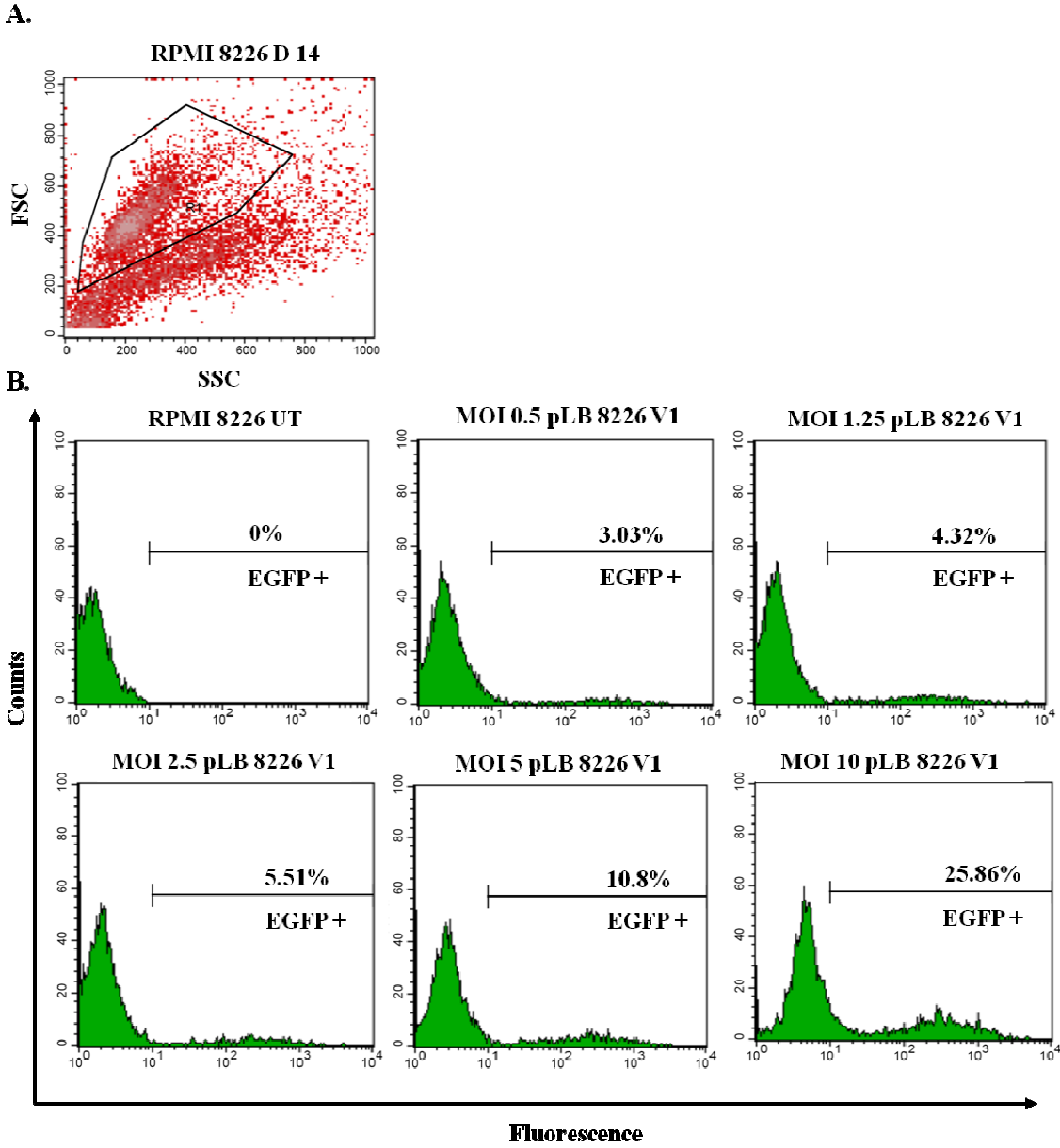
Figure 7.2. Evaluation of enhanced green fluorescent protein 14 d following exposure to pLB 8226 V1 expressing lentiviral particles. pLB 8226 V1 transduced 8226 cells were held in culture for 14 d. A) Forward (FSC) and side scatter (SSC) analysis of untreated 8226 cells were used to generate regions of interest. B) Markers were drawn to exclude negative cells on channel FL-1 allowing for selection of cells positive for EGFP expression. Viral titer is noted at top of histogram while percentage represents the proportion of positive cells in each culture.

A.

Day 7

B.

Day 21
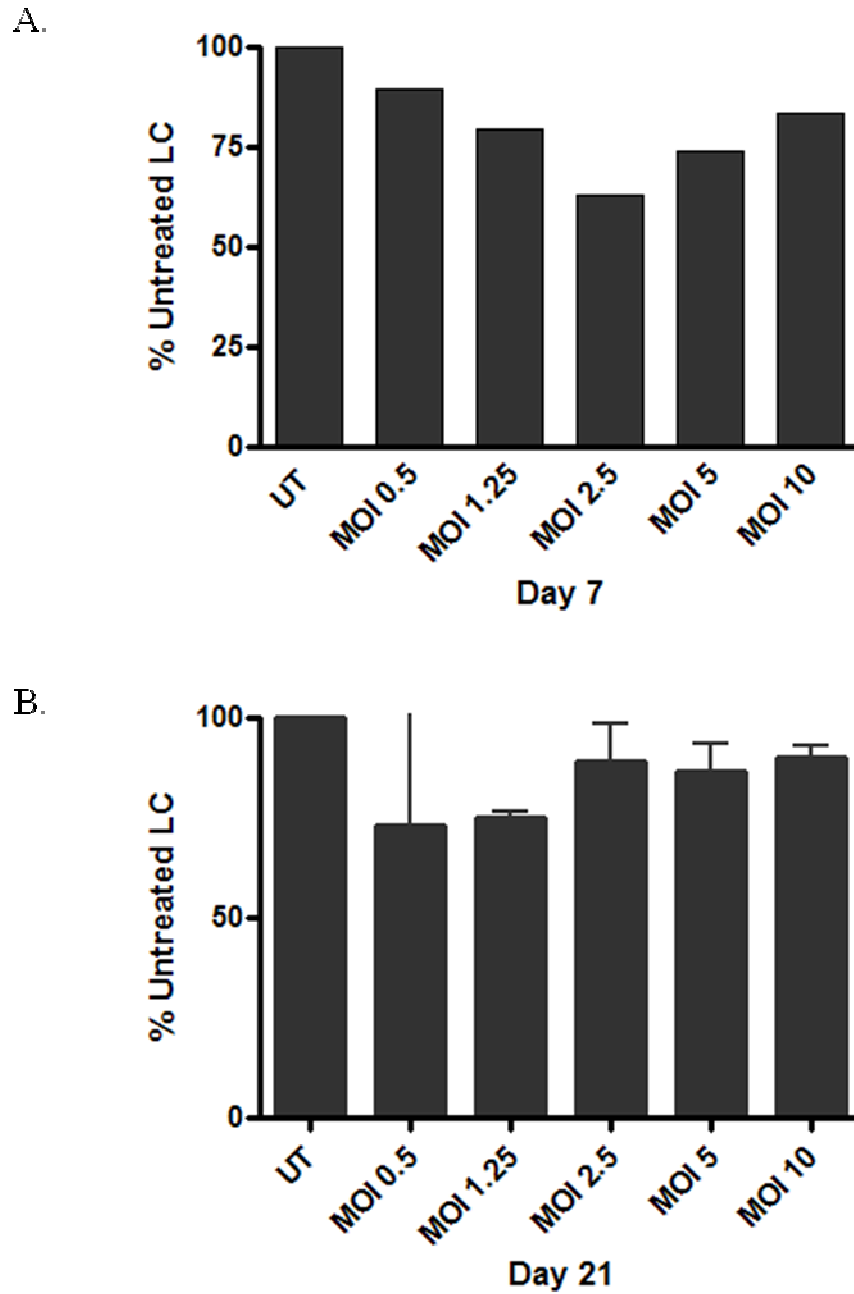
Figure 7.3 Secreted LC from 8226 cells exposed to pLB 8226 V1 lentiviral vectors. At A.) 7 (n=1) and B.) 21 d (n=3) following transduction with increasing concentrations of lentivirus pLB 8226 V1 cells were cultured and supernatants analyzed for secreted LC by ELISA. Data were expressed as percent untreated 8226 LC and at d 21 data were analyzed by One-way ANOVA (* denotes significance; $p < 0.05$)

MOI 5 or 10 of the same viral construct were shown to contain 86 and 90% of controls, respectively (Figure 7.3 B).

To test whether exposure to higher levels of virus would improve results viral titers were raised 10-fold by reducing the number of 8226 cells plated from 1×10^6 - 1×10^5 cells per well while retaining the amount of virus added (Figure 7.4 A-B). Additionally, cells exposed to lentiviral particles containing empty expression vector pLB were included in these experiments (Figure 7.4 C).

In cells that received a 10-fold increase in viral particles, no corresponding increase in EGFP-positive cells was observed. The singular exception to this was seen in cells exposed to an MOI 50 of pLB 8226 V1 lentiviral particles, and in this case the increase was modest (30% v. 25%) when compared with cells previously exposed to the same particles at an MOI of 5 (Figure 7.1). These results were mirrored in 8226 cells which received empty pLB vector bearing particles with 31% of these cells considered positive for EGFP expression at 24 h.

Similar to cells transduced with lower titer shRNA-expressing lentiviral particles, cells from the high MOI treatment group were plated to 24-well plates at 2×10^5 in fresh media and incubated overnight at 7 d post-transduction. The following day, supernatants were harvested and secreted LC was measured by ELISA. Significantly ($p<0.05$) reduced amounts of LC protein were found in cells which had received lentiviral particles at MOI of 10 (42% decrease) and 50 (41% decrease) as compared with those treated with particles containing empty pLB plasmid (vector control) (Figure 7.5). The cells treated with an MOI of 25 showed reduced LC secretion relative to empty vector control cells, but this change did not reach significance (Figure 7.5).

A.

RPMI 8226 24 h

B.

RPMI 8226 UT

1.04%

EGFP +

MOI 10 pLB 8226 V1

5.64%

EGFP +

MOI 25 pLB 8226 V1

15.04%

EGFP +

MOI 50 pLB 8226 V1

30.02%

EGFP +

C.

**MOI 50 pLB Empty**

31.87%

EGFP +
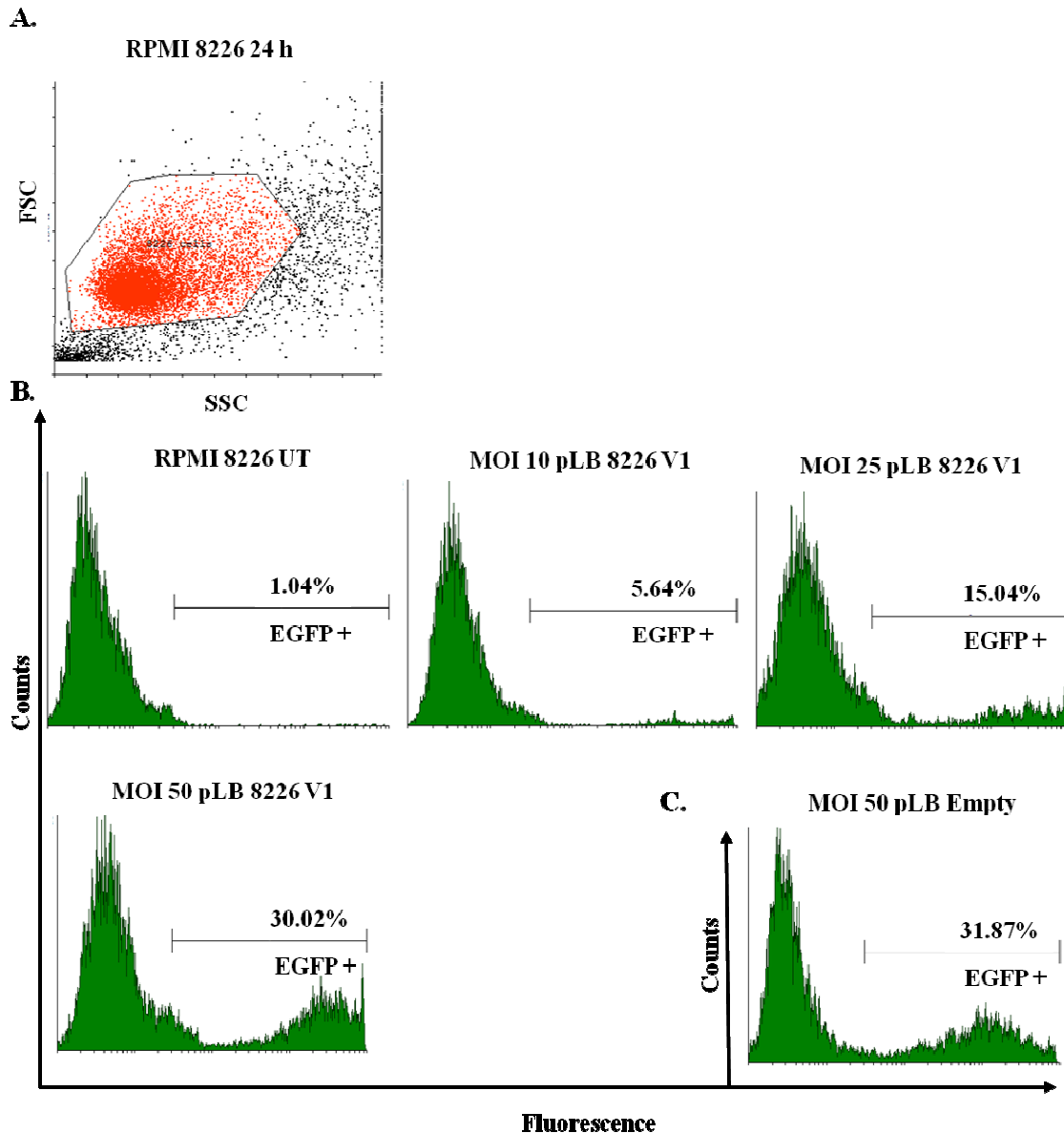
Fluorescence

Figure 7.4. Evaluation of enhanced green fluorescent protein 24 h following exposure to high MOI pLB 8226 V1 or control lentiviral particles. RPMI 8226 cells were exposed to 10-fold higher amounts of lentiviral particles and evaluated for EGFP expression at 24 h. A) FSC and SSC profiles of untreated 8226 cells cultured under similar conditions to those exposed to viral vectors were used to draw regions around cell populations. B) Untreated cells were used to set marker regions for cells considered positive for EGFP. Each panel represents an individual transduction experiment, in which cells were exposed to shRNA expressing lentiviral particles at increasing MOI. Percentages above marker region represent the proportion of EGFP positive cells from the total population. Similarly, in C) 8226 cells were exposed to viral particles encoding empty pLB expression vector.

120
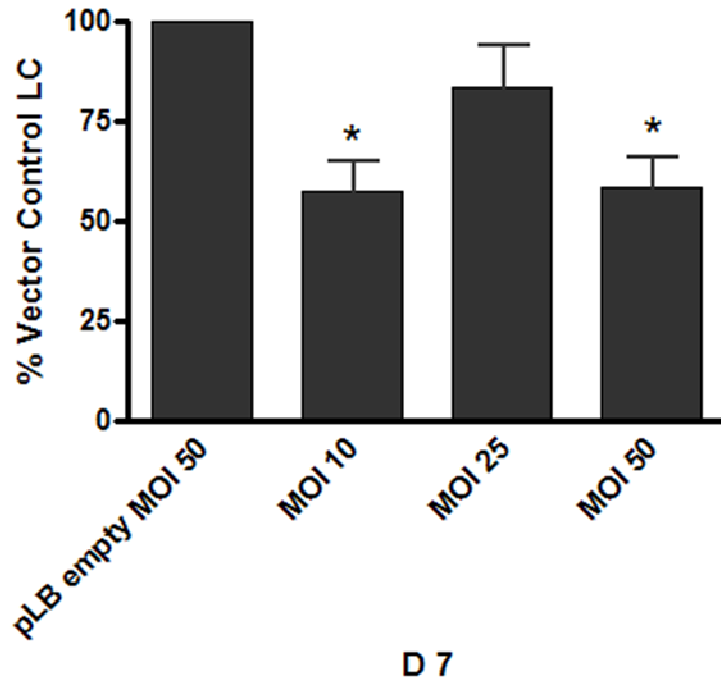
Figure 7.5 Exposure to higher levels of shRNA expressing lentiviral particles. RPMI 8226 cells exposed to either MOI 10 or 50 shRNA 8226 V1 expressing lentiviral particles demonstrated a significant (n=3; *denotes significance $p < 0.05$) reduction in secreted LC protein as compared with control cells which had received MOI 50 lentiviral particles when analyzed by One-way ANOVA.

Transduction of cell line SP2/O-λ6

Initial transductions of the cell line SP2/O-λ6 were performed using lower concentrations of lentiviral particles. Surprisingly, analysis of the transduced cells 24 h post exposure revealed no EGFP expression in the cells even at the highest concentrations of virus used in this study (i.e., MOI 5-10) (Figure 7.6). Following this, SP2/O-λ6 cells were plated at a lower number of cells per well (1 x10^5 cells) and were exposed to 10-fold increased amounts of pLB Wil V1 virus from a new, unopened stock.

As with the earlier results, SP2/O-λ6 cells receiving Wil Vλ lentivirus at MOI 12.5 and 25 demonstrated no increase in fluorescence as compared with controls (Figure 7.7 A-B). Those receiving viral particles at an MOI of 50 demonstrated a small population (1.8 v. 0.9%, respectively) of cells exhibiting an increased fluorescence as compared to controls. It was only when cells were exposed to the highest amount of virus tested in these studies, MOI 100, that a substantial (6.87%) population of cells were evidenced by EGFP expression (Figure 7.7 B). Examination of FSC and SSC for this population also revealed an increased number of dying cells as assessed by size and complexity (Figure 7.7 C).

To determine if the differences observed in transduction efficiency as compared with the 8226 line were a function of the SP2/O-λ6 line, or the pLB Wil V1 virus a series of cross exposure experiments were conducted. In the first series of studies, SP2/O-λ6 cells were plated as above and received either lentiviral vectors expressing pLB 8226 V1 plasmid or empty pLB plasmid at an MOI of 50, followed by analysis by flow cytometery. Evaluation of those exposed to pLB 8226 V1 revealed 12.33% of cells expressing EGFP, while exposure to the same levels of particles expressing pLB empty vector resulted in 1.25% of the population being positive for green fluorescence (Figure 7.8 A-B).
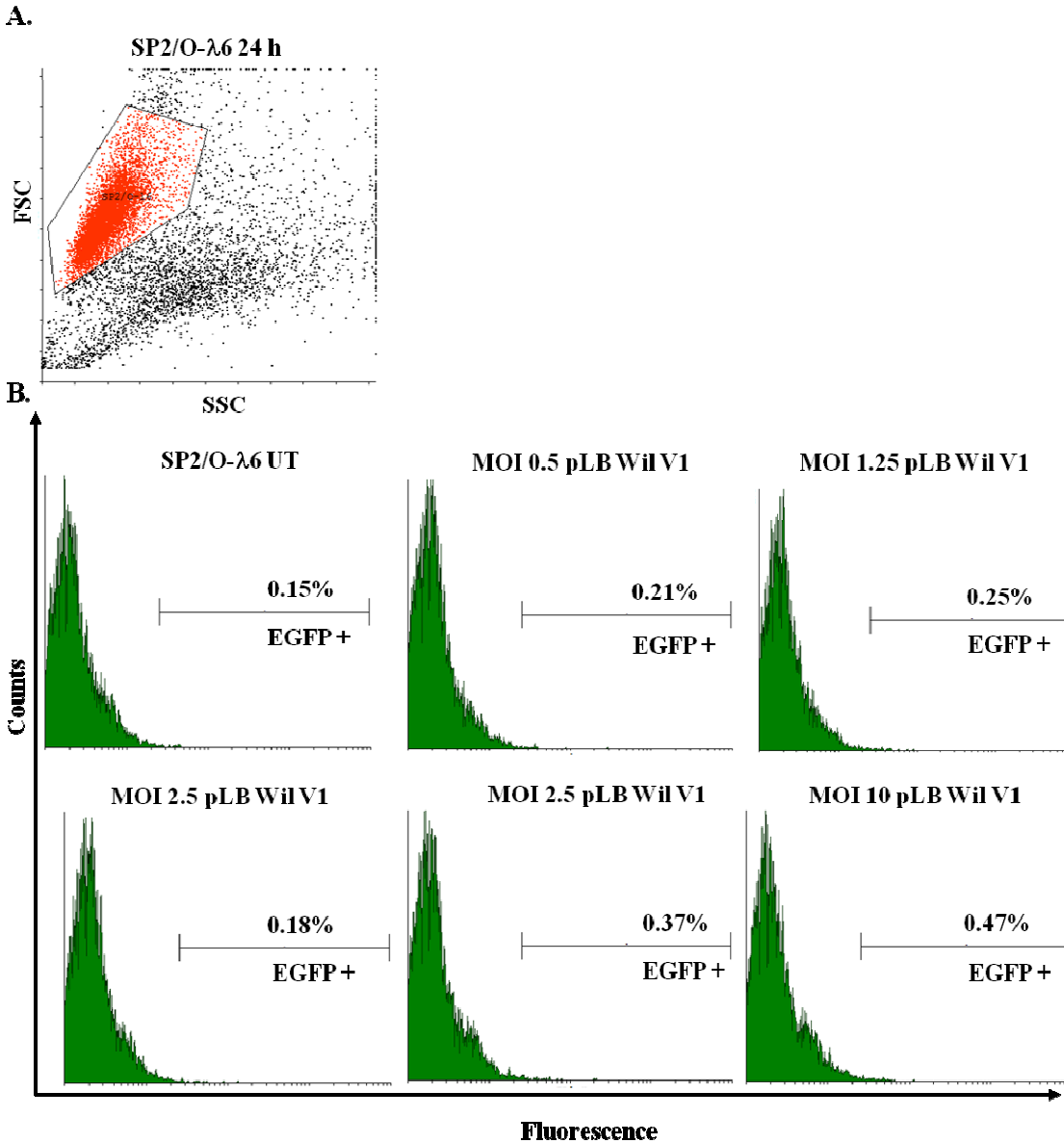
Figure 7.6 Evaluation of enhanced green fluorescent protein 14 d following exposure to pLB Wil V1 expressing lentiviral particles. pLB Wil V1 transduced SP2/O-λ6 cells were held in culture for 14 d. A) Regions of interest were drawn based on FSC and SSC profiles of untreated SP2/O-λ6 cells. B) Evaluation of fluorescence from untreated populations was used to generate a marker region to exclude negative cells on channel FL-1. Panels illustrate EGFP expression from untreated or treated cells. Viral titer is noted at top of histogram while percentage represents the proportion of positive cells in each culture.
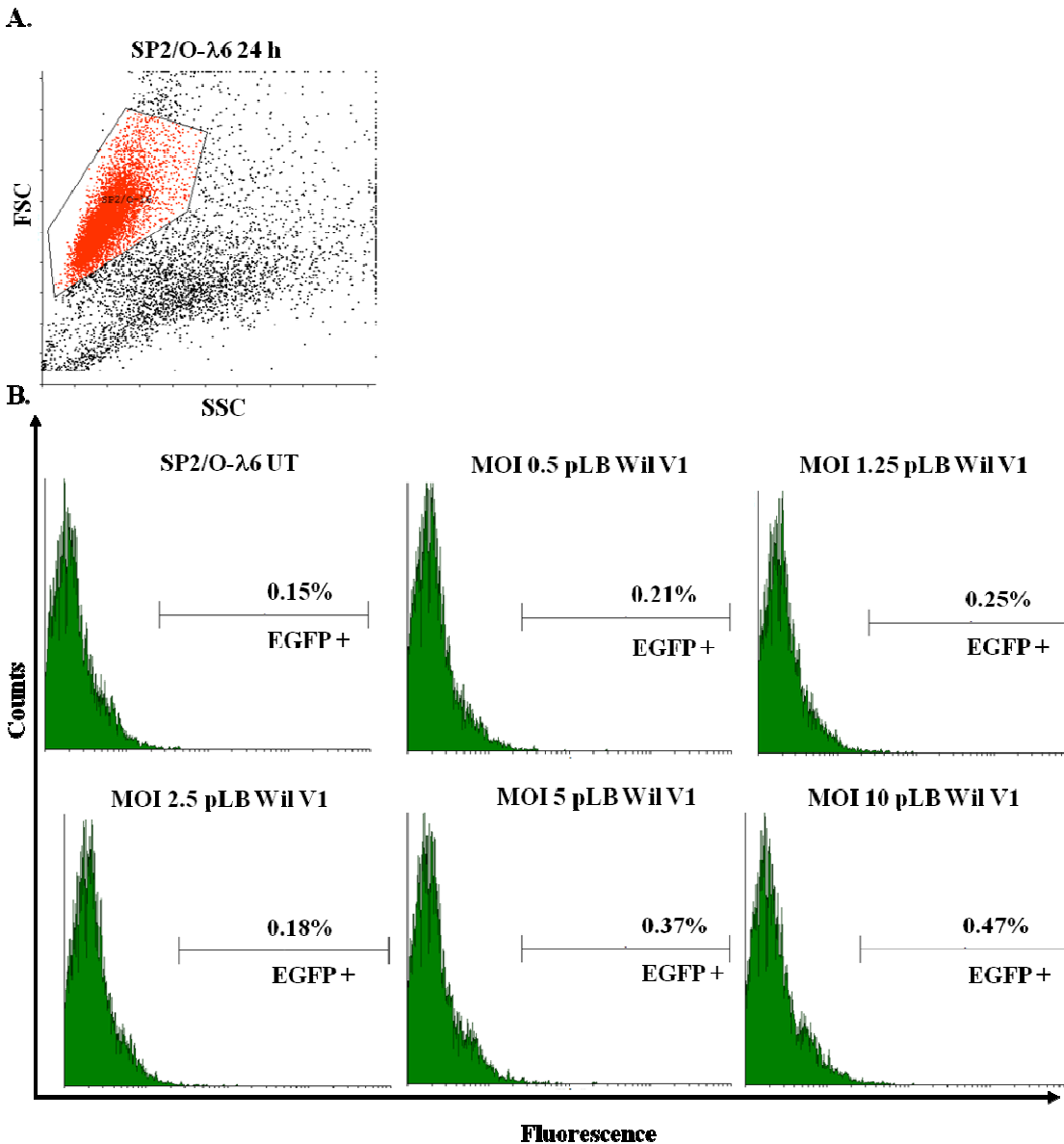
Figure 7.7 Evaluation of enhanced green fluorescent protein 24 h following exposure to high MOI pLB Wil V1 lentiviral particles. SP2/O-λ6 cells were exposed to 10-fold higher amounts of lentiviral particles and evaluated for EGFP expression at 24 h. A) FSC and SSC profiles of untreated SP2/O-λ6 cells cultured under similar conditions to those exposed to viral vectors were used to draw regions around cell populations. B) Untreated cells were used to set marker regions for cells considered positive for EGFP. Each panel represents an individual transduction experiment, in which cells were exposed to shRNA expressing lentiviral particles at increasing MOI. Percentages above marker region represent the proportion of EGFP positive cells from the total population. C.) FSC and SSC profiles of SP2/O-λ6 demonstrate an increased population of cells considered non-viable (Blue) with increasing concentration of viral particles.
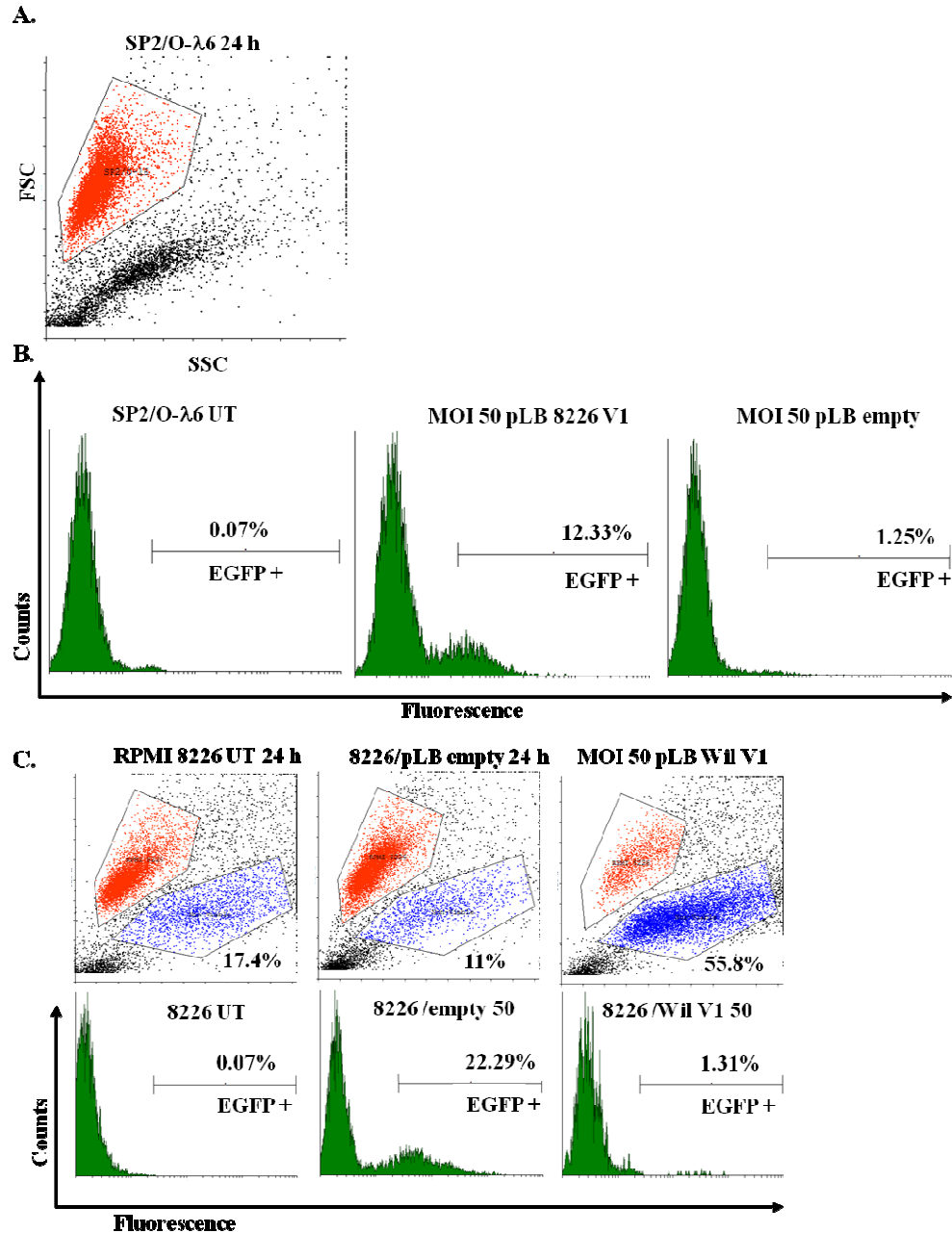
Figure 7.8 Evaluation of EGFP expression in SP2/O-λ6 and 8226 cells following exposure to pLB Wil V1, 8226 V1 or pLB empty lentiviral vectors. A.) FSC and SSC profiles of untreated SP2/O-λ6 cells were used to generate regions of interest. B.) To determine if lack of transfection efficiency was caused by lentiviral particles SP2/O-λ6 cells were exposed to either pLB empty or 8226 V1 lentiviral particles at MOI 50. Fluorescence was assessed at 24h by flow cytometry. C.) Lentiviral particles (MOI 50) encoding pLB Wil V1 were used to infect 8226 cells alongside pLB empty and pLB 8226 particles. Panels illustrate FSC and SSC profiles for each transduction experiment, with regions colored red considered the primary 8226 population while those in blue considered non-viable (denoted by percentages). Below, FL-1 profiles of cells following treatment, where percentages represent EGFP positive cells.

125

In a parallel series of experiments, the human myeloma line 8226 was exposed to viral particles

encoding pLB Wil Vλ (MOI 50), while cells exposed to particles encoding pLB vector were

used as a positive control population. From evaluation by flow cytometry it is evident that

transductions with the pLB empty vector viral particles was successful, with 22.29% of cells

expressing EGFP. Conversely, exposure to pLB Wil V1 resulted in a much lower proportion of

EGFP positive cells with only 1.34% of cells demonstrating increased fluorescence.

The difference in viability observed in cell line SP2/O-λ6 was also mirrored in 8226 cells

exposed to Wil Vλ viral particles where 55.8% of cells were considered non-viable as compared

with 11% and 17% in untreated and vector control treated cells, respectively (Figure 7.8 C).

Generation of stably transduced 8226 clones

While exposure to the 8226 line to shRNA expressing lentivirus produced a population of cells

positive for EGFP expression and elicited, a modest, but significant reduction in secreted LC

protein (Figure 7.4) it was of interest to know what the maximal level of LC silencing might be.

To approach this, samples of 8226 cells transduced with either pLB 8226 V1 or pLB empty

lentiviral expression systems were collected and clonal populations generated by limiting

dilution. For cells exposed to pLB 8226V18226 V1, 8 clones were generated which

demonstrated a >90% population of cells shown to express EGFP as measured by flow

cytometry (Figure 7.9). Likewise, 3 clones were generated from 8266 cells exposed to pLB

empty vector which were shown to exhibit equivalent levels of EGFP positive cells.

Initial screening of secreted LC protein from clones was measured following 24 hour incubations

in 24-well plates in 1 ml DMEM-F12 of 200,000 cells per well by using the total λ ELISA A

(Chapter 3.9). Analysis of ELISA results by One-way ANOVA demonstrate that clones

A.

8226 UT

82266 UT

0.17%

EGFP +

B.

13C7

97.2%

EGFP +

13C7 B

97%

EGFP +

13A3

95.5%

EGFP +

13A2

95%

EGFP +

13A5

95%

EGFP +

13B2

95%

EGFP +

13B9

98%

EGFP +

16B2

99%
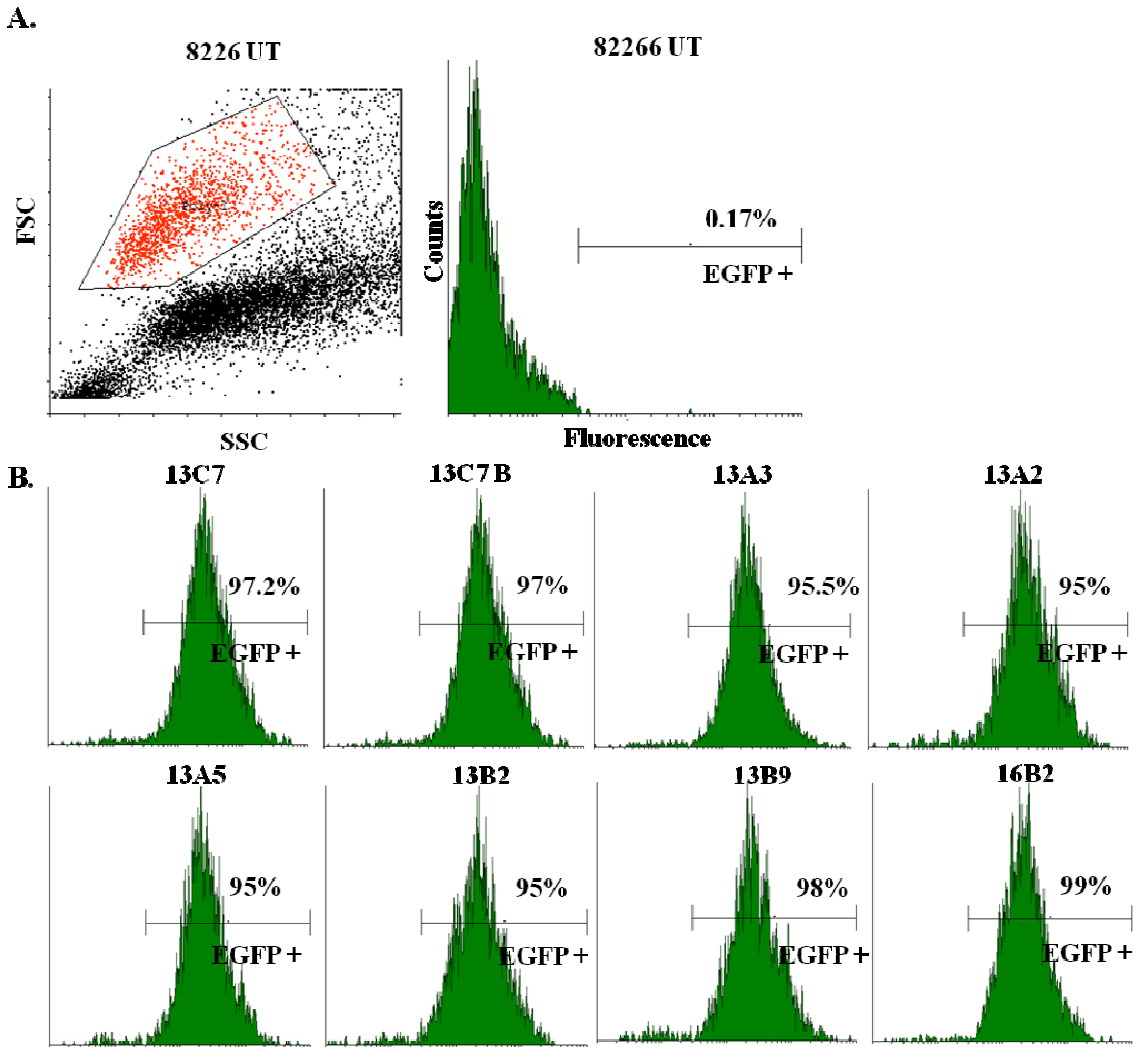
EGFP +

Figure 7.9 RPMI 8226 cells exposed to 8226 V1 shRNA bearing lentiviral particles were analyzed for EGFP expression by flow cytometry. A.) Regions of interest were drawn around populations of untreated 8226 cells based of FSC and SSC profiles. A Marker (EGFP +) was drawn on histograms based on fluorescence channel FL-1 to exclude negative cells. B.) Screening of 8226 clones from cells exposed to lentivirus pLB 8226 V1 (MOI 10) demonstrate a near homogenous population of cells expressing EGFP.

127

expressing the 8226 V1 shRNA produced a significantly reduced amount of LC 8226 with a mean ~20% of that seen with untreated control cells (n = 2; * p< 0.05). Of these, clones 13A2, 13B2, and 13A5 demonstrated the most striking reductions of secreted LC; generating 13%, 21%, and 22% of LC protein relative to untreated control cells. Following these, clones 13C7, 16B2, 13A3, and 13B9 also secreted significantly reduced (25% - 39%) amounts of LC protein as compared to untreated 8226 cells (Figure 7.10 A).

In contrast, with singular exception (clone E1D4), no significant reduction in secreted LC product was detected in clones generated from cells transduced with lentivirus bearing empty pLB vector (Figure 7.10 B). In clone E1D4, secreted LC product was found at levels which were reduced by 44% to those found in the untreated parental line, possibly owing to a general reduction in protein synthesis as a consequence of the site of insertion of the pLB construct within the DNA of this clone.

Cell growth and viability were assessed for individual clones following overnight incubation of 2×10^5 cells in fresh DMEM F-12 by trypan blue dye exclusion assay and counting on a hemacytometer. Analysis of these data by One-way ANOVA revealed no significant differences in the number of viable cells from treated or control population (Figure 7.11 A). However, the percentage of viable cells was slightly reduced (10%) in clone 13A2 as compared with the untreated 8226 line (Figure 7.11 B). Similarly, clones derived from empty vector treated cells showed no difference in cell number (Figure 7.11 C) or viability (Figure 7.11 D) as compared with untreated control cells.

From these initial characterization studies, three clones (13A2, 13C7, 16B2) were selected from the 8226 V1 shRNA-transduced group, and one (E1G3) from the pLB empty vector group and
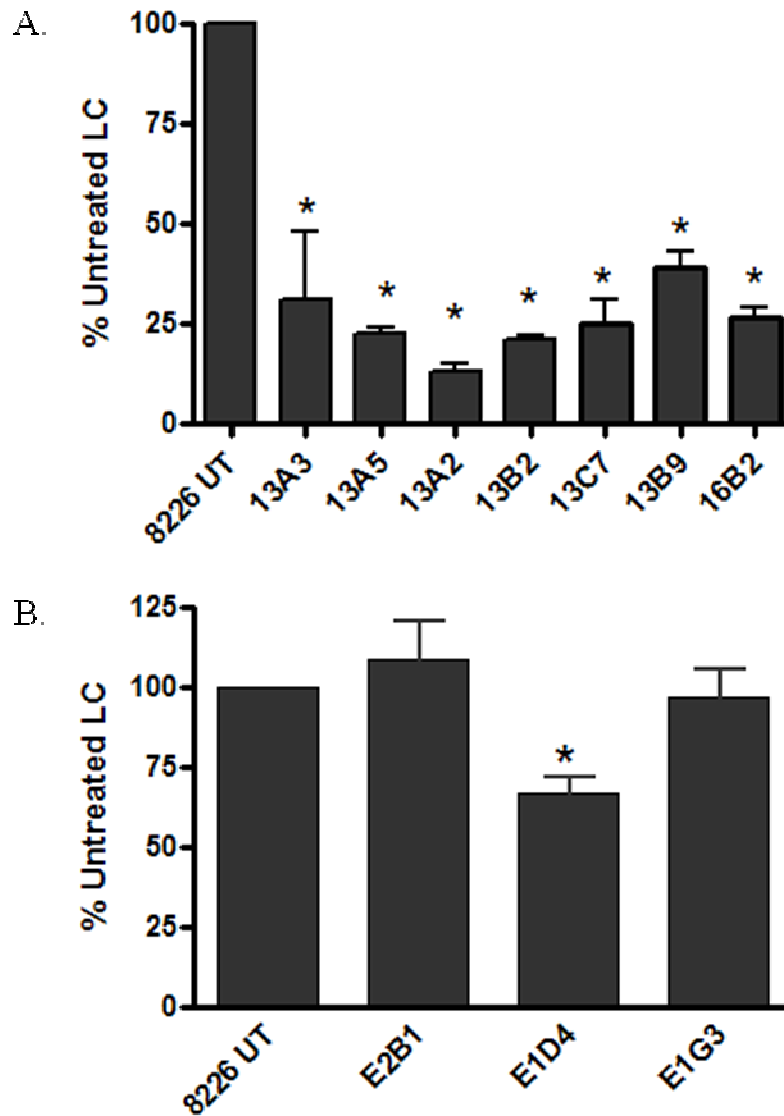
Figure 7.10 Measurement of secreted LC from lentiviral 8226 clones. Clones from 8226 cells exposed to A.) 8226 V1 shRNA (n=2) or B.) pLB empty (E2B1, E1D4 n=9; E1G3 n=18; 8226 UT n=15) lentiviral particles were cultured overnight in 24-well plates and secreted LC measured by ELISA and results expressed as percent LC as compared with 8226 UT. Results were analyzed for significant differences by One-way ANOVA and Dunnett's multiple comparison test (* denotes significance; $p < 0.05$).
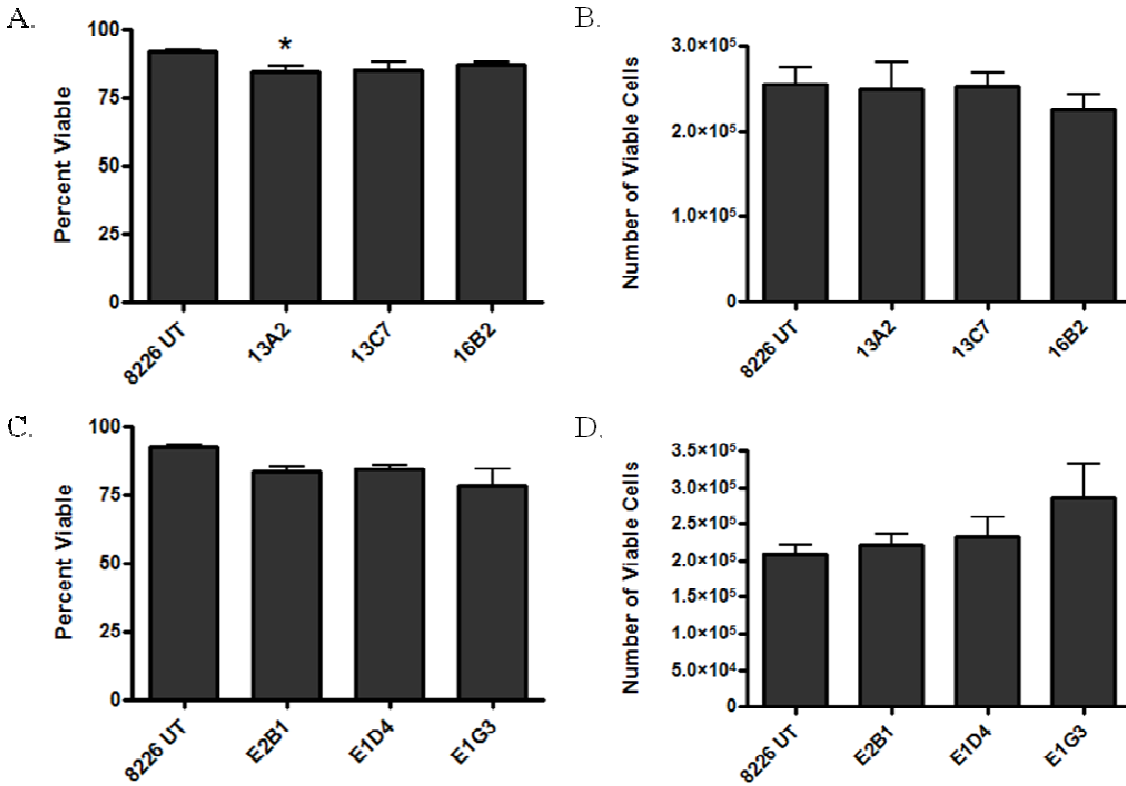
Figure 7.11 Cell number and viability of pLB 8226V1 and pLB empty clones following overnight incubation. Selected clones from cells exposed to either pLB 8226 V1 or pLB empty infected cells were plated at 2×10^5 cells per well in 24 well plates. The following day, cells were counted and viability assessed by trypan blue dye exclusion and counting on hemacytometer. Data were pooled and analyzed for differences using One-way ANOVA and Dunnett's Multiple Comparisons tests (n=9; * denotes significance $p < 0.05$) A.) No differences were found in clones 13C7 or 16B2, while clone 13A2 was found to have a slight (10%), but significant decrease in viability as compared with untreated cells. B) no differences were found in cell numbers of clones exposed to pLB 8226 V1 as compared with untreated cells. Likewise, no differences were found in C.) viability, or D.) number in cells exposed to pLB empty vector as compared with controls.

were maintained under standard conditions (Chapter 3.1), while the remaining clones were stored at -80°C.

LC mRNA levels

For the shRNA 8226 V1 expressing clones 13A2, 13C7, and 16B2 and clone E1G3, derived from cells transduced with the empty pLB vector, total RNA was extracted and analyzed for relative LC 8226 gene expression by real time PCR using primers specific to LC 8226, while human β-actin served as a reference gene (Chapter 3.5) (Figure 7.12 A). As compared to untreated 8226 cells, samples collected from clones 13A2, 13C7, and 16B2 demonstrated significantly reduced (25, 30, 45%, respectively) levels of LC 8226-encoding messenger RNA as compared to the parental 8226 line. In contrast, no differences were found in cells from group E1G3 as compared to untreated cells.

Secreted LC protein

As before, clones 13A2, 13C7, 16B2 were transferred to individual wells of a 24-well plate in 1 mL fresh media. Untreated 8226 cells and the empty vector clone E1G3 were cultured alongside shRNA-expressing clones and served as untreated and vector controls, respectively. Following a24 h incubation, cells were harvested and supernatants analyzed for human LC, this time, because of technical difficulties with total λ ELISA A, using total λ ELISA B (Chapter 3.9). Data were expressed as percent untreated 8226 LC and analyzed by one-way ANOVA. As with the previous ELISA (Figure 8.10), 8226 shRNA clones were shown to produce significantly reduced levels of LC 8226 as compared with controls (n = 9; p >0.01). As shown in Figure
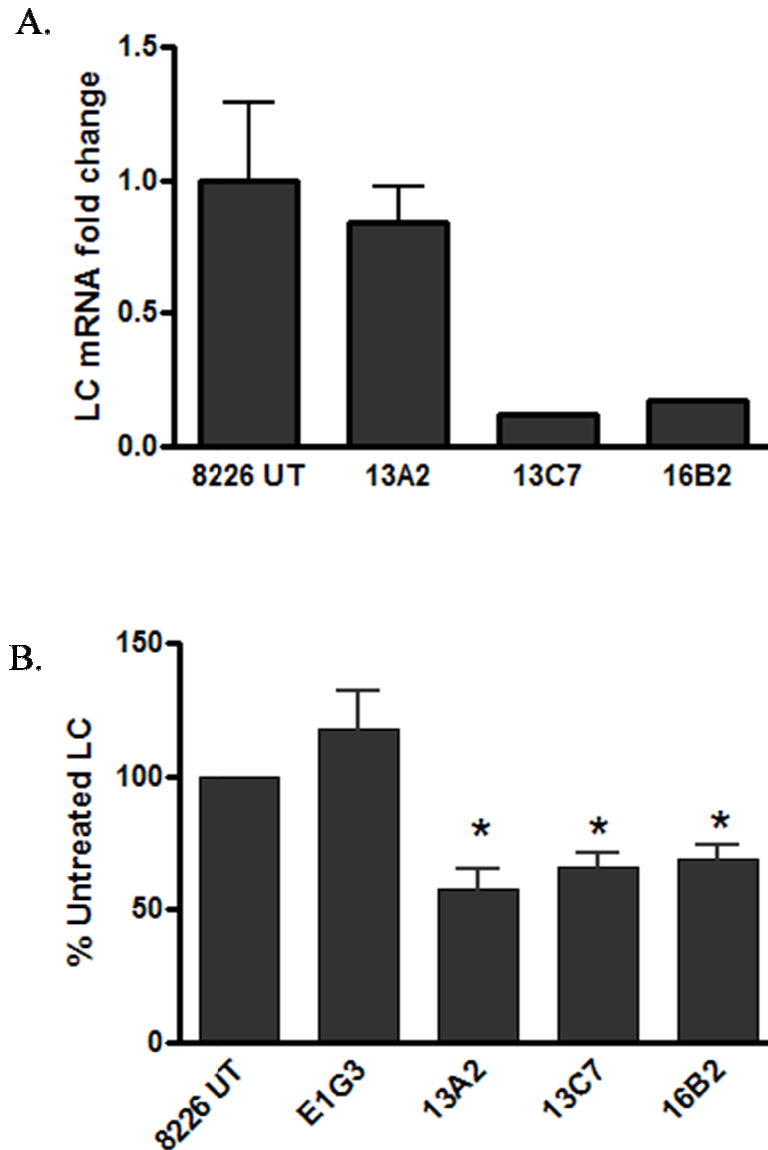
Figure 7.12 Real time PCR analysis of LC 8226 mRNA and ELISA analysis of protein LC 8226 in clones exposed to either pLB 8226 V1 or pLB empty lentiviral particles. A.) Clones from cells exposed to 8226 V1 shRNA expressing lentiviral particles were evaluated for LC 8226 gene products by Real-time PCR, and demonstrate a trend towards reduced LC 8226 mRNA levels (n=3). B.) To confirm earlier ELISA results, clones were cultured overnight and supernatants analyzed using total λ ELISA B. Results were expressed as percent untreated 8226 LC and analyzed by One-way ANOVA and Dunnett's Multiple Comparisons test (n=9; * denotes significance p < 0.01). Clone E1G3 was generated from 8226 cells receiving pLB empty lentiviral particles and demonstrates no differences in secreted LC protein as compared with controls. Whereas, clones 13A2, 13C7, and 16B2 demonstrate significant reductions in LC as compared with untreated 8226 cells.

7.10, supernatants taken from wells containing clones 13A2, 13C7, and 16B2 had LC protein levels that were reduced by 58%, 66%, and 70% as compared to the untreated parental 8226 line. As expected, no difference was detected in LC concentrations from supernatants collected from wells containing clone E1G3 as compared with untreated 8226 cells (Figure 7.12 B).

7.4 Discussion

Transduction of myeloma cell lines

As shown in Chapter 6, the introduction of synthetic siRNA molecules which are designed to target products of the LC gene to the human myeloma line 8226 and the mouse myeloma line SP2/O-λ6 resulted in reductions of LC protein. While significant, these reductions were transient, and levels of LC protein and messenger RNA recovered by ~ 72 h post transfection. In addition, the chemical transfectants utilized in these experiments are not amenable for administering siRNAs *in vivo.* To address these issues, several options were considered for delivery of silencing RNAs. A review of the literature revealed several publications in which viral vectors were used to deliver shRNAs to B-lineage cells or for inducing RNAi *in vivo* (212, 220, 221). From these searches it was found that in a comparison among viral vectors systems based on lentiviral particles were most successful at transducing human myeloma lines *in vitro* (213). Further, in a biodistribution study it was reported that mice receiving EGFP expressing lentiviral particles demonstrated presence of expression cassettes in both primary bone marrow stem cells and populations of circulating B-cells (214). Based on these earlier studies it was determined that a lentiviral delivery system might be appropriate for delivery of anti-LC shRNAs, although it remained to be seen whether the expression of the silencing RNAs would be robust enough to effect LC production.

As described in Chapter 6, lentiviral expression constructs were designed to express shRNA molecules targeting LC 8226 and LC Wil. These constructs along with a lentiviral expression vector lacking an shRNA expression construct were prepared and packaged by the UT Viral Vector Core Facility at the University of Tennessee, Memphis (219). In a series of experiments, both the 8226 line and the SP2/O-λ6 line were exposed to these lentiviral vectors at a range of concentrations. It was found that 8226 cells exposed to lentiviral particles demonstrated effective transduction as evidenced by both an increased number of cells expressing the EGFP reporter protein and decreased levels of LC as compared to controls.

Conversely, and for reasons that are not understood, exposure of the cell line SP2/O-λ6 to lentiviral particles containing the pLB Wil V1 vector elicited no increase in fluorescence or decrease in LC production. It was initially thought that the cell line may be refractory to transduction with the selected lentiviral system, so a series of experiments were conducted in which the SP2/O line was exposed to either 8226 V1 shRNA-expressing or pLB empty lentiviral particles. Results from these seemed to confirm our hypothesis; however in parallel experiments in which 8226 cells were treated with pLB Wil expressing lentivirus it was found that these cells too had failed to be effectively transduced by the viral particles. In both cases, increasing levels of viral particles failed to increase the number of transduced cells, but did however generate a cytotoxic response as evidenced by using flow cytometery. Because of these findings both the SP2/O-λ6 line and the pLB Wil V1 lentiviral groups were dropped from the remaining experiments.

Generation of stably transduced RPMI 8226 clones

While a modest reduction in LC was noted with 8226 cells receiving higher levels of lentiviral particles, these data were collected on mixed populations of cells containing at best ~30% transduced cells. To determine the amount of silencing that may be expected with a homogenous population of infected cells it was decided to generate several clones from these initial groups. Indeed, when assayed in the absence of untransfected cells, those 8226 clones exposed to pLB 8226 V1 shRNA-expressing lentiviral particles were shown to express lower quantities of LC protein to their untreated 8226 cohorts, while those generated from cells treated with particles expressing empty pLB vector retained the ability to produce normal levels of LC protein. Further, this reduction was not due to a decreased tolerance of infected cells as cell viability was not compromised.

Taken together, these data demonstrate that exposure of myeloma lines to shRNA-expressing lentiviral systems can elicit a similar response to that seen when cells were exposed to synthetic siRNAs. A >60% reduction in LC protein secretion appears to be the maximum attainable from a population of > 90% virally-transduced cells. It is possible that the rate of transcription for LC gene products is outpacing the production of shRNA molecules, resulting in only a portion of target being degraded. Alternately, the rate of LC mRNA turnover is greater than that of the rate of degradation within the RNAi process, allowing some mRNAs to bypass the RNAi pathway. While these are both possibilities, further study would be required to determine the true cause of partial silencing in these cases.

Chapter 8

Mouse models of LC expression

8.1 Introduction

While earlier experiments demonstrated the silencing effects of administering siRNA molecules

to cells *in vitro* [Chapters 5, 6, 7], these studies did not address whether a similar reduction in LC

gene products may be attained in an *in vivo* model system. Several published reports have

shown that synthetic siRNAs or vector-delivered shRNA molecules can be used, but with

varying degrees of success (172, 214, 222). While none of these studies specifically targeted the

LC protein, there is at least one example in which shRNA bearing lentiviral vectors were shown

to infect both bone marrow and circulating b-lymphocytes in mice (214).

To test the hypothesis that RNAi therapy affords a rational approach to reducing free LC

burden *in vivo,* human 8226 plasma cell tumors were generated in severely compromised

immuno-deficient beige (SCID) or mice deficient in active Recombinase Activating Gene 1

(RAG1 -/-). The SCID/beige model was first identified in the early 1980's by Bosma *et al*. and

is deficient in both B and T cell responses. There is a lack of immunoglobulin production due to

a deficiency in the recombinase activity within the IgL gene locus; while mice retain normal

macrophage and natural killer cell function (223, 224). Similarly, the RAG1 -/- knockout mice

are immunodeficient due to a lack of the RAG1gene, which is crucial for B and T cell

maturation, and thus these animals contain no mature B or T lymphocytes (225).

For these studies both mouse strains were implanted with either pLB empty vector clones or pLB

8226 V1 shRNA clones (Chapter 7), and LC production monitored over a period of 4 weeks.

To study the effects of treating an established tumor with siRNAs, immunocompromised mice were implanted with 8226 cells and monitored for tumor growth. Mice were then treated with lentiviral expression vectors encoding either 8226V1 shRNA transcript or empty pLB vector by direct tumoral injection. Mouse sera was collected prior to and post-injection with viral vectors and the secretion of LC monitored by various techniques over the course of these studies.

8.2 Methods

Mice

Fox Chase SCID/beige (SCID) mice were acquired from Charles Rivers Laboratories (Wilmington, MA) and were housed in the animal care facilities at the University of Tennessee Medical Center, Knoxville. RAG1 -/- mice were a gift from the HICP and were housed as above. Animals were maintained under 12 hour light/dark cycles while food and water were given *ad libitum*. All care and animal manipulations were approved by the University of Tennessee Animal Care and Use Committee.

Cells

Clones of cell line 8226 containing either pLB empty or pLB shRNA 8226 V1 expression constructs were generated as described in Chapter 9. For this series of experiments the 8226 V1 shRNA-expressing clones 13A2 and 13C7 were used, while cells generated from the pLB empty vector clone E1G3 were used as a control. In addition, the parental cell line 8226 was included as control for LC expression.

Lentiviral vectors

Lentiviral vectors pLB 8226 V1 and pLB empty were characterized as described in Chapter 6.

Xenograft models and treatment

On the day of experiment, cells were counted and viability assessed by trypan blue dye exclusion assay as described in Chapter 4. Cells from line 8226 or the stably transfected clones 13A2, 13C7 and E1G3 were harvested by centrifugation. Cells were washed 3x and resuspended in ice cold sterile 200 μl PBS. For intraperitoneal (I.P.) injections, female SCID mice (n = 4) were lightly anesthetized using isoflurane and received 1 x 10^7 8226 or 8226 lentivirus-transduced clone (n = 4 per group) cells by direct introduction of cells to the intraperitoneal cavity using a ½ inch 30 gauge needle.

Subcutaneous (S.C.) injections of 1 x 10^7 either 8226 untreated, pLB 8226 V1, or pLB empty clones were administered to the left inguinal region in the mammary fat pads of female RAG1 -/- mice (n = 4) using ½ inch 30 gauge needles. On days 7, 14, and 28 blood was collected via the retroorbital sinus from anesthetized mice. Samples were held for 1 h at RT to generate serum. When possible, urine was also collected from animals by first placing them over squares of parafilm™ and gently scruffing the animal. Sera and urine samples were stored at 0°C until time of analysis. On day 28, mice were euthanized and spleen, kidney, heart, and liver tissues harvested at necropsy. Samples of each organ were preserved in buffered formalin solution for microscopic analysis. Solid tumor, when present, was also harvested and preserved in formalin. Samples of spleen and tumor tissue were also stored in RNA later solution for molecular analysis (Ambion, Austin, TX).

In a separate series of experiments, 8 female SCID mice received 1 x 10^7 8226 cells suspended in 100 μl ice cold PBS, injected to the inguinal mammary fat pad as above. Mice were monitored for tumor development. Once tumors formed, measurements of height, length, and width were taken using calipers. When the tumor volume reached ~5 mm^3, mice received 10^7 of either pLB 8226 V1 or pLB empty expressing lentiviral particles. Particles were diluted in 100 μl ice cold PBS and injections were given directly into tumor mass (intratumoral; I.T.). Mouse sera were harvested both immediately prior to administration of virus and at 7 and 14 days following treatment. Tumor size was assessed on the day of each collection. On day 14 animals were euthanized and tissue harvested as above.

ELISA of sera LC

Mouse sera was diluted 1:10 in PBS + 0.5% tween and analyzed by total λ ELISA B as described in Chapter 3.9. Serial dilutions of the patient derived human BJP (Cott) was used to generate standard curves. Filtered mouse sera (Sigma-Aldrich) was used as a negative control.

Immunohistochemistry

Tissue was fixed in 10% neutral-buffered formalin for ~24 h, embedded in paraffin and 4 μm-thick sections cut. Sections were placed on Tissue Path Superfrost Plus Gold Slides (Fisher Scientific). For each animal, one slide was prepared with hematoxylin and eosin stain. At the time of analysis slides were de-paraffinized and antigen retrieval performed using Target Retrieval Solution S1700 (Dako) as directed. For detection of LC, rabbit anti-human total λ pAB (Dako) was applied at a 1:15,000 dilution and the sections incubated overnight at 4°C. For detection of EGFP, Rabbit monoclonal anti-EGFP (Invitrogen) was applied at a 1:250 dilution

and incubated overnight at 4°C.   Reactivity was visualized with the IHC for Rabbit antibodies

on Mouse/Rat tissues kit (Biogenex, San Ramon, CA) following manufacturer's instructions.

Color development was achieved using ImmPACT™ DAB peroxidase substrate (Vector

Laboratories, Burlingame, CA) following manufacturer's instructions. Images were captured by

microscopy as described in Chapter 3.8.

Statistical Analysis

For data sets with comparisons between more than two groups data were analyzed by One-Way

ANOVA followed by Dunnett's Multiple Comparisons Test. In cases where comparisons were

made between two groups data were analyzed by Non-Paired Student's T-test. All analyses were

conducted using GraphPad Prism version 4.0 (GraphPad Software Inc.). Data are reported as

mean ± standard error.

8.3 Results

I.P. injection of SCID mice

SCID mice were randomly assigned to receive pLB shRNA expressing clones 13A2, 13C7 or

pLB empty expression vector clone E1G3 (vector control; VC), while those receiving untreated

8226 cells served as no treatment control (n = 4 per group). Animals from groups SCID 8226 UT

and SCID 13A2 were the first to receive myeloma cells, with groups SCID VC and SCID 13C7

exposed on a separate day. Sera collected from SCID 8226 or SCID 13A2 mice demonstrated

detectable levels of human λ LC (289.8 ± 87.21 µg/mL; n = 3 and 85.54 ± 34.35 µg/mL; n = 4,

respectively) when analyzed by ELISA (Figure 8.1 A). In the case of mouse SCID 8226 UT 1,

repeated ELISA of sera revealed no increased LC production, and the animal was excluded from

analysis. Although at day 7 post tumor implantation there appeared to be a trend towards decreased LC production in group SCID 13A2 (85.54 ± 34.35 μg/mL; n = 4) as compared with SCID UT (289.8 ± 87.21 μg/mL; n = 3) this did not reach significance (p = 0.11).

On day 14 there was also a similar trend toward decreased LC production in sera from mice in the SCID 13A2 group with mean concentrations of serum LC 86.88 ± 23.00 μg/mL (n = 4) as compared to 312.5 μg/mL ± 71.90 (n = 3) in animals from group SCID UT (8.1 B), although, due to the low animal numbers per group, the data failed to achieve significance (p = 0.06), Because 2 animals from group 13A2 (mice 13A2 1 and 13A2 3) expired while under anesthesia, we limited LC analysis of sera to day 28 for the remaining animals to avoid further losses. As an alternative, mouse urine was analyzed as a metric of LC production, although as assay of urine from individuals taken on the same day yielded highly disparate results, this approach was also dismissed.

Analysis of mean LC production from sera collected from animals in groups SCID UT and SCID 13A2 revealed a high level of variability as evidenced by large standard errors within groups. As such, LC data were graphed for individual animals from groups SCIT UT and SCID 13A2 over time (Figure 8.2 A, B). Likewise, sera LC values for individuals from groups SCID 13C7 and SCID VC were graphed from samples collected at day 28 (Figure 8.2 C, D).

These data demonstrated an overall > 2-fold increase of LC protein within the sera of animals from group SCID 8226 with a minimum value of ~ 250 μg/ml (mouse SCID UT 2). A similar increase in serum light chain concentration was observed in 2 of the 13A2 mice (SCID 13A2 1 and SCID 13A2 3); however the maximum level attained by these animals at day 28 pi
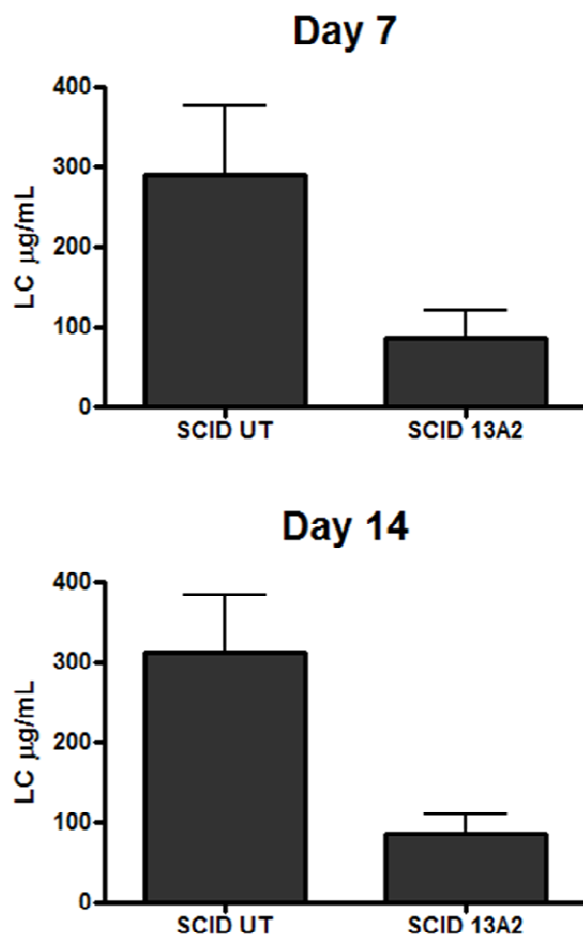
Figure 8.1 Mean Serum LC concentration of SCID mice at 7 and 14 days following I.P. injection of myeloma cells. Female SCID/beige mice received either 1 x 107 RPMI 8226 or clone 13A2 cells by intraperitoneal injection. Serum was harvested at A.) 7 or B.) 14 days and analyzed for total human l LC by ELISA. Data were analyzed using a Student's t-test.
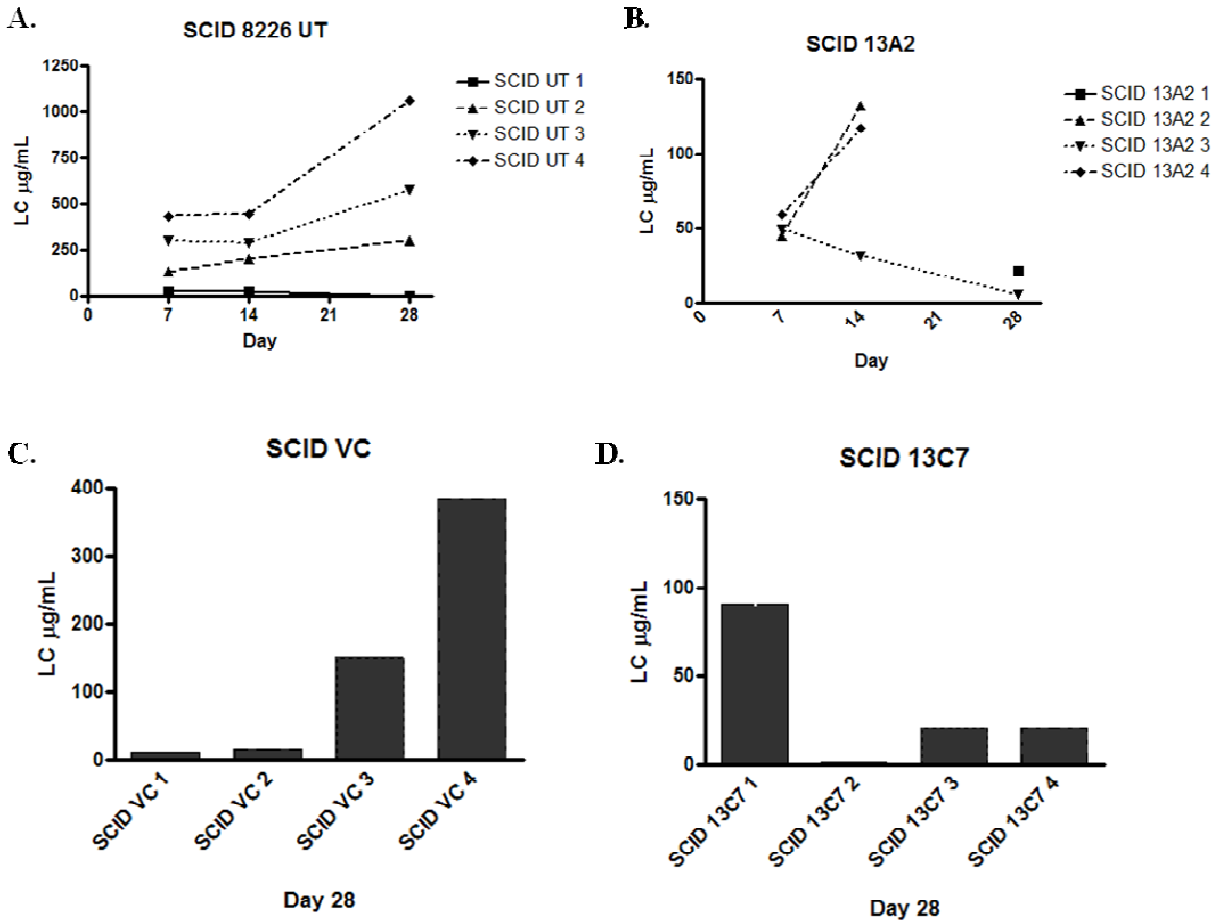
Figure 8.2 Serum concentration of human LC in individual mice. Serum LC concentrations for mice from groups A.) SCID UT and B.) SCID 13A2 were plotted over time. Serum LC increased in 3 of 4 animals from group SCID UT over the course of the study, while increasing LC was observed in 2 of 4 mice from group SCID 13A2. C.) In Animals from group SCID VC two animals were found to have serum LC concentrations above 100 mg/mL, while two were near 0. D.) Three mice from group SCID 13C7 were shown to lack or have low levels of human LC protein in the serum, while mouse 13C7 1 was shown to have 89 mg/mL.

was only ~130 µg/ml (Figure 8.2 A, B). Exclusion of the non-responding animals from group

SCID 13A2 at day 14 increased the mean LC concentration from 86 ± 23.00 µg/mL (n = 4) to

124.4 ± 7.500 µg/mL (n = 2) and reduced the standard error (SEM 7.5 v. 73.5), but did not affect

significance (p=0.061) when compared with group SCID UT 8226 (312.5 ± 71.90 µg/mL; n =

3).Analysis of mean LC concentration in sera collected at 28 d pi indicated a significant

difference ($p < 0.05$) between the untreated control group SCID UT (648.3 ± 222.3 µg/mL; n =

3) and the treated group SCID 13C7 (19.55 ± 1.667; n = 3) (Figure 9.3). While no differences

were detected between SCID UT and SCID VC (267 ± 116 µg/mL; n = 2).

Tissue samples harvested at day 28 pi mice were studied by using IHC. In the case of

animals SCID UT 2 - 4, tumor cells were observed outside the abdominal wall of the peritoneal

cavity near the site of injection. Regardless, the lesion size, presence or absence of tumors

corresponded well with whether serum LC was detectable for the given animal. It was not

known whether the extra-peritoneal lesions resulted from inadvertent S.C. injection of cells, or

due to implantation of a small number of cells from backflow at the time of injection.

S.C. injection of RAG1 -/- mice

While data from I.P implantation of SCID mice appeared compelling, a major concern with the

model was the lack of visible tumor. Further, the single parameter which might offer a measure

of tumor burden in the mice, sera LC concentration, was also the protein which should be

affected by treatment, and could therefore not be used as surrogate marker of tumor size or

growth in an *in vivo* silencing experiment. Additionally, due to loss of animals, group sizes were

smaller than desirable, likely contributing to the lack of statistical significance. To address these

issues, a second mouse model was developed. For this, the clones 13A2, 13C7, and E1G3 (VC)
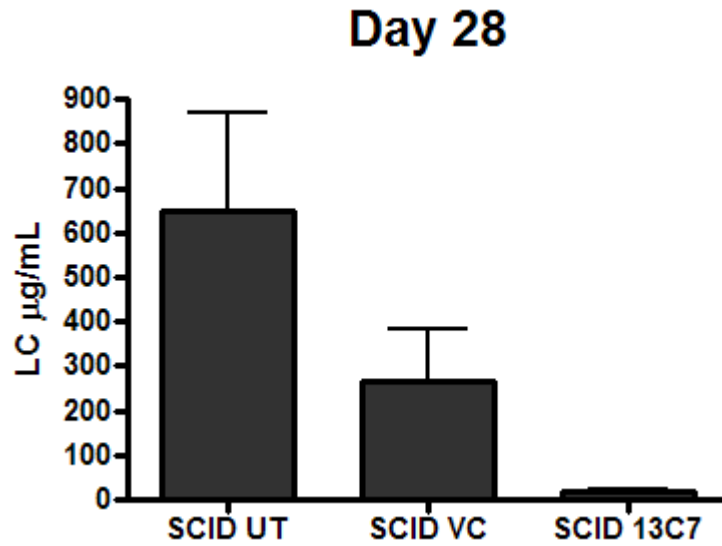
Figure 8.3 Analysis of sera from groups SCID UT, SCID VC, and SCID 13C7 at 28 days following I.P. myeloma cell injection. Serum from taken from animals within each tumor group were analyzed for human LC by ELISA. Mean concentrations were compared among SCID UT (n = 3), SCID VC (n = 2), and SCID 13C7 (n = 3). Data were analyzed by One-way ANOVA.

were again utilized, in addition to untreated 8226 cells, to generate S.C. xenograft tumor in the

inguinal fat pad in RAG1 -/- mice. As before, mice were held up to 28 days and sera were

harvested at 7, 14, and 28 d. At day 28 mice were euthanized, necropsies performed, and tissues

collected for IHC analysis. By day 7, small (approximately 33 mm^3) tumors were palpable in 3

of 4 mice receiving untreated 8226 cells (RAG UT 2, 3, and 4), in all vector control animals

(RAG VC 1, 2, 3), 3 of 4 mice receiving clone 13A2 (RAG 13A2 2, 3, and 4), and all mice

receiving clone 13C7 (RAG 13C7; n = 4). The serum LC levels measured on d 7 yielded were

not significantly different between groups (Figure 8.4A); however, as seen in the SCID mice, the

8226 tumor-bearing animals had higher mean LC concentrations (106 ± 46.59 µg/ml; n = 4) as

compared to the silenced clones, 13A2 (21.24 ± 4.27 µg/ml; n = 4), and 13C7 (47.49 ± 13.52; n

= 4). Sera from mice bearing vector control cells contained 76.99 ± 23.46 µg/ml human LC.

Reassessment of sera LC at 14 days revealed a similar, but more dramatic pattern, with 8226

tumor-bearing mice having 128 ± 48 µg/mL (n = 4), and those bearing clone 13A2 or 13C7 had

much lower levels (7.490 ± 1.936 µg/mL; n = 3 and 2.493 ± 1.039 µg/mL; n = 4, respectively)

(Figure 8.4 B).

Because of the apparent decrease in serum LC from the clone groups as compared with

concentrations assayed at day 7 mice were rechecked for tumor lesions. Animals which had been

found with lesions at site of injection prior to day 7 had retained the lesions, although tumor sizes

were still below that which could be accurately measured by calipers. The decrease in serum

free LC in these mice could therefore not be explained by the loss of tumor mass.

Analysis of serum samples collected on day 28 showed that this trend continued (Figure

8.4 C); however, while there were large differences in mean serum LC concentrations between
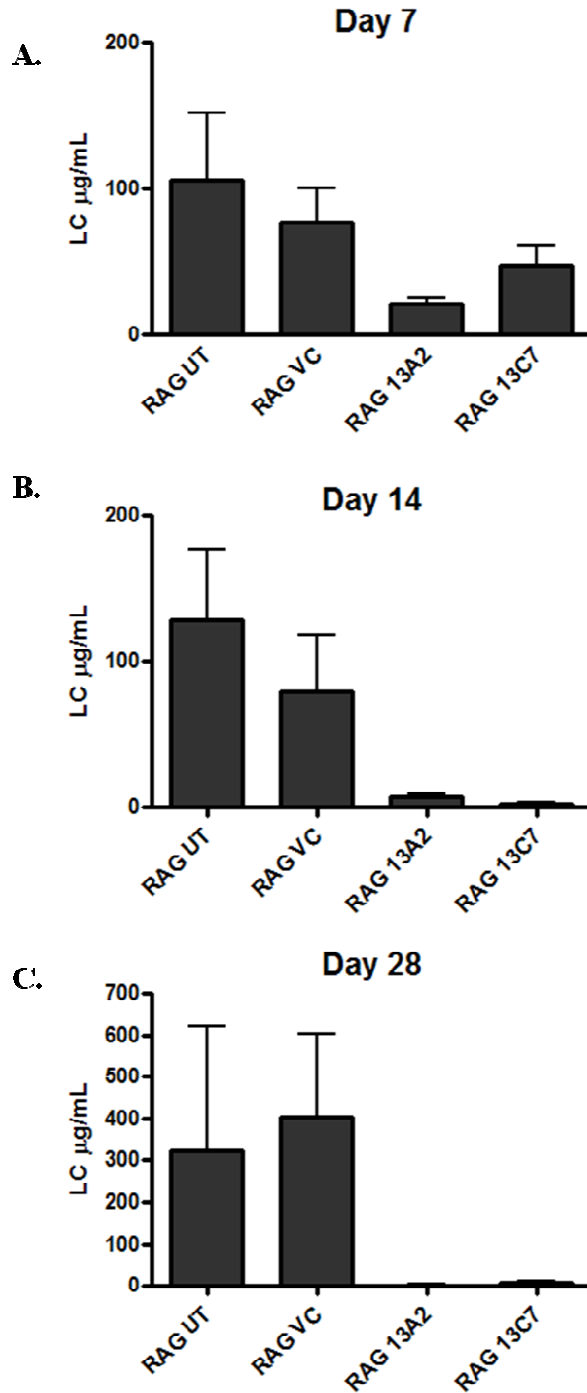
Figure 8.4 ELISA analysis of sera from shRNA treated 8226 clone tumor bearing mice. For each group (N=4), female RAG 1-/- mice were injected with 1 x 107 myeloma cells. Mouse sera was collected at A.) 7 days post tumor implantation and assayed for serum human LC by ELISA. This was repeated at B.) 14, and C.) 28 days. Mean LC concentrations among groups were analyzed for each day by One-Way ANOVA.

groups there were still no significant differences among animals. At necropsy on d 28, tumor lesions were identified in 3 of the control animals (Rag UT1, 3, and 4) and 3 of the vector control animals (RAG VC 1, 3). Interestingly, no evidence of lesions was identified from animals bearing 13A2 or 13C7 clones. Results of necropsies are summarized in Table 8.1 for each animal, reporting presence of tumors, weight of mass at time of necropsy, and whether each animal demonstrated LC production by ELISA from samples collected on day 28.

Due to the high variability in LC serum concentrations among animals from the same group, the LC production of individual animals were analyzed over time to determine whether patterns may emerge which would help explain the above results. Beginning with animals bearing untreated 8226 tumors one of the 4 animals (RAG UT 1) demonstrated the expected increase in LC production throughout the experimental period (112, 244, and 1,036 µg/mL at 7, 14, and 28 d, respectively), while RAG UT 2 began with a higher concentration of LC at day 7 (236.99 µg/mL) this value decreased to 168 µg/mL by day 14, and disappeared by day 28 (Figure 8.5 A). For the remaining animals, assessment of LC production at d 7 revealed much lower concentrations of serum LC (35 and 43 µg/mL) compared with the other animals within this group. LC concentrations from mouse RAG UT 4 showed a modest increase in LC at d 14 (60 µg/mL) which persisted to d 28 (54 µg/mL), and mouse RAG UT 3 exhibited a similar pattern at d 14 with LC concentrations of 37 µg/mL, although in this case, there was a drastic reduction in detectable LC by d 28 (4.59 µg/mL) (Figure 8.5 A).

In animals injected with vector control cells, two animals, VC 1 and VC 3, demonstrated increasing amounts of serum LC protein over the experimental period beginning with 65 and 121 µg/mL LC at day 7. The concentration of LC assayed from sera collected at day 14 was

Table 8.1 Comparisons of tumors and LC data in RAG 1 -/- mice

Group	Mouse	LC in sera (µg/mL)		Tumor Present		Weight (g)
		D 7	**D 28**	D 7	D 28	
RAG UT	1	112	1215	No	Yes	0.189
	2	236	4	Yes	No	
	3	34	8	Yes	Yes	0.002
	4	43	54	Yes	Yes	0.002
Vector Control	1	65	607	Yes	Yes	0.118
	2	42	0	No	No	
	3	121	597	Yes	Yes	0.102
13A2	1	11	6	Yes	No	
	2	15	0	Yes	N/A	
	3	27	0	Yes	No	
	4	28	0	Yes	N/A	
13C7	1	35	13	Yes	No	
	2	87	12	Yes	No	
	3	31	2	No	No	
	4	33	7	No	No	

Legend: No data available for animals marked N/A
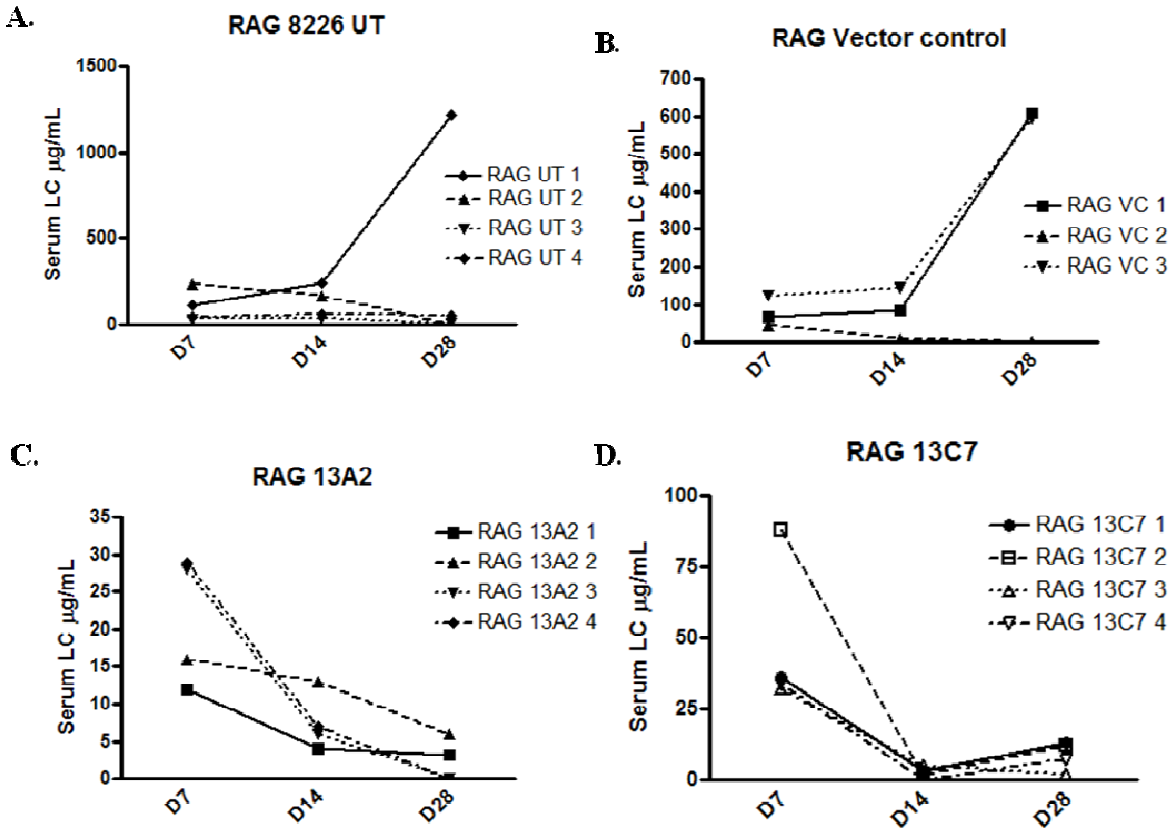
Figure 8.5 Serum LC concentrations from animals bearing myeloma cell tumors. Sera LC concentrations were plotted for RAG 1-/- mice which had been implanted with A.) untreated 8226 cells, B.) Vector control clones, C.) shRNA clone 13A2, or D.) shRNA clone 13C7at 7, 14, and 28 days

increased in both animals to 85 and 142 µg/mL, and reached peak concentrations at d 28 with

samples containing 607 and 597 µg/mL, respectively (Figure 8.5 B). While LC was detectable

in the sera from the remaining animal at d 7 (42.99 µg/mL), there was a steep reduction by d 14

(8.99 µg/mL) and no detectable LC by d 28 (Figure 8.5 B).

Of the mice injected with clone 13A2, two (RAG 13A2 1 and RAG 13A2 2), showed

lower serum LC concentrations at d 7 as compared with their cohorts (RAG 13A2 3 and 4) with

12 and 16 µg/mL versus 27 and 28 µg/mL, respectively. By day 14 LC concentrations had

decreased to > 5 µg/mL for all but RAG 13A2 2, which had a reduced sera LC level of 12.9

µg/mL. By day 28 serum LC was below detectable limits for all animals from this group (Figure

8.5 C).

Mice bearing 13C7 tumors demonstrated a similar pattern to that of mice from group

13A2, with the highest levels of LC observed at d 7 (Figure 8.5 D).

Since LC was detectable in the sera of animals from all groups at day 7 this data was

reanalyzed and 2 animals from the RAG UT group removed (RAG UT 3, 4). The rationale for

this is that over the experimental period serum LC did not increase appreciably from day 7,

possibly indicating problems with the tumor cells. Removal of these animals increased the mean

LC concentration for the RAG UT group from 106± 49 µg/mL (n = 4) to 172±64 µg/mL (n = 2).

Comparisons among the groups without these values using One-Way ANOVA followed by

Dunnett's Multiple Comparisons Test now revealed significant differences among between both

animals from both 13A2 and 13C7 groups as compared with untreated controls, while no

differences were detected between animals bearing untreated 8226 cells and those bearing vector

control tumors (Figure 8.6).
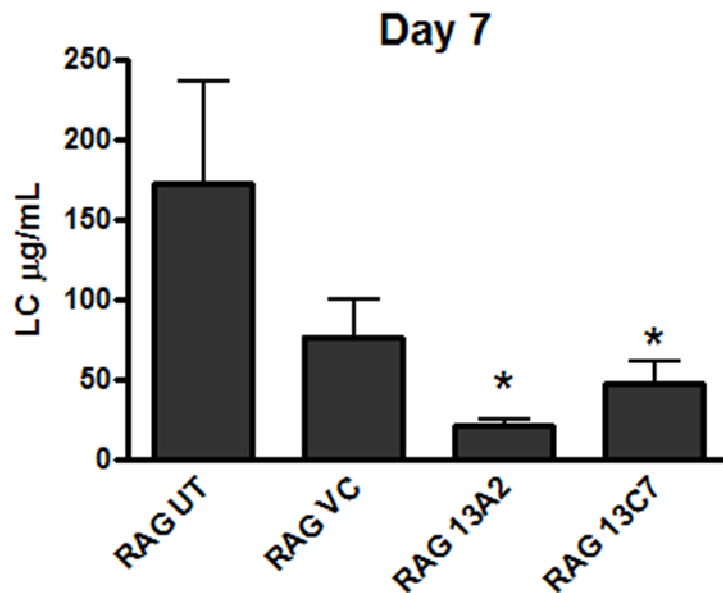
Figure 8.6 Analysis of RAG mice bearing myeloma clone tumors. Serum concentrations of human LC were reanalyzed by One-Way ANOVA following removal of mice RAG UT3, and RAG UT 4. Removal of these animals from analysis reveal a significant ($p > 0.01$) reduction in the serum LC concentration of animals from the RAG 13A2 (mean LC 21.24 ± 4.27 mg/mL) group as compared with RAG UT controls (Mean LC 172.5 ± 64.5 mg/mL). These data also indicicate a significant ($p < 0.05$) reduction in the mean LC concentration of animals from group RAG 13C7 (47.49 ± 13.52 mg/mL)

Treatment of *in vivo* S.C. human 8226 tumors with shRNA-bearing lentivirus

To determine the efficacy of administering a shRNA expression vector to pre-established tumors 8 female SCID mice received 1 x 10^7 8226 cells S.C in the inguinal mammary fat pad. Unfortunately, 2 of the mice expired under anesthesia during implantation. The remaining animals were monitored for up to 25 days for tumor growth, prior to injection of lentivirus and for up to 14 days following treatment - these data are summarized in Table 8.2 and Figure 8.7. Of these, one mouse (8226 V1 1) was found to have developed a mass of appropriate size 15 days pi of cells (Table 8.2). By 21 d two more mice (pLB 1 and 8226 V1 2) had developed masses of similar size (Table 8.2). Tumors were identified in the final 2 mice (8226 UT and pLB 2) at day 30 and 35, respectively (Table 8.2). The final animal from this group had no apparent tumorigenesis over the course of the study.

Animals which had developed tumors (n = 5) were randomly assigned to receive 10^7 lentiviral particles containing either pLB empty vector (group pLB; n = 2) or pLB 8226 V1 shRNA expressing constructs (group 8226V1; n = 2), while the remaining mouse received no treatment and served as a control (8226 UT). In each animal, sera were harvested immediately prior to administration of lentivirus, followed by sampling at 14 d. The presence of human λ LC was measured by ELISA (Chapter 3.9; Total λ ELISA B). Prior to treatment with lentivirus (Day 0) animals randomly assigned to the 8226 V1 group had slightly elevated LC concentration in the sera (972.4 ± 135.9 µg/mL, n = 2) as compared to those from the pLB group (2167 ± 386.4 µg/mL, n = 2), although this was not statistically significant (Figure 8.8 A). By day 14 this trend had reversed itself, with animals from the 8226 V1 group having mean sera LC concentrations of 2,133 ± 1683 µg/mL, while those from the pLB group were found to have mean LC concentrations of 3,685 ± 364.3 µg/mL (Figure 8.8 B).

Table 8.2 Tumor sizes in SCID mice

Group	Mouse	Day 0*		Day 7		Day 14		
		L x W x H	mm^3	L x W x H	mm^3	L x W x H	mm^3	W (g)
pLB	1	4 x 6 x 3	37.7	5 x 9 x 4	188	14 x 9 x 6	395	0.805
	2	4 x 5 x 4	41.9	7 x 6 x 5	87.9	10 x 7 x 6	219	0.457
8226 V1	1	7 x 4 x 4	58.6	7 x 4 x 2	29.3	12 x 10 x 6	377	0.790
	2	7 x 7 x 7	179	9 x 7 x 4	131	14 x 16 x 4	469	0.989
8226 UT	1			9 x 6 x 4	113	11 x 7 x 12	483	1.01

* Timing measured relative to injection of lentivirus

SCID est tumor size over time
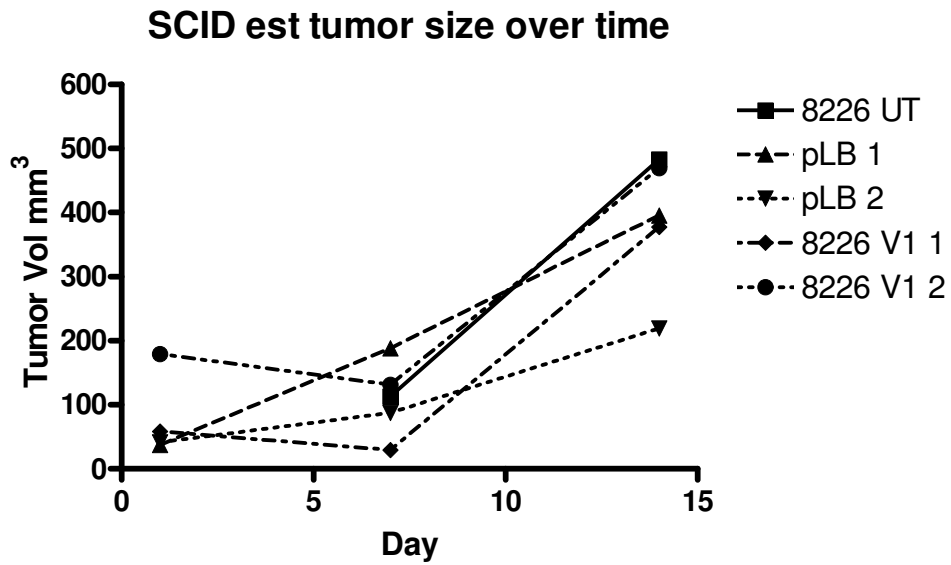
Figure 8.7 Calculated tumor volumes from individual animals over time. Female SCID mice received 1 x 10^{7} 8226 cells as S.C. injections to the inguinal mammary fat pads. Tumor growth was estimated in each animal by measuring height, length, and width of tumors using calipers and calculating tumor volume using the formula $4/3\pi(ABC)$.
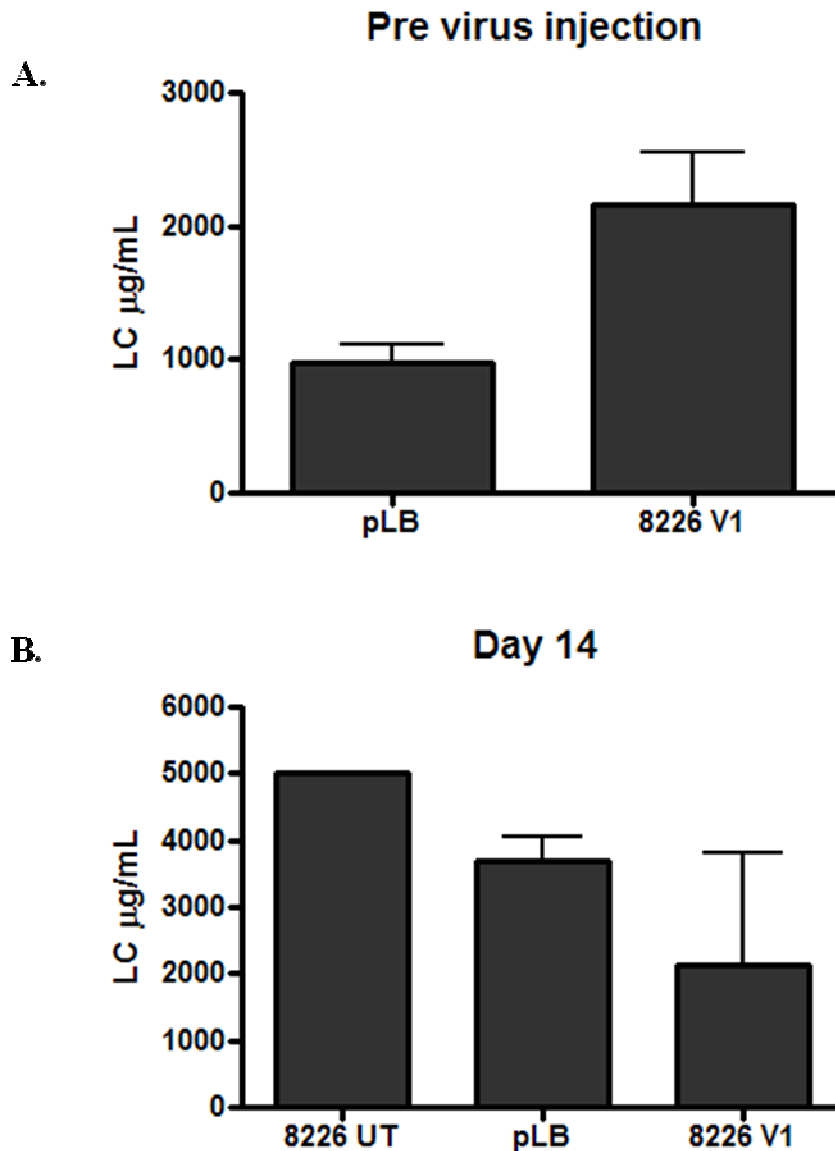
Figure 8.8 Serum LC from 8226 xenograft tumor bearing mice pre- and post-treatment with lentiviral expression vectors. Female SCID bearing 8226 xenograft tumors were treated with 10^7 lentiviral particles (pLB N=2; 8226 V1 N=2), whereas 8226 UT received no injection (N=1). For each animal, sera were analyzed for human LC by ELISA. Mean LC concentrations from sera are shown for A.) pre-treatment or C.) 14 days following administration of virus. Data were analyzed by One-Way ANOVA.

As a reference the 8226 UT mouse was found to have 5,016 µg/mL serum LC (Figure 8.8 B).

To account for the differences in tumor size among animals, data collected regarding tumor

volume (Figure 8.7) along with serum LC ELISA results were used to generate ratios of serum

LC concentration to tumor volumes for animals from each group at day 14, and the mean ratio

for each of these groups were plotted (Figure 8.9). From this, it was found that the average ratio

of LC production per mm^3 of tumor volume for group pLB was 12.63 ± 2.375 µg/mL LC/mm^3

tumor, with the single 8226 UT animal producing 10 µg/mL LC/mm^3 tumor, and mice injected

with 8226 V1 vector producing 4.615 ± 3.515 µg/mL LC/mm^3 tumor.

Sections of kidney and tumor tissue taken from mice and stained were stained by IHC using

antibodies specific to human λ LC. Comparisons of tumors from these animals revealed little

difference in the intensity of antibody binding, but do reveal that tumor size along with the

amount of vascularization and necrotic regions were equivalent among mice. Evaluation of

kidneys from animals taken from each of the three groups do, however, reveal differences in the

amount of antibody binding along the luminal surfaces of the renal tubules as well as within the

cytoplasm of the renal tubule cells (Figure 8.10 A, B, C). This difference is most apparent in the

tubules themselves, where heavy binding is observed along the borders with animals from

control groups (8226 UT or pLB empty) as compared with those treated with 8226 V1 shRNA

expressing particles.

8.4 Discussion

While it is difficult to draw definitive conclusions about the results of these experiments, they do

demonstrate that shRNA expression vectors can continue to exhibit their inhibitory effect *in vivo*
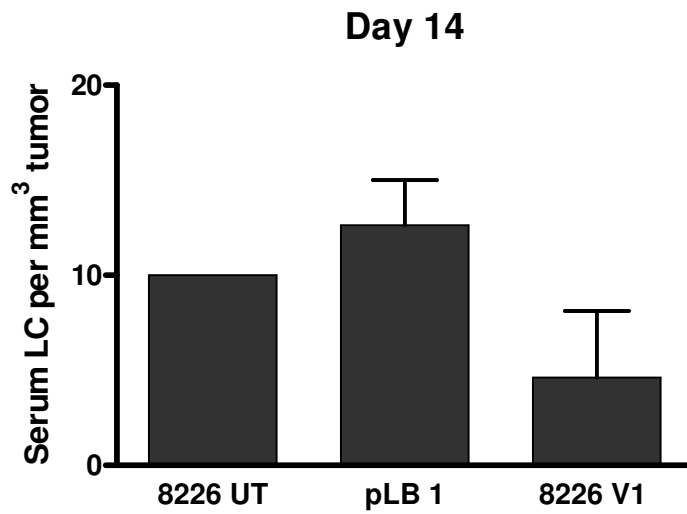
Day 14

Figure 8.9 Serum LC production normalized to tumor volume. Serum LC concentrations from ELISA for human LC protein were collected from mice at day 14. Values were normalized to estimated tumor size by dividing LC content by tumor volume and data expressed as µg/mL LC/ mm^3 tumor.
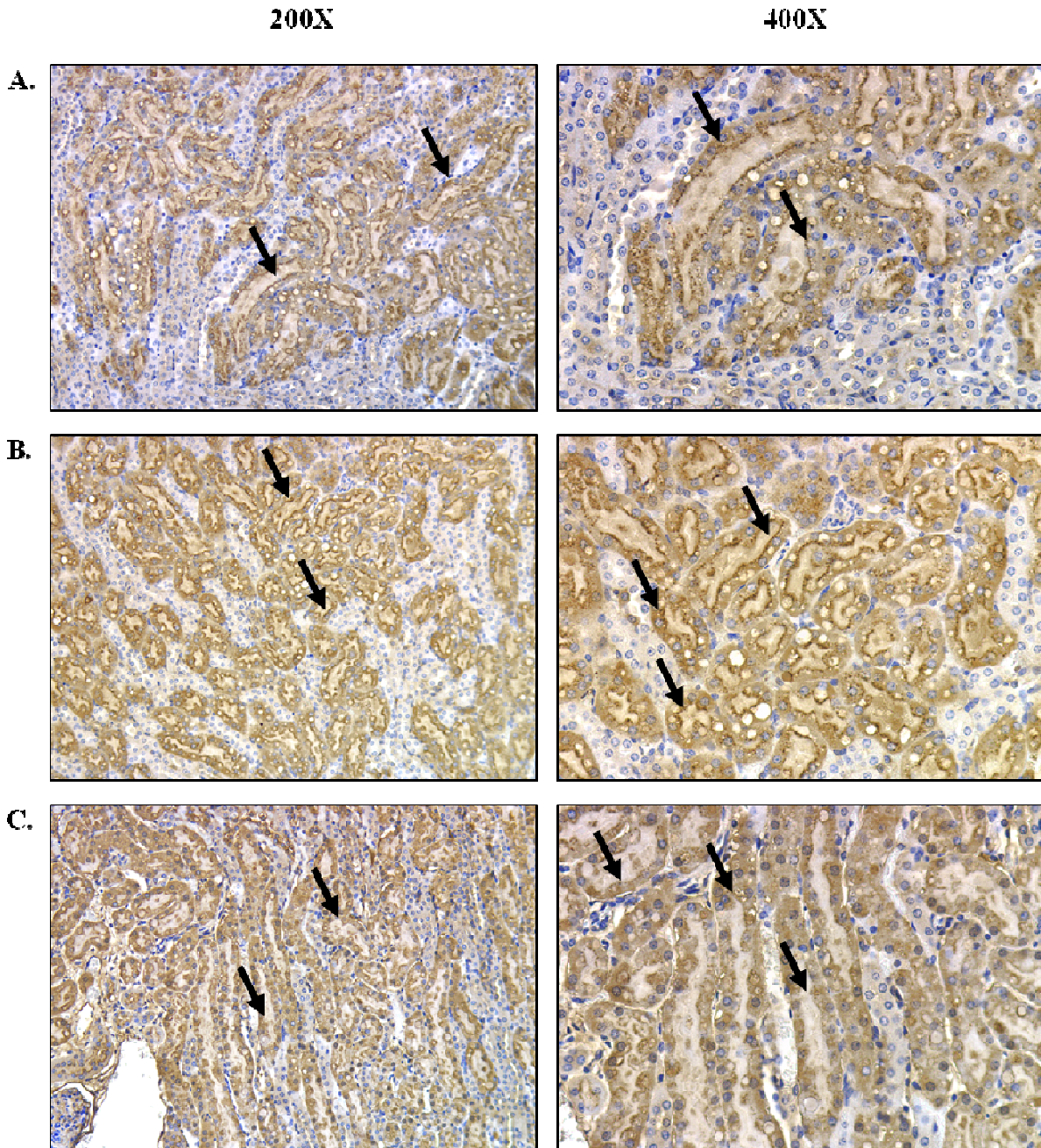
Figure 8.10 Detection of λ LC in mouse kidneys following treatment with shRNA expression vectors. Mice were sacrificed at 14 d p.i. and kidneys stained for human LC. Images were taken from 200X (left column) and 400X (right column) fields for animal bearing 8226 xenograft tumors and receiving A.) no treatment (8226 UT), B.) Vector pLB, or C.) pLB 8226 V1 lentiviral particles. Arrows show regions along the luminal borders of tubules or renal tubular epithelial cells.

following implantation as xenografts in mice; as was the case at the earlier time points from the SCID I.P. and the RAG1 S.C. experiments.

Some concerns about these models remain, however, and would to need be addressed in future studies. One of the most problematic issues that arose with the tumor models used herein was the large degree of variability in tumor development both among and between groups. In some cases, the standard SEM within a given treatment group for serum LC content was almost identical to the mean itself, making it difficult to draw conclusions about outcomes with any statistical certainty.

Another concern was the apparent loss of tumors observed in the RAG1 mouse line after the day 14 time point following implantation of shRNA-treated myeloma clones. While tumors were not present in some of the untreated and vector control animals in this group, all mice receiving shRNA clones 13A2 and 13C7 were devoid of perceptible lesions at time of necropsy. While differences in cell growth and viability were not apparent during *in vitro* studies [Chapter 8], these clones appear to be less fit than the untreated or vector control groups regarding survival *in vivo*. Re-submission of the shRNA sequence used to generate the 8226 V1 expression vector to the NCBI BLAST algorithm using the RefSeq_RNA database as reference revealed no known RNA transcripts with more than ~50% homology to the siRNA sequence used. While this does not remove the possibility that the encoded shRNA sequence could reduce survival of the cells *in vivo*, it does reduce the likelihood that off-target effects are responsible. Another possibility is that the selected clones were less hardy than untreated 8226 cells because of lack of variability within the cell population. Although, it would not be expected that two unique clones would be equally susceptible, and the findings that vector control clones were successful at colonization also argues against this fact. At least one study has reported

hepatotoxicity in mice receiving lentiviral vectors by tail vein injection. In this case, expression

of the shRNA construct was controlled by an RNA polymerase III, as is the case with the system

used here. It was hypothesized by the authors that the cytotoxic effects were induced when the

constitutively expressed shRNA construct overwhelmed the cells natural miRNA pathways,

resulting in loss of essential post-transcriptional gene silencing (204). A final alternative that

may explain the fact that many of the mice did not develop tumors is that the RAG1 -/- knockout

strain has been shown to be "leaky" and that in some cases the mice develop the capacity to

produce immunoglobulin (Kennel, *et. Al.* unpublished data). If this were the case then the lack

of tumors in many of the mice used in this study may be due to the animals mounting a humoral

response to the cells of human origin.

Regarding the variability among groups, it would be desirable to increase the number of

animals per group to determine whether statistical significance might be possible with a larger

sample size, given the apparent trends towards decreased LC seen among both the I.P. and S.C.

models. As for the survival issues with shRNA expressing clones, one potential series of

experiments would be to redesign the shRNA constructs to target various regions along the LC

gene transcript, and generate several clones based on each of these vectors. Here, differences in

survival among clones might offer evidence to whether the loss of tumors is a problem of design

or inherent to infection with lentiviral vectors.

As for the final series of experiments in which established 8226 tumors were treated with

empty or shRNA expressing lentiviral particles a larger cohort of animals would be crucial to

assess the efficacy of this approach. Given the small sample size (n = 2 per treatment), these

experiments represent a preliminary study, although the data shown in figure 9.9 seem

promising, given the decrease in the ratio of LC production with given tumor size. In

conclusion, establishing that the effects of silencing LC proteins using siRNA or shRNA

molecules *in vivo* is crucial in translating effects observed in the earlier chapters to a clinical

model. These data, while limited, provide the impetus for further study along these lines.

Chapter 9

Summary and Conclusions

9.1 Design of siRNA molecules targeting LC products

Based on sequencing data acquired from PCR amplification of individual LC gene products (Figure 4.1), several candidate small interfering RNA molecules were designed which corresponded to sequences along the V, J, and C region for the respective targets (Table 4.2). SiRNA sequences targeting the V, or J region of each LC were designed to sites such as the borders of framework- and complimentarity defining regions, or recombination sites between the V and J regions of the LC molecule. These sites were selected because they represent areas of the molecules which are most likely to house sequences that are significantly different to their respective LC germline genes or to other LCs within the same isotype sub-class (i.e., λ or κ) (226, 227). Alternately, sites of conserved homology were selected within the C region for both λ and κ isotypes. Selection of these regions allowed for the design and synthesis of class specific siRNAs which could target a broad range of LC molecules of a given sub-type.

Initial experiments in silencing LC products were carried out in both κ and λ producing human myeloma lines (cell lines Bur and RPMI 8226) as well as a transgenic mouse myeloma line engineered to produce a patient derived amyloidogenic recombinant λ6 LC molecule (SP2/O-λ6; Wil). Screenings of various transfection reagents using fluorescently labeled non-silencing siRNA molecules to transfect these lines were conducted (Table 4.3) and a suitable reagent (HiperFect) was identified which could efficiently (> 90% of cells transfected; Figure

4.3) deliver the nucleic acid cargo to all cell lines used in these studies without inducing a cytotoxic response.

9.2 Effect of targeted siRNA molecules on LC synthesis

As demonstrated in Chapter 5, exposure of either mouse or human myeloma lines to siRNAs targeting V, J, and C regions of their secreted LC gene products elicited significant reductions in target mRNA (25-61%) and secreted protein (25-75%) when compared with untreated control cells (Figure 5.2, 5.4). The effect of these interfering RNAs on LC production was observable within 24 hrs of exposure, and appeared to be maintained for 48-72 hrs afterwards. Additionally, neither the addition of siRNAs or transfection reagent to cell cultures seemed to negatively affect cell growth or viability (Figure 5.3).

While these results indicate the potential of siRNAs to affect LC production, it is evident that this is a transient reduction in secreted product. One possible explanation for this loss of activity is the loss of siRNA molecules over time. Supporting this hypothesis, Figure 5.1 depicts histograms generated using flow cytometry to detect the presence of a fluorescently labeled siRNA molecule at 24 h, 48 h and 72 h following exposure to either mouse (SP2/O-λ6) or human (8226) myeloma lines. In this case, both lines exhibit a high degree of uptake for labeled siRNA molecules (> 95% of cells were positive) at 24 hrs. Following along with line SP2/O-λ6, a reduction in positive cells is apparent by 48 h (~60% positive), which is further reduced by 72 h (~40% positive). When these data are compared with those for cell number and viability (Figure 5.3) it appears that the greatest decrease in the number of positive cells (24-48 hrs; 96%-59%) also corresponds to the time period (24-48h) demonstrating the largest increase in cell number (2 x 10^5 - > 2 x 10^6 cells well^{-1}) for this line.

Although the population of 8226 cells remained >90% positive for the duration of the experiments, careful examination of the flow cytometry histograms over the time periods assayed reveals an apparent decrease in fluorescent intensity among cells. Although it is unclear whether this loss is attributable to decreased signal from the fluorescent label over time or due to dilution of the siRNA molecules across cell divisions, it is interesting that a similar population of cells appeared as a "shoulder" of cells with decreased fluorescence at 48 h in the SP2/O-λ6 line and 72 h in the 8226 line, and that the appearance of this population is most apparent at time points when lines were seen to noticeably increase in cell number.

A final piece of evidence that the observed loss of effect on LC production was a function of loss of siRNA molecules per cell is seen in flow cytometry experiments using clones of cell line 8226 which had been stably transfected with constructs which produce both shRNA molecules as well as enhanced green fluorescent protein (EGFP) as a reporter molecule (Figure 7.9). In this case, the production of EGFP is expected to be maintained among daughter cells following division, and as a result, the "shoulder" observed in the previous model system is not seen.

9.3 Design and generation of lentiviral expression vectors

The data summarized in Section 9.2 are promising, and demonstrate the utility of siRNA molecules in reducing LC production in myeloma lines, although the transient nature of this reduction remains a concern. One approach to address this was to alter the delivery system of effector molecules from one that provided a single "dose" of siRNAs, to one that offered a renewable, and thus, a sustainable supply of silencing molecules. It has been reported in myeloma lines that silencing of various proteins has been achieved using viral mediated delivery

165

of constructs which express shRNA molecules (213, 217). While these studies did not specifically target LC proteins, they do demonstrate the successful transfer of gene expression to these cells from viral particles.

To test whether the level of silencing mediated by a shRNA expression system would be robust enough to effect a reduction in LC protein expression, two constructs (Wil V1 and 8226 V1), which had been shown effective at reducing LC production (Figure 5.4), were modified to incorporate a hairpin-loop structure (Table 6.1) and were cloned into the pLB lentiviral expression plasmid (Figure 6.2). These constructs were shown to effectively produce visible quantities of EGFP protein when transiently transfected to the kidney line HEK 293t by fluorescent microscopy (not shown). These constructs were also shown to be functional following packaging within lentiviral particles by exposing naïve HEK 293t cells to supernatants from cultures which had been previously co-transfected with plasmids encoding viral coat proteins and packaging signal sequences along with pLB expression vectors (Figure 6.6). A lack of EGFP expression was seen in human myeloma lines following exposure to supernatants, although this was likely due to the low amount of virus produced from this system, as there was no way to concentrate viral particles to a higher titer solution.

9.4 Effect of shRNA expressing lentiviral vectors on LC production

Cell supernatants containing high titers of infective lentiviral particles encoding either the empty pLB plasmid (pLB) or plasmids which include constructs encoding shRNAs directed to either LC 8226 (pLB 8226V1) or LC Wil (pLB Wil V1).

By 24 h exposure of the human myeloma line 8226 to viral particles containing plasmid pLB or those encoding pLB 8226V1 induced the expression of the reporter protein EGFP. The

166

proportions of cells expressing EGFP were found to increase for both lentiviral vectors as the MOI for each virus was increased over a range of 0.5-50 (Figure 7.2, 7.4). Assessment by flow cytometry revealed that exposure to either virus at levels of MOI 100 resulted in the maximum number of EGFP positive cells attainable (~30%) without inducing cytotoxicity (Figure 7.4). Among the populations of cells exposed to lower amounts of virus (MOI 0.5-10) there appeared to be a dose dependant reduction of secreted LC as compared with control cells when supernatants were assayed at day 7, which seemed to peak at around MOI 2.5 (Figure 7.3). When supernatants from cells exposed to higher viral titer (MOI 10-50) were assayed, two of the groups (MOI 10 and MOI 50), were found to be producing significantly reduced amounts of protein when compared with untreated cells (Figure 7.5).

Unexpectedly, similar exposures of the mouse myeloma line SP2/O-λ6 to increasing levels of virus pLB Wil V1 failed to elicit EGFP expression in cells (Figure 7.7). This was likely a combination of poor virus preparation combined with cells which were refractory to transduction as exposure of 8226 cells to pLB Wil V1 yielded no increase in EGFP and exposure of the SP2/O line to pLB 8226 V1 resulted in a slight increase in EGFP positive cells (Figure7.8).

Observations were also made regarding LC productions in clonal populations of 8226 cells which had been positively transfected with both virus pLB and pLB 8226 V1 (Figure 7.9). Several of the lines exposed to the shRNA expressing viral particles were shown to secrete reduced amounts of LC mRNA and protein as compared with untreated cells (Figure 7.10, 7.12), while, with a single exception, those exposed to pLB were found to secrete equivalent levels (Figure 7.10).

9.5 LC secretion by shRNA expressing clones in vivo

Of the shRNA expressing clones generated, 2 were selected for injection to the peritoneal cavity of immunocompromised SCID mice alongside mice receiving either untreated 8226 cells or those receiving a clone generated from pLB empty infected cells. Assay of sera taken from one group mice implanted with shRNA clone cells or untreated 8226 cells at 7 and 14 days p.i. revealed increased levels of LC (Figure 8.1). From this figure it also appears that the amount of LC in the sera from mice bearing the shRNA expressing cells was lower than that from animals bearing the parental line. While similar results were observed at day 28 in mice receiving the alternate shRNA expressing clone, it is difficult to determine if this reduction is due to a reduction in LC secretion or due to the loss of clonal cells.

Following these studies a second immunocompromised mouse line (RAG1 -/-) received either shRNA expressing clones, pLB empty clone, or untreated 8226 cells as s.c. injections. From these mice, tumor growth was apparent for up to 14 days post injection, as assessed by manual palpation of animals (Table 9.1). Although, beyond the 14 day timepoint lesions were not detectable in animals bearing the shRNA expressing cells (Table 9.1). While the cause of tumor regression is undetermined several possibilities were postulated in Chapter 8.4.

Analysis of sera taken from animals at day 7 did reveal reductions in LC content from mice receiving either shRNA expressing clones as compared with animals bearing untreated 8226 tumors (Figure 8.6).

9.6 Treatment of established tumors with lentiviral particles

In a final series of experiments, xenograft tumors consisting of 8226 cells were generated within the mammary fat pad of 5 female SCID mice. Tumor growth was monitored and when lesions reached roughly equivalent sizes mice received intratumoral injections of viral particles bearing either pLB empty or pLB 8226 V1 expression plasmids. While assay of sera from animals prior to injection revealed mice from group 8226 V1 had higher levels of LC to those receiving pLB empty vector particles, by day 14 this trend appeared to have reversed (Figure 8.8). Ratios of tumor size versus sera LC production from day 14 also revealed that tumors from animals in group 8226 V1 appeared be producing lower levels of LC per mm^3 than animals receiving sham injection, or the animal bearing untreated 8226 cells.

Perhaps the most compelling data taken from this series of experiments was shown in Figure 8.9, which depicts the IHC staining for human λ LC within renal tubules from animals receiving pLB 8226 V1 particles versus pLB empty or untreated control animals. From these images it appears that tubules stain more strongly in control animals than in those receiving virus bearing functional shRNA expression vectors. Most striking is the almost lack of staining for LC along the luminal epithelia of these animals. In contrast, animals from both control groups were shown to be highly positive for staining along this region.

9.7 Conclusions of studies

Taken together, these data demonstrate that exposure to myeloma cells to silencing RNAs will induce a targeted reduction in LC molecules. Studies from cells in culture provided positive evidence that this reduction can be elicited by either viral or non-viral delivery of interfering RNAs and provided the basis for the constructs used for *in vivo* studies. While tumors formed by these clones generate measureable amounts of LC which is secreted to the sera, further studies should be conducted to confirm that these reductions are a result of the shRNA construct and not a consequence of viral transduction. Along those lines, additional RAG1 -/- might be implanted with a larger variety of clonal 8226 cells to test whether some cells might be more fit for implantation *in vivo*. Also, the inclusion of a third control group, composed of cells transduced with constructs expressing non-silencing shRNAs should be included to answer whether the constitutive expression of shRNA molecules may impact survival.

To further strengthen the case that shRNA expressing lentiviral particles can indeed effect LC production in established tumors a larger number of mice should be recruited for study. In addition, mice could also be given a higher number of viral particles than used in the current study in order to account for increased cell numbers found in tumors which are large enough for injection. Further, staining of tumor tissue for presence of EGFP positive cells either by PCR amplification of gene products or by IHC staining might provide insight to the efficiency of silencing in these mice by determining the proportion of transduced versus non-transduced cells.

As the field of siRNA delivery is constantly growing, alternative means to viral delivery should be explored for the transfection of cells *in vivo*. Although the viral vectors used for these studies provided a relatively safe method of treatment for mice bearing established tumors it may be desirable to identify a non-viral means to introduce silencing RNAs in a clinical setting.

9.8 Closing Remarks

The goal of personalized gene therapy using siRNA molecules currently remains unrealized, however, as this study has shown RNAi provides a robust and flexible means to reducing the production of pathologic moieties. This section contains a brief narrative of how the inclusion of siRNAs might alter the treatment of a patient with AL amyloidosis.

Figure 1.6 outlines the current treatment strategy of patients diagnosed with a PCD. This process starts with the diagnosis of pathology along with staging of the disease. In this case the patient presents with elevated serum creatnine levels along with abnormal findings by echocardiogram along with the presence of BJP in the urine. Staining of fat and renal biopsy tissue with Congo red reveals congophilic bodies, which exhibit apple green birefringence when viewed under polarized light. N-terminal protein sequencing of this material confirms it is composed of $\lambda2$ LC, and yields a partial 12 amino acid sequence. IHC evaluation of bone marrow aspirates reveals a small cadre of clonal plasma cells composing ~3% of the total cell population. Whole body CT scans fail to identify presence of lytic bone lesions.

The patient begins conventional chemotherapy with a combination of Melphalan and Prednisone. Upon re-evaluation renal function has worsened and BJP content of the urine has increased. Because of the patient's age (60 yrs) they would be eligible for ASCT (Chapter 1.3) however, because of renal involvement they are a poor candidate. As other studies have shown that reduction of serum LC content can lead to improved organ function and outcomes in AL (160) the patient elects to receive siRNA therapy to reduce LC production. As it was previously determined that the LC involved in deposition was a member of the λ sub-type the patient receives synthetic siRNA molecules designed to the λ C region as an i.v. infusion using a neutral

peptide carrier. Evaluation of patient serum and urine reveals a ~25% reduction in LC levels 2 days p.i. compared with the pre-injection values and a 15% reduction at 5 days.

DNA sequencing of the pathologic LC was conducted by first translating the N-terminal protein sequence to nucleotides, which were used to generate an LC specific primer. Primers specific to the λ2 C region provide the reverse template. The patient LC is sequenced and a 60-bp shRNA molecule is designed with an 18 bp stem region complimentary to the pathologic LC, but shares less than 50% homology to the λ 2 germline gene. This shRNA construct is cloned into a tissue specific viral expression vector and is driven by the LC V region promoter and Cμ enhancer element. These expression plasmids are packaged as self-inactivating viral particles, which have been pseudotyped with coat proteins which target CD 138, which has been shown to be upregulated in neoplastic plasma cells (228). This system provides both a targeted delivery of gene products as well as an expression system which is driven by B-cell specific regulatory elements.

Following secondary evaluation, the patient receives an injection of viral particles and is monitored for unwanted immune responses. Patient sera is re-evaluated over a 2 week period and shown to contain consistently less LC than the pre-injection levels. Subsequent evaluation of renal function shows improvement and the patient begins the process for ASCT.

As mentioned in the opening of this section, this scenario is based solely on conjecture and provides a "what if?" scenario for illustrative purposes only.

List of References

1.   Napoli C, Lemieux C, Jorgensen R. Introduction of a Chimeric Chalcone Synthase Gene into Petunia Results in Reversible Co-Suppression of Homologous Genes in trans. Plant Cell. 1990; **2**(4): 279-89.

2.   Pal-Bhadra M, Bhadra U, Birchler JA. Cosuppression in Drosophila: gene silencing of Alcohol dehydrogenase by white-Adh transgenes is Polycomb dependent. Cell. 1997; **90**(3): 479-90.

3.   Romano N, Macino G. Quelling: transient inactivation of gene expression in Neurospora crassa by transformation with homologous sequences. Mol Microbiol. 1992; **6**(22): 3343-53.

4.   Fire A, Xu S, Montgomery MK, Kostas SA, Driver SE, Mello CC. Potent and specific genetic interference by double-stranded RNA in Caenorhabditis elegans. Nature. 1998; **391**(6669): 806.

5.   Obbard DJ, Gordon KH, Buck AH, Jiggins FM. The evolution of RNAi as a defence against viruses and transposable elements. Philos Trans R Soc Lond B Biol Sci. 2009; **364**(1513): 99-115.

6.   Grishok A, Pasquinelli AE, Conte D, Li N, Parrish S, Ha I, Baillie DL, Fire A, Ruvkun G, Mello CC. Genes and mechanisms related to RNA interference regulate expression of the small temporal RNAs that control C. elegans developmental timing. Cell. 2001; **106**(1): 23-34.

7.   Lagos-Quintana M, Rauhut R, Lendeckel W, Tuschl T. Identification of novel genes coding for small expressed RNAs. Science. 2001; **294**(5543): 853-8.

8.   Lagos-Quintana M, Rauhut R, Yalcin A, Meyer J, Lendeckel W, Tuschl T. Identification of tissue-specific microRNAs from mouse. Curr Biol. 2002; **12**(9): 735-9.

9.   Wightman B, Ha I, Ruvkun G. Posttranscriptional regulation of the heterochronic gene lin-14 by lin-4 mediates temporal pattern formation in C. elegans. Cell. 1993; **75**(5): 855-62.

174

10.   Schwarz DS, Hutvagner G, Haley B, Zamore PD. Evidence that siRNAs function as guides, not primers, in the Drosophila and human RNAi pathways. Mol Cell. 2002; **10**(3): 537-48.

11.   Elbashir SM, Lendeckel W, Tuschl T. RNA interference is mediated by 21- and 22-nucleotide RNAs. Genes Dev. 2001; **15**(2): 188-200.

12.   Elbashir SM, Harborth J, Lendeckel W, Yalcin A, Weber K, Tuschl T. Duplexes of 21-nucleotide RNAs mediate RNA interference in cultured mammalian cells. Nature. 2001; **411**(6836): 494-8.

13.   Bagasra O, Prilliman KR. RNA interference: the molecular immune system. J Mol Histol. 2004; **35**(6): 545-53.

14.   JOSHUA-TOR L. The Argonautes. Cold Spring Harbor Symposia on Quantitative Biology. 2006; **71**: 67-72.

15.   Schwarz DS, Hutvagner G, Du T, Xu Z, Aronin N, Zamore PD. Asymmetry in the assembly of the RNAi enzyme complex. Cell. 2003; **115**(2): 199-208.

16.   Filipowicz W. RNAi: The Nuts and Bolts of the RISC Machine. Cell. 2005; **122**(1): 17-20.

17.   Paddison PJ. RNA interference in mammalian cell systems. Curr Top Microbiol Immunol. 2008; **320**: 1-19.

18.   Yi R, Qin Y, Macara IG, Cullen BR. Exportin-5 mediates the nuclear export of pre-microRNAs and short hairpin RNAs. Genes Dev. 2003; **17**(24): 3011-6.

19.   Yi R, Doehle BP, Qin Y, Macara IG, Cullen BR. Overexpression of exportin 5 enhances RNA interference mediated by short hairpin RNAs and microRNAs. RNA. 2005; **11**(2): 220-6.

20.   Lund E, Guttinger S, Calado A, Dahlberg JE, Kutay U. Nuclear export of microRNA precursors. Science. 2004; **303**(5654): 95-8.

21.   Bohnsack MT, Czaplinski K, Gorlich D. Exportin 5 is a RanGTP-dependent dsRNA-binding protein that mediates nuclear export of pre-miRNAs. RNA. 2004; **10**(2): 185-91.

22.   Ambros V. microRNAs: Tiny Regulators with Great Potential. Cell. 2001; **107**(7): 823-6.

23.   Lee Y, Kim M, Han J, Yeom KH, Lee S, Baek SH, Kim VN. MicroRNA genes are transcribed by RNA polymerase II. EMBO J. 2004; **23**(20): 4051-60.

24.   Kim VN. MicroRNA biogenesis: coordinated cropping and dicing. Nat Rev Mol Cell Biol. 2005; **6**(5): 376-85.

25.   Aagaard L, Rossi JJ. RNAi therapeutics: principles, prospects and challenges. Adv Drug Deliv Rev. 2007; **59**(2-3): 75-86.

26.   Tuschl T, Zamore PD, Lehmann R, Bartel DP, Sharp PA. Targeted mRNA degradation by double-stranded RNA in vitro. Genes Dev. 1999; **13**(24): 3191-7.

27.   Zamore PD, Tuschl T, Sharp PA, Bartel DP. RNAi: double-stranded RNA directs the ATP-dependent cleavage of mRNA at 21 to 23 nucleotide intervals. Cell. 2000; **101**(1): 25-33.

28.   Kim TK, Eberwine JH. Mammalian cell transfection: the present and the future. Anal Bioanal Chem. **397**(8): 3173-8.

29.   Gopalakrishnan B, Wolff J. siRNA and DNA transfer to cultured cells. Methods Mol Biol. 2009; **480**: 31-52.

30.   Mykhaylyk O, Zelphati O, Rosenecker J, Plank C. siRNA delivery by magnetofection. Curr Opin Mol Ther. 2008; **10**(5): 493-505.

31.   Sandy P, Ventura A, Jacks T. Mammalian RNAi: a practical guide. Biotechniques. 2005; **39**(2): 215-24.

32.   Maess MB, Buers I, Robenek H, Lorkowski S. Improved Protocol for Efficient Nonviral Transfection of Premature THP-1 Macrophages. Cold Spring Harb Protoc. **2011**(5).

33.   Tanaka M, Asaoka M, Yanagawa Y, Hirashima N. Long-Term Gene-Silencing Effects of siRNA Introduced by Single-Cell Electroporation into Postmitotic CNS Neurons. Neurochem Res.

34.   Tanaka M, Yanagawa Y, Hirashima N. Transfer of small interfering RNA by single-cell electroporation in cerebellar cell cultures. J Neurosci Methods. 2009; **178**(1): 80-6.

35.   Moore CB, Guthrie EH, Huang MT, Taxman DJ. Short hairpin RNA (shRNA): design, delivery, and assessment of gene knockdown. Methods Mol Biol. **629**: 141-58.

36.   Virella G, Wang AC. Immunoglobulin structure. Immunol Ser. 1993; **58**: 75-90.

37.   Goldsby RA. Kuby Immunology. 4th ed. New York: W.H. Freeman and Company; 2001.

38.   Schatz DG, Spanopoulou E. Biochemistry of V(D)J recombination. Curr Top Microbiol Immunol. 2005; **290**: 49-85.

39.   Neuberger MS. Antibody diversification by somatic mutation: from Burnet onwards. Immunol Cell Biol. 2008; **86**(2): 124.

40.   Teng G, Papavasiliou FN. Immunoglobulin Somatic Hypermutation. Annual Review of Genetics. 2007; **41**(1): 107-20.

41.   Peled JU, Kuang FL, Iglesias-Ussel MD, Roa S, Kalis SL, Goodman MF, Scharff MD. The biochemistry of somatic hypermutation. Annu Rev Immunol. 2008; **26**: 481-511.

42.   Hardy RR, Hayakawa K. B CELL DEVELOPMENT PATHWAYS. Annual Review of Immunology. 2001; **19**(1): 595-621.

43.   Kondo M, Scherer DC, King AG, Manz MG, Weissman IL. Lymphocyte development from hematopoietic stem cells. Current Opinion in Genetics & Development. 2001; **11**(5): 520.

44.   Jankovic M, Casellas R, Yannoutsos N, Wardemann H, Nussenzweig MC. RAGs AND REGULATION OF AUTOANTIBODIES. Annual Review of Immunology. 2004; **22**(1): 485.

45.   De Felice FG, Vieira MN, Saraiva LM, Figueroa-Villar JD, Garcia-Abreu J, Liu R, Chang L, Klein WL, Ferreira ST. Targeting the neurotoxic species in Alzheimer's disease: inhibitors of Abeta oligomerization. Faseb J. 2004; **18**(12): 1366-72.

46.   Ozsan GH, Dispenzieri A. Serum free light chain analysis in multiple myeloma and plasma cell dyscrasias. Expert Review of Clinical Immunology. **7**(1): 65(9).

47.   Kyle RA, Gertz MA, Witzig TE, Lust JA, Lacy MQ, Dispenzieri A, Fonseca R, Rajkumar SV, Offord JR, Larson DR, Plevak ME, Therneau TM, Greipp PR. Review of 1027 patients with newly diagnosed multiple myeloma. Mayo Clin Proc. 2003; **78**(1): 21-33.

48.   Bradwell AR, Carr-Smith HD, Mead GP, Harvey TC, Drayson MT. Serum test for assessment of patients with Bence Jones myeloma. The Lancet. 2003; **361**(9356): 489-91.

49.   Kyle RA. Sequence of testing for monoclonal gammopathies. Arch Pathol Lab Med. 1999; **123**(2): 114-8.

50.   Waldenstrom J. Abnormal proteins in myeloma. Adv Intern Med. 1952; **5**: 398-440.

51.   Kyle RA. Monoclonal gammopathy of undetermined significance. Natural history in 241 cases. Am J Med. 1978; **64**(5): 814-26.

52.   Rajkumar SV, Dispenzieri A, Kyle RA. Monoclonal gammopathy of undetermined significance, Waldenstrom macroglobulinemia, AL amyloidosis, and related plasma cell disorders: diagnosis and treatment. Mayo Clin Proc. 2006; **81**(5): 693-703.

53.   Sirohi B, Powles R. Epidemiology and outcomes research for MGUS, myeloma and amyloidosis. European Journal of Cancer. 2006; **42**(11): 1671.

54.   Harousseau J-L, Shaughnessy J, Jr., Richardson P. Multiple Myeloma. Hematology. 2004; **2004**(1): 237.

55.   San Miguel JF, Gutierrez NC, Mateo G, Orfao A. Conventional diagnostics in multiple myeloma. European Journal of Cancer. 2006; **42**(11): 1510.

56.   Kyle RA, Rajkumar SV. Multiple Myeloma. New England Journal of Medicine. 2004; **351**(18): 1860-73.

57.   Rajkumar SV, Kyle RA. Multiple myeloma: diagnosis and treatment. Mayo Clin Proc. 2005; **80**(10): 1371-82.

58.   Sezer O. Myeloma bone disease. Hematology. 2005; **10**: 19.

59.   Jacobson JL, Hussein MA, Barlogie B, Durie BGM, Crowley JJ. A new staging system for multiple myeloma patients based on the Southwest Oncology Group (SWOG) experience. British Journal of Haematology. 2003; **122**(3): 441-50.

60.   Durie BGM, Salmon SE. A clinical staging system for multiple myeloma correlation of measured myeloma cell mass with presenting clinical features, response to treatment, and survival. Cancer. 1975; **36**(3): 842-54.

61.   Greipp P, Lust J, O'Fallon W, Katzmann J, Witzig T, Kyle R. Plasma cell labeling index and beta 2-microglobulin predict survival independent of thymidine kinase and C-reactive protein in multiple myeloma [see comments]. Blood. 1993; **81**(12): 3382-7.

62.   Greipp PR, Miguel JS, Durie BGM, Crowley JJ, Barlogie B, Bladé J, Boccadoro M, Child JA, Avet-Loiseau H, Kyle RA, Lahuerta JJ, Ludwig H, Morgan G, Powles R, Shimizu K, Shustik C, Sonneveld P, Tosi P, Turesson I, Westin J. International Staging System for Multiple Myeloma. Journal of Clinical Oncology. 2005; **23**(15): 3412-20.

63.   Alexanian R, Balcerzak S, Bonnet JD, Gehan EA, Haut A, Hewlett JS, Monto RW. Prognostic factors in multiple myeloma. Cancer. 1975; **36**(4): 1192-201.

64.   Durie BG, Stock-Novack D, Salmon SE, Finley P, Beckord J, Crowley J, Coltman CA. Prognostic value of pretreatment serum beta 2 microglobulin in myeloma: a Southwest Oncology Group Study. Blood. 1990; **75**(4): 823-30.

65.   Bataille R, Durie BG, Grenier J, Sany J. Prognostic factors and staging in multiple myeloma: a reappraisal. J Clin Oncol. 1986; **4**(1): 80-7.

66.   Bataille R, Magub M, Grenier J, Donnadio D, Sany J. Serum beta-2-microglobulin in multiple myeloma: relation to presenting features and clinical status. Eur J Cancer Clin Oncol. 1982; **18**(1): 59-66.

67.   Becker N. Epidemiology of multiple myeloma. Recent Results Cancer Res. **183**: 25-35.

68.   Howlader N NA, Krapcho M, Neyman N, Aminou R, Waldron W, Altekruse SF, Kosary CL, Ruhl J, Tatalovich Z, Cho H, Mariotto A, Eisner MP, Lewis DR, Chen HS, Feuer EJ, Cronin KA. SEER Cancer Statistics Review, 1975-2008. 2010 2011 [cited; Available from: http://seer.cancer.gov/csr/1975_2008/

69.   Howe HL, Wu X, Ries LAG, Cokkinides V, Ahmed F, Jemal A, Miller B, Williams M, Ward E, Wingo PA, Ramirez A, Edwards BK. Annual report to the nation on the status of cancer, 1975–2003, featuring cancer among U.S. Hispanic/Latino populations. Cancer. 2006; **107**(8): 1711-42.

70.   Kyle R, Beard C, O'Fallon W, Kurland L. Incidence of multiple myeloma in Olmsted County, Minnesota: 1978 through 1990, with a review of the trend since 1945. Journal of Clinical Oncology. 1994; **12**(8): 1577-83.

71.   Benjamin M, Reddy S, Brawley OW. Myeloma and race: A review of the literature. Cancer and Metastasis Reviews. 2003; **22**(1): 87-93.

72.   Waxman AJ, Mink PJ, Devesa SS, Anderson WF, Weiss BM, Kristinsson SY, McGlynn KA, Landgren O. Racial disparities in incidence and outcome in multiple myeloma: a population-based study. Blood. **116**(25): 5501-6.

73.   Kohler BA, Ward E, McCarthy BJ, Schymura MJ, Ries LAG, Eheman C, Jemal A, Anderson RN, Ajani UA, Edwards BK. Annual Report to the Nation on the Status of Cancer, 1975â€"2007, Featuring Tumors of the Brain and Other Nervous System. Journal of the National Cancer Institute.

74.   Friedman GD, Herrinton LJ. Obesity and multiple myeloma. Cancer Causes Control. 1994; **5**(5): 479-83.

75.   Baris D, Brown LM, Silverman DT, Hayes R, Hoover RN, Swanson GM, Dosemeci M, Schwartz AG, Liff JM, Schoenberg JB, Pottern LM, Lubin J, Greenberg RS, Fraumeni JF, Jr. Socioeconomic status and multiple myeloma among US blacks and whites. Am J Public Health. 2000; **90**(8): 1277-81.

76.   Brown LM, Gridley G, Pottern LM, Baris D, Swanso CA, Silverman DT, Hayes RB, Greenberg RS, Swanson GM, Schoenberg JB, Schwartz AG, Fraumeni JF, Jr. Diet and nutrition as risk factors for multiple myeloma among blacks and whites in the United States. Cancer Causes Control. 2001; **12**(2): 117-25.

77.   Neriishi K, Nakashima E, Suzuki G. Monoclonal gammopathy of undetermined significance in atomic bomb survivors: incidence and transformation to multiple myeloma. Br J Haematol. 2003; **121**(3): 405-10.

78.   Preston DL, Kusumi S, Tomonaga M, Izumi S, Ron E, Kuramoto A, Kamada N, Dohy H, Matsuo T, Matsui T, et al. Cancer incidence in atomic bomb survivors. Part III. Leukemia, lymphoma and multiple myeloma, 1950-1987. Radiat Res. 1994; **137**(2 Suppl): S68-97.

79.   De Raeve HR, Vanderkerken K. The role of the bone marrow microenvironment in multiple myeloma. Histol Histopathol. 2005; **20**(4): 1227-50.

80.   Yeh HS, Berenson JR. Myeloma bone disease and treatment options. European Journal of Cancer. 2006; **42**(11): 1554.

81.   Gahrton G, Iacobelli S, Bjorkstrand B, Bourhis J, Corradini P, Crawley C, Morris C, Niederwieser D. Role of stem cell transplantation in myeloma. Hematology. 2005; **10 Suppl 1**: 127-8.

82.   Bergman LW, Kuehl WM. Co-translational modification of nascent immunoglobulin heavy and light chains. J Supramol Struct. 1979; **11**(1): 9-24.

83.   Bergman LW, Kuehl WM. Formation of intermolecular disulfide bonds on nascent immunoglobulin polypeptides. Journal of Biological Chemistry. 1979; **254**(13): 5690-4.

84.   Abraham RS, Clark RJ, Bryant SC, Lymp JF, Larson T, Kyle RA, Katzmann JA. Correlation of Serum Immunoglobulin Free Light Chain Quantification with Urinary Bence Jones Protein in Light Chain Myeloma. Clin Chem. 2002; **48**(4): 655-7.

85.   Katzmann JA, Clark RJ, Abraham RS, Bryant S, Lymp JF, Bradwell AR, Kyle RA. Serum Reference Intervals and Diagnostic Ranges for Free {kappa} and Free {lambda} Immunoglobulin Light Chains: Relative Sensitivity for Detection of Monoclonal Light Chains. Clin Chem. 2002; **48**(9): 1437-44.

86.   Pesce AJ, Clyne DH, Pollak VE, Kant SK, Foulkes EC, Selenke WM. Renal tubular interactions of proteins. Clinical Biochemistry. 1980; **13**(5): 209-15.

87.   Torra R, Blade J, Cases A, Lopez-Pedret J, Montserrat E, Rozman C, Revert L. Patients with multiple myeloma requiring long-term dialysis: presenting features, response to therapy, and outcome in a series of 20 cases. Br J Haematol. 1995; **91**(4): 854-9.

88.   Irish AB, Winearls CG, Littlewood T. Presentation and survival of patients with severe renal failure and myeloma. QJM. 1997; **90**(12): 773-80.

89.   Blade J, Fernandez-Llama P, Bosch F, Montoliu J, Lens XM, Montoto S, Cases A, Darnell A, Rozman C, Montserrat E. Renal Failure in Multiple Myeloma: Presenting Features and Predictors of Outcome in 94 Patients From a Single Institution. Arch Intern Med. 1998; **158**(17): 1889-93.

90.   Sanders PW, Booker BB. Pathobiology of cast nephropathy from human Bence Jones proteins. J Clin Invest. 1992; **89**(2): 630-9.

91.   Pote A, Zwizinski C, Simon EE, Meleg-Smith S, Batuman V. Cytotoxicity of Myeloma Light Chains in Cultured Human Kidney Proximal Tubule Cells. American Journal of Kidney Diseases. 2000; **36**(4): 735.

92.   Wall J, Schell M, Murphy C, Hrncic R, Stevens FJ, Solomon A. Thermodynamic instability of human lambda 6 light chains: correlation with fibrillogenicity. Biochemistry. 1999; **38**(42): 14101-8.

93.   Bellotti V, Merlini G, Bucciarelli E, Perfetti V, Quaglini S, Ascari E. Relevance of class, molecular weight and isoelectric point in predicting human light chain amyloidogenicity. Br J Haematol. 1990; **74**(1): 65-9.

94.   Perfetti V, Casarini S, Palladini G, Vignarelli MC, Klersy C, Diegoli M, Ascari E, Merlini G. Analysis of VÎ»-JÎ» expression in plasma cells from primary (AL) amyloidosis and normal bone marrow identifies 3r(Î»III) as a new amyloid-associated germline gene segment. Blood. 2002; **100**(3): 948-53.

95.   Pozzi C, D'Amico M, Fogazzi GB, Curioni S, Ferrario F, Pasquali S, Quattrocchio G, Rollino C, Segagni S, Locatelli F. Light chain deposition disease with renal involvement: clinical characteristics and prognostic factors. Am J Kidney Dis. 2003; **42**(6): 1154-63.

96.   Comenzo RL, Zhang Y, Martinez C, Osman K, Herrera GA. The tropism of organ involvement in primary systemic amyloidosis: contributions of Ig V L germ line gene use and clonal plasma cell burden. Blood. 2001; **98**(3): 714-20.

97.   Batuman V, Verroust PJ, Navar GL, Kaysen JH, Goda FO, Campbell WC, Simon E, Pontillon F, Lyles M, Bruno J, Hammond TG. Myeloma light chains are ligands for cubilin (gp280). Am J Physiol Renal Physiol. 1998; **275**(2): F246-54.

98.   Batuman V, Guan S. Receptor-mediated endocytosis of immunoglobulin light chains by renal proximal tubule cells. Am J Physiol. 1997; **272**(4 Pt 2): F521-30.

99.   Basic-Jukic N, Kes P, Labar B. Myeloma kidney: pathogenesis and treatment. Acta Med Croatica. 2001; **55**(4-5): 169-75.

100.   Fletcher AP, Neuberger A, Ratcliffe WA. Tamm-Horsfall urinary glycoprotein. The subunit structure. Biochem J. 1970; **120**(2): 425-32.

101.   Huang ZQ, Kirk KA, Connelly KG, Sanders PW. Bence Jones proteins bind to a common peptide segment of Tamm-Horsfall glycoprotein to promote heterotypic aggregation. J Clin Invest. 1993; **92**(6): 2975-83.

102.   Bachmann S, Metzger R, Bunnemann B. Tamm-Horsfall protein-mRNA synthesis is localized to the thick ascending limb of Henle's loop in rat kidney. Histochemistry. 1990; **94**(5): 517-23.

103.   Holland MD, Galla JH, Sanders PW, Luke RG. Effect of urinary pH and diatrizoate on Bence Jones protein nephrotoxicity in the rat. Kidney Int. 1985; **27**(1): 46-50.

104.   Huang ZQ, Sanders PW. Biochemical interaction between Tamm-Horsfall glycoprotein and Ig light chains in the pathogenesis of cast nephropathy. Lab Invest. 1995; **73**(6): 810-7.

105.   Merlini G, Pozzi C. Mechanisms of renal damage in plasma cell dyscrasias: an overview. Contrib Nephrol. 2007; **153**: 66-86.

106.   Defronzo RA, Humphrey RL, Wright JR, Cooke CR. Acute renal failure in multiple myeloma. Medicine (Baltimore). 1975; **54**(3): 209-23.

107.   Batuman V, Sastrasinh M, Sastrasinh S. Light chain effects on alanine and glucose uptake by renal brush border membranes. Kidney Int. 1986; **30**(5): 662-5.

108.   Batuman V, Guan S, O'Donovan R, Puschett JB. Effect of myeloma light chains on phosphate and glucose transport in renal proximal tubule cells. Ren Physiol Biochem. 1994; **17**(6): 294-300.

109.   Randall RE, Williamson Jr WC, Mullinax F, Tung MY, Still WJS. Manifestations of systemic light chain deposition. The American Journal of Medicine. 1976; **60**(2): 293-9.

110.   RONCO PM, ALYANAKIAN M-A, MOUGENOT B, AUCOUTURIER P. Light Chain Deposition Disease: A Model of Glomerulosclerosis Defined at the Molecular Level. Journal of the American Society of Nephrology. 2001; **12**(7): 1558-65.

111.   Masai R, Wakui H, Togashi M, Maki N, Ohtani H, Komatsuda A, Sawada K. Clinicopathological features and prognosis in immunoglobulin light and heavy chain deposition disease. Clin Nephrol. 2009; **71**(1): 9-20.

112.   Tsakiris DJ, Stel VS, Finne P, Fraser E, Heaf J, de Meester J, Schmaldienst S, Dekker F, Verrina E, Jager KJ. Incidence and outcome of patients starting renal replacement therapy for end-stage renal disease due to multiple myeloma or light-chain deposit disease: an ERA-EDTA Registry study. Nephrol Dial Transplant. **25**(4): 1200-6.

113.   Teng J, Russell WJ, Gu X, Cardelli J, Jones ML, Herrera GA. Different types of glomerulopathic light chains interact with mesangial cells using a common receptor but exhibit different intracellular trafficking patterns. Lab Invest. 2004; **84**(4): 440.

114.   Keeling J, Teng J, Herrera GA. AL-amyloidosis and light-chain deposition disease light chains induce divergent phenotypic transformations of human mesangial cells. Lab Invest. 2004; **84**(10): 1322.

115.   Zhu L, Herrera GA, Murphy-Ullrich JE, Huang ZQ, Sanders PW. Pathogenesis of glomerulosclerosis in light chain deposition disease. Role for transforming growth factor-beta. Am J Pathol. 1995; **147**(2): 375-85.

116.   Lorenz EC, Gertz MA, Fervenza FC, Dispenzieri A, Lacy MQ, Hayman SR, Gastineau DA, Leung N. Long-term outcome of autologous stem cell transplantation in light chain deposition disease. Nephrol Dial Transplant. 2008; **23**(6): 2052-7.

117.   Fujita H, Hishizawa M, Sakamoto S, Kondo T, Kadowaki N, Ishikawa T, Itoh J, Fukatsu A, Uchiyama T, Takaori-Kondo A. Durable hematological response and improvement of nephrotic syndrome on thalidomide therapy in a patient with refractory light chain deposition disease. Int J Hematol.

118.   Harada K, Akai Y, Sakan H, Yamaguchi Y, Nakatani K, Iwano M, Saito Y. Resolution of mesangial light chain deposits 3 years after high-dose melphalan with autologous peripheral blood stem cell transplantation. Clin Nephrol. **74**(5): 384-8.

119.   Westermark P, Benson MD, Buxbaum JN, Cohen AS, Frangione B, Ikeda S, Masters CL, Merlini G, Saraiva MJ, Sipe JD. A primer of amyloid nomenclature. Amyloid. 2007; **14**(3): 179-83.

120.   Westermark P, Benson MD, Buxbaum JN, Cohen AS, Frangione B, Ikeda S, Masters CL, Merlini G, Saraiva MJ, Sipe JD. Amyloid: toward terminology clarification. Report from the Nomenclature Committee of the International Society of Amyloidosis. Amyloid. 2005; **12**(1): 1-4.

121.   Pepys MB. Amyloidosis. Annu Rev Med. 2005.

122.   Gertz MA, Lacy MQ, Dispenzieri A, Hayman SR. Amyloidosis. Best Pract Res Clin Haematol. 2005; **18**(4): 709-27.

123.   Gahrton G, Durie BGM, Samson DM. Multiple myeloma and related disorders. London New York, NY: Arnold ;

Distributed in the United States of America by Oxford University Press; 2004.

124.   Rajkumar SV, Gertz MA, Kyle RA. Primary systemic amyloidosis with delayed progression to multiple myeloma. Cancer. 1998; **82**(8): 1501-5.

125.   Dykxhoorn DM, Schlehuber LD, London IM, Lieberman J. Determinants of specific RNA interference-mediated silencing of human beta-globin alleles differing by a single nucleotide polymorphism. PNAS. 2006; **103**(15): 5953-8.

126.   Gertz MA. Immunoglobulin light chain amyloidosis: 2011 update on diagnosis, risk-stratification, and management. American Journal of Hematology. **86**(2): 180-6.

127.   Wall JS, Gupta V, Wilkerson M, Schell M, Loris R, Adams P, Solomon A, Stevens F, Dealwis C. Structural basis of light chain amyloidogenicity: comparison of the thermodynamic properties, fibrillogenic potential and tertiary structural features of four Vlambda6 proteins. J Mol Recognit. 2004; **17**(4): 323-31.

128.   Solomon A, Frangione B, Franklin EC. Bence Jones proteins and light chains of immunoglobulins. Preferential association of the V lambda VI subgroup of human light chains with amyloidosis AL (lambda). J Clin Invest. 1982; **70**(2): 453-60.

129.   Falk RH, Comenzo RL, Skinner M. The systemic amyloidoses. N Engl J Med. 1997;
337(13): 898-909.

130.   Kyle RA, Gertz MA. Primary systemic amyloidosis: clinical and laboratory features in 474
cases. Semin Hematol. 1995; **32**(1): 45-59.

131.   Hawkins PN, Richardson S, MacSweeney JE, King AD, Vigushin DM, Lavender JP, Pepys
MB. Scintigraphic quantification and serial monitoring of human visceral amyloid deposits provide
evidence for turnover and regression. Q J Med. 1993; **86**(6): 365-74.

132.   Slifka MK, Antia R, Whitmire JK, Ahmed R. Humoral immunity due to long-lived plasma
cells. Immunity. 1998; **8**(3): 363-72.

133.   Gianni L, Bellotti V, Gianni AM, Merlini G. New drug therapy of amyloidoses: resorption
of AL-type deposits with 4'-iodo-4'-deoxydoxorubicin. Blood. 1995; **86**(3): 855-61.

134.   Pepys MB, Herbert J, Hutchinson WL, Tennent GA, Lachmann HJ, Gallimore JR, Lovat
LB, Bartfai T, Alanine A, Hertel C, Hoffmann T, Jakob-Roetne R, Norcross RD, Kemp JA,
Yamamura K, Suzuki M, Taylor GW, Murray S, Thompson D, Purvis A, Kolstoe S, Wood SP,
Hawkins PN. Targeted pharmacological depletion of serum amyloid P component for treatment of
human amyloidosis. Nature. 2002; **417**(6886): 254-9.

135.   Hrncic R, Wall J, Wolfenbarger DA, Murphy CL, Schell M, Weiss DT, Solomon A.
Antibody-mediated resolution of light chain-associated amyloid deposits. Am J Pathol. 2000;
157(4): 1239-46.

136.   Durie BG, Kyle RA, Belch A, Bensinger W, Blade J, Boccadoro M, Child JA, Comenzo R,
Djulbegovic B, Fantl D, Gahrton G, Harousseau JL, Hungria V, Joshua D, Ludwig H, Mehta J,
Morales AR, Morgan G, Nouel A, Oken M, Powles R, Roodman D, San Miguel J, Shimizu K,
Singhal S, Sirohi B, Sonneveld P, Tricot G, Van Ness B. Myeloma management guidelines: a

consensus report from the Scientific Advisors of the International Myeloma Foundation. Hematol J. 2003; **4**(6): 379-98.

137.   Fenk R, Schneider P, Kropff M, Huenerlituerkoglu AN, Steidl U, Aul C, Hildebrandt B, Haas R, Heyll A, Kobbe G. High-dose idarubicin, cyclophosphamide and melphalan as conditioning for autologous stem cell transplantation increases treatment-related mortality in patients with multiple myeloma: results of a randomised study. Br J Haematol. 2005; **130**(4): 588-94.

138.   Rajkumar SV, Kyle RA. Conventional therapy and approach to management. Best Pract Res Clin Haematol. 2005; **18**(4): 585-601.

139.   Blokhin N, Larionov L, Perevodchikova N, Chebotareva L, Merkulova N. [Clinical experiences with sarcolysin in neoplastic diseases]. Ann N Y Acad Sci. 1958; **68**(3): 1128-32.

140.   Salmon SE, Shadduck RK, Schilling A. Intermittent high-dose prednisone (NSC-10023) therapy for multiple myeloma. Cancer Chemother Rep. 1967; **51**(3): 179-87.

141.   Barlogie B, Smith L, Alexanian R. Effective treatment of advanced multiple myeloma refractory to alkylating agents. N Engl J Med. 1984; **310**(21): 1353-6.

142.   McElwain TJ, Powles RL. High-dose intravenous melphalan for plasma-cell leukaemia and myeloma. Lancet. 1983; **2**(8354): 822-4.

143.   McElwain TJ, Selby PJ, Gore ME, Viner C, Meldrum M, Millar BC, Malpas JS. High-dose chemotherapy and autologous bone marrow transplantation for myeloma. Eur J Haematol Suppl. 1989; **51**: 152-6.

144.   Barlogie B, Hall R, Zander A, Dicke K, Alexanian R. High-dose melphalan with autologous bone marrow transplantation for multiple myeloma. Blood. 1986; **67**(5): 1298-301.

145.   Barlogie B, Alexanian R, Dicke K, Zagars G, Spitzer G, Jagannath S, Horwitz L. High-dose chemoradiotherapy and autologous bone marrow transplantation for resistant multiple myeloma. Blood. 1987; **70**(3): 869-72.

146.   Barlogie B. The role of transplant in multiple myeloma. Clin Adv Hematol Oncol. 2005; **3**(8): 604-6.

147.   Harousseau JL, Attal M, Divine M, Milpied N, Marit G, Leblond V, Stoppa AM, Bourhis JH, Caillot D, Boasson M, et al. Comparison of autologous bone marrow transplantation and peripheral blood stem cell transplantation after first remission induction treatment in multiple myeloma. Bone Marrow Transplant. 1995; **15**(6): 963-9.

148.   Harousseau JL, Attal M. The role of autologous hematopoietic stem cell transplantation in multiple myeloma. Semin Hematol. 1997; **34**(1 Suppl 1): 61-6.

149.   Murphy CL, Kestler DP, Foster JS, Wang S, Macy SD, Kennel SJ, Carlson ER, Hudson J, Weiss DT, Solomon A. Odontogenic ameloblast-associated protein nature of the amyloid found in calcifying epithelial odontogenic tumors and unerupted tooth follicles. Amyloid. 2008; **15**(2): 89-95.

150.   Attal M, Harousseau J-L, Stoppa A-M, Sotto J-J, Fuzibet J-G, Rossi J-Fo, Casassus P, Maisonneuve H, Facon T, Ifrah N, Payen C, Bataille Rg. A Prospective, Randomized Trial of Autologous Bone Marrow Transplantation and Chemotherapy in Multiple Myeloma. New England Journal of Medicine. 1996; **335**(2): 91-7.

151.   Child JA, Morgan GJ, Davies FE, Owen RG, Bell SE, Hawkins K, Brown J, Drayson MT, Selby PJ. High-Dose Chemotherapy with Hematopoietic Stem-Cell Rescue for Multiple Myeloma. New England Journal of Medicine. 2003; **348**(19): 1875-83.

152.   Palumbo A, Triolo S, Argentino C, Bringhen S, Dominietto A, Rus C, Omedè P, Tarella C, Pileri A, Boccadoro M. Dose-Intensive Melphalan With Stem Cell Support (MEL100) Is Superior to Standard Treatment in Elderly Myeloma Patients. Blood. 1999; **94**(4): 1248-53.

153.   Palumbo A, Bringhen S, Petrucci MT, Musto P, Rossini F, Nunzi M, Lauta VM, Bergonzi C, Barbui A, Caravita T, Capaldi A, Pregno P, Guglielmelli T, Grasso M, Callea V, Bertola A, Cavallo F, Falco P, Rus C, Massaia M, Mandelli F, Carella AM, Pogliani E, Liberati AM, Dammacco F, Ciccone G, Boccadoro M. Intermediate-dose melphalan improves survival of myeloma patients aged 50 to 70: results of a randomized controlled trial. Blood. 2004; **104**(10): 3052-7.

154.   San Miguel JF, Lahuerta JJ, Garcia-Sanz R, Alegre A, Blade J, Martinez R, Garcia-Larana J, De La Rubia J, Sureda A, Vidal MJ, Escudero A, Perez-Esquiza E, Conde E, Garcia-Ruiz JC, Cabrera R, Caballero D, Moraleda JM, Leon A, Besalduch J, Hernandez MT, Rifon J, Hernandez F, Solano C, Palomera L, Parody R, Gonzalez JD, Mataix R, Maldonado J, Constela J, Carrera D, Bello JL, De Pablos JM, Perez-Simon JA, Torres JP, Olanguren J, Prieto E, Acebede G, Penarrubia MJ, Torres P, Diez-Martin JL, Rivas A, Sanchez JM, Diaz-Mediavilla J. Are myeloma patients with renal failure candidates for autologous stem cell transplantation? Hematol J. 2000; **1**(1): 28-36.

155.   Hales BF. Thalidomide on the comeback trail. Nat Med. 1999; **5**(5): 489-90.

156.   Olson KB, Hall TC, Horton J, Khung CL, Hosley HF. Thalidomide (N-Phthaloylglutamimide) in the Treatment of Advanced Cancer. Clin Pharmacol Ther. 1965; **6**: 292-7.

157.   Godal HC, Borchgrevink CF. The effect of plasmapheresis on the hemostatic function in patients with macroglobulinemia Waldenstrom and multiple myeloma. Scand J Clin Lab Invest. 1965; **17**: Suppl 84:133-7.

158.   Feest TG, Burge PS, Cohen SL. Successful treatment of myeloma kidney by diuresis and plasmaphoresis. Br Med J. 1976; **1**(6008): 503-4.

159.   Dispenzieri A, Kyle RA, Lacy MQ, Therneau TM, Larson DR, Plevak MF, Rajkumar SV, Fonseca R, Greipp PR, Witzig TE, Lust JA, Zeldenrust SR, Snow DS, Hayman SR, Litzow MR, Gastineau DA, Tefferi A, Inwards DJ, Micallef IN, Ansell SM, Porrata LF, Elliott MA, Gertz MA. Superior survival in primary systemic amyloidosis patients undergoing peripheral blood stem cell transplantation: a case-control study. Blood. 2004; **103**(10): 3960-3.

160.   Katayama I, Sawada Y, Yokozeki H, Nishioka K, Akiba T. Successful treatment of systemic amyloidosis by combination chemotherapy and plasmapheresis. Effect on plasma IL6 and serum amyloid protein A. Int J Dermatol. 1994; **33**(9): 672-3.

161.   El-Achkar TM, Sharfuddin AA, Dominguez J. Approach to Acute Renal Failure With Multiple Myeloma: Role of Plasmapheresis. Therapeutic Apheresis and Dialysis. 2005; **9**(5): 417-22.

162.   Helen J. Lachmann RGJDGHDC-SARBMBPPNH. Outcome in systemic AL amyloidosis in relation to changes in concentration of circulating free immunoglobulin light chains following chemotherapy. British Journal of Haematology. 2003; **122**(1): 78-84.

163.   Maroun Khoury VEGCAGRYCLDSCJFA. Efficient suppression of murine arthritis by combined anticytokine small interfering RNA lipoplexes. Arthritis & Rheumatism. 2008; **58**(8): 2356-67.

164.   Gu W, Putral L, Hengst K, Minto K, Saunders NA, Leggatt G, McMillan NAJ. Inhibition of cervical cancer cell growth in vitro and in vivo with lentiviral-vector delivered short hairpin RNA targeting human papillomavirus E6 and E7 oncogenes. Cancer Gene Therapy. 2006; **13**(11): 1023.

165.   Bilanges B, Stokoe D. Direct comparison of the specificity of gene silencing using antisense oligonucleotides and RNAi. Biochem J. 2005; **388**(Pt 2): 573-83.

166.   He S, Zhang D, Cheng F, Gong F, Guo Y. Applications of RNA interference in cancer therapeutics as a powerful tool for suppressing gene expression. Molecular Biology Reports.

167.   Elders RC, Holder A, Baines SJ, Argyle D, Catchpole B. Targeted knockdown of canine KIT (stem cell factor receptor) using RNA interference. Veterinary Immunology and Immunopathology. **141**(1-2): 151-6.

168.   Frank-Kamenetsky M, Grefhorst A, Anderson NN, Racie TS, Bramlage B, Akinc A, Butler D, Charisse K, Dorkin R, Fan Y, Gamba-Vitalo C, Hadwiger P, Jayaraman M, John M, Jayaprakash KN, Maier M, Nechev L, Rajeev KG, Read T, Rohl I, Soutschek J, Tan P, Wong J, Wang G, Zimmermann T, de Fougerolles A, Vornlocher H-P, Langer R, Anderson DG, Manoharan M, Koteliansky V, Horton JD, Fitzgerald K. Therapeutic RNAi targeting PCSK9 acutely lowers plasma cholesterol in rodents and LDL cholesterol in nonhuman primates. Proceedings of the National Academy of Sciences. 2008; **105**(33): 11915-20.

169.   Lan-Yang Ca, Chin-Ping Y, Besl L, Schell M, Solomon A. Identification and characterization of a functional human Ig V[lambda]VI germline gene. Molecular Immunology. 1994; **31**(7): 531-6.

170.   Matsuoka Y, Moore GE, Yagi Y, Pressman D. Production of free light chains of immunoglobulin by a hematopoietic cell line derived from a patient with multiple myeloma. Proc Soc Exp Biol Med. 1967; **125**(4): 1246-50.

171.   Stewart SA, Dykxhoorn DM, Palliser D, Mizuno H, Yu EY, An DS, Sabatini DM, Chen IS, Hahn WC, Sharp PA, Weinberg RA, Novina CD. Lentivirus-delivered stable gene silencing by RNAi in primary cells. RNA. 2003; **9**(4): 493-501.

172.   Kissler S, Stern P, Takahashi K, Hunter K, Peterson LB, Wicker LS. In vivo RNA interference demonstrates a role for Nramp1 in modifying susceptibility to type 1 diabetes. Nat Genet. 2006; **38**(4): 479-83.

173.   Abe M, Goto T, Kennel SJ, Wolfenbarger D, Macy SD, Weiss DT, Solomon A. Production and immunodiagnostic applications of antihuman light chain monoclonal antibodies. Am J Clin Pathol. 1993; **100**(1): 67-74.

174.   Martinez J, Patkaniowska A, Urlaub H, Lührmann R, Tuschl T. Single-Stranded Antisense siRNAs Guide Target RNA Cleavage in RNAi. Cell. 2002; **110**(5): 563-74.

175.   Kurosawa T, Igarashi S, Nishizawa M, Onodera O. Selective silencing of a mutant transthyretin allele by small interfering RNAs. Biochem Biophys Res Commun. 2005; **337**(3): 1012-8.

176.   Ralph GS, Radcliffe PA, Day DM, Carthy JM, Leroux MA, Lee DC, Wong LF, Bilsland LG, Greensmith L, Kingsman SM, Mitrophanous KA, Mazarakis ND, Azzouz M. Silencing mutant SOD1 using RNAi protects against neurodegeneration and extends survival in an ALS model. Nat Med. 2005; **11**(4): 429-33.

177.   Kim DH, Behlke MA, Rose SD, Chang MS, Choi S, Rossi JJ. Synthetic dsRNA Dicer substrates enhance RNAi potency and efficacy. Nat Biotechnol. 2005; **23**(2): 222-6.

178.   Gu S, Jin L, Zhang F, Huang Y, Grimm D, Rossi JJ, Kay MA. Thermodynamic stability of small hairpin RNAs highly influences the loading process of different mammalian Argonautes. Proceedings of the National Academy of Sciences.

179.   Turner JJ, Jones S, Fabani MM, Ivanova G, Arzumanov AA, Gait MJ. RNA targeting with peptide conjugates of oligonucleotides, siRNA and PNA. Blood Cells, Molecules, and Diseases. **In Press, Corrected Proof**.

180.   Toub N, Malvy C, Fattal E, Couvreur P. Innovative nanotechnologies for[no-break space]the[no-break space]delivery of[no-break space]oligonucleotides and[no-break space]siRNA. Biomedecine & Pharmacotherapy. 2006; **60**(9): 607.

181.   Merlini G, Stone MJ. Dangerous small B-cell clones. Blood. 2006; **108**(8): 2520-30.

182.   Pozzi C, Locatelli F. Kidney and liver involvement in monoclonal light chain disorders. Semin Nephrol. 2002; **22**(4): 319-30.

183.   Yoshita M, Ishida C, Yanase D, Yamada M. Immunoglobulin light-chain (AL) amyloidosis with myasthenic symptoms and echocardiographic features of dilated cardiomyopathy. Intern Med. 2006; **45**(3): 159-62.

184.   Keller LS, Faull RJ, Smith P, Swift J, Bannister KM, Otto S, Peh CA. Crystalloid deposits in the kidney. Nephrology (Carlton). 2005; **10**(1): 81-3.

185.   Lacy MQ, Gertz MA. Acquired Fanconi's syndrome associated with monoclonal gammopathies. Hematol Oncol Clin North Am. 1999; **13**(6): 1273-80.

186.   Tanenbaum ND, Howell DN, Middleton JP, Spurney RF. Lambda light chain deposition disease in a renal allograft. Transplant Proc. 2005; **37**(10): 4289-92.

187.   Comenzo RL, Gertz MA. Autologous stem cell transplantation for primary systemic amyloidosis. Blood. 2002; **99**(12): 4276-82.

188.   Herrera GA, Joseph L, Gu X, Hough A, Barlogie B. Renal Pathologic Spectrum in an Autopsy Series of Patients With Plasma Cell Dyscrasia. Archives of Pathology & Laboratory Medicine. 2004; **128**(8): 875.

189.   Leung N, Gertz MA, Zeldenrust SR, Rajkumar SV, Dispenzieri A, Fervenza FC, Kumar S, Lacy MQ, Lust JA, Greipp PR, Witzig TE, Hayman SR, Russell SJ, Kyle RA, Winters JL. Improvement of cast nephropathy with plasma exchange depends on the diagnosis and on reduction of serum free light chains. Kidney Int. 2008; **73**(11): 1282-8.

190.   Ohno S, Yoshimoto M, Honda S, Miyachi S, Ishida T, Itoh F, Endo T, Chiba S, Imai K. The antisense approach in amyloid light chain amyloidosis: identification of monoclonal Ig and inhibition of its production by antisense oligonucleotides in in vitro and in vivo models. J Immunol. 2002; **169**(7): 4039-45.

191.   Shi Y. Mammalian RNAi for the masses. Trends Genet. 2003; **19**(1): 9-12.

192.   Yin J, Ma Z, Selliah N, Shivers DK, Cron RQ, Finkel TH. Effective gene suppression using small interfering RNA in hard-to-transfect human T cells. J Immunol Methods. 2006.

193.   Baker BE, Kestler DP, Ichiki AT. Effects of siRNAs in combination with Gleevec on K-562 cell proliferation and Bcr-Abl expression. J Biomed Sci. 2006; **13**(4): 499-507.

194.   Lin W, Zhang J, Zhang J, Liu X, Fei Z, Li X, Davidovic L, Tang Z, Shen L, Deng Y, Yang A, Han H, Zhang X, Yao L. RNAi-mediated inhibition of MSP58 decreases tumor growth, migration and invasion in a human glioma cell line. J Cell Mol Med. 2008.

195.   Wang W, Yen H, Chen CH, Soni R, Jasani N, Sylvestre G, Reznik SE. The endothelin-converting enzyme-1/endothelin-1 pathway plays a critical role in inflammation-associated premature delivery in a mouse model. Am J Pathol. 2008; **173**(4): 1077-84.

196.   Ramy AR, Gardner L, Mahrous E, Taxman DJ, Legros LL, Rowe S, Ting JP, Geller AM, Kotb M. Selective targeting of leukemic cells growth in vivo and in vitro using a gene silencing approach to diminish S-adenosylmethionine (SAMe) synthesis. J Biol Chem. 2008.

197.   Whelan J. First clinical data on RNAi. Drug Discov Today. 2005; **10**(15): 1014-5.

198.   DeVincenzo J, Cehelsky JE, Alvarez R, Elbashir S, Harborth J, Toudjarska I, Nechev L, Murugaiah V, Van Vliet A, Vaishnaw AK, Meyers R. Evaluation of the safety, tolerability and pharmacokinetics of ALN-RSV01, a novel RNAi antiviral therapeutic directed against respiratory syncytial virus (RSV). Antiviral Res. 2008; **77**(3): 225-31.

199.   Lee GM, Kim JH, Lee HG. Flow cytometric analysis of antibody producing cells using double immunofluorescent staining. Biotechnology Techniques. 1996; **10**(8): 615.

200.   Bertrand J-R, Pottier M, Vekris A, Opolon P, Maksimenko A, Malvy C. Comparison of antisense oligonucleotides and siRNAs in cell culture and in vivo. Biochemical and Biophysical Research Communications. 2002; **296**(4): 1000.

201.   Feng X, Zhao P, He Y, Zuo Z. Allele-specific silencing of Alzheimer's disease genes: The amyloid precursor protein genes with Swedish or London mutations. Gene. **In Press, Corrected Proof**.

202.   Low J, Shuguang H, Dowless M, Blosser W, Vincent T, Davis S, Hodson J, Koller E, Marcusson E, Blanchard K, Stancato L. High-Content Imaging Analysis of the Knockdown Effects of Validated siRNAs and Antisense Oligonucleotides. J Biomol Screen. 2007; **12**(6): 775-88.

203.   Hiroi N, Funahashi A, Kitano H. Comparative studies of suppression of malignant cancer cell phenotype by antisense oligo DNA and small interfering RNA. Cancer Gene Ther. 2006; **13**(1): 7-12.

204.   Grimm D, Streetz KL, Jopling CL, Storm TA, Pandey K, Davis CR, Marion P, Salazar F, Kay MA. Fatality in mice due to oversaturation of cellular microRNA/short hairpin RNA pathways. Nature. 2006; **441**(7092): 537.

205.   Ma Z, Li J, He F, Wilson A, Pitt B, Li S. Cationic lipids enhance siRNA-mediated interferon response in mice. Biochem Biophys Res Commun. 2005; **330**(3): 755-9.

206.   Fedorov Y, Anderson EM, Birmingham A, Reynolds A, Karpilow J, Robinson K, Leake D, Marshall WS, Khvorova A. Off-target effects by siRNA can induce toxic phenotype. Rna. 2006; **12**(7): 1188-96.

207.   Soutschek J, Akinc A, Bramlage B, Charisse K, Constien R, Donoghue M, Elbashir S, Geick A, Hadwiger P, Harborth J, John M, Kesavan V, Lavine G, Pandey RK, Racie T, Rajeev KG, Rohl I, Toudjarska I, Wang G, Wuschko S, Bumcrot D, Koteliansky V, Limmer S, Manoharan M, Vornlocher H-P. Therapeutic silencing of an endogenous gene by systemic administration of modified siRNAs. Nature. 2004; **432**(7014): 173.

208.   Akhtar S, Benter IF. Nonviral delivery of synthetic siRNAs in vivo. J Clin Invest. 2007; **117**(12): 3623-32.

209.   Shao Y, Chan CY, Maliyekkel A, Lawrence CE, Roninson IB, Ding Y. Effect of target secondary structure on RNAi efficiency. Rna. 2007; **13**(10): 1631-40.

210.   Sioud M. siRNA Delivery In Vivo. Methods Mol Biol. 2005; **309**: 237-50.

211.   Ohara PT, Vit J-P, Bhargava A, Jasmin L. Evidence for a role of connexin 43 in trigeminal pain using RNA interference in vivo. J Neurophysiol. 2008: 90722.2008.

212.   Fernandes MS, Gomes EM, Butcher LD, Hernandez-Alcoceba R, Chang D, Kansopon J, Newman J, Stone MJ, Tong AW. Growth Inhibition of Human Multiple Myeloma Cells by an

Oncolytic Adenovirus Carrying the CD40 Ligand Transgene. Clinical Cancer Research. 2009; **15**(15): 4847-56.

213.   De Vos J, Bagnis C, Bonnafoux L, Requirand G, Jourdan M, Imbert MC, Jourdan E, Rossi JF, Mannoni P, Klein B. Comparison of murine leukemia virus, human immunodeficiency virus, and adeno-associated virus vectors for gene transfer in multiple myeloma: lentiviral vectors demonstrate a striking capacity to transduce low-proliferating primary tumor cells. Hum Gene Ther. 2003; **14**(18): 1727-39.

214.   Pan D, Gunther R, Duan W, Wendell S, Kaemmerer W, Kafri T, Verma IM, Whitley CB. Biodistribution and toxicity studies of VSVG-pseudotyped lentiviral vector after intravenous administration in mice with the observation of in vivo transduction of bone marrow. Mol Ther. 2002; **6**(1): 19-29.

215.   Couto LB, High KA. Viral vector-mediated RNA interference. Current Opinion in Pharmacology. **10**(5): 534-42.

216.   Dull T, Zufferey R, Kelly M, Mandel RJ, Nguyen M, Trono D, Naldini L. A third-generation lentivirus vector with a conditional packaging system. J Virol. 1998; **72**(11): 8463-71.

217.   Rabin N, Kyriakou C, Coulton L, Gallagher OM, Buckle C, Benjamin R, Singh N, Glassford J, Otsuki T, Nathwani AC, Croucher PI, Yong KL. A new xenograft model of myeloma bone disease demonstrating the efficacy of human mesenchymal stem cells expressing osteoprotegerin by lentiviral gene transfer. Leukemia. 2007; **21**(10): 2181-91.

218.   Zhang S, Suvannasankha A, Crean CD, White VL, Chen CS, Farag SS. The novel histone deacetylase inhibitor, AR-42, inhibits gp130/Stat3 pathway and induces apoptosis and cell cycle arrest in multiple myeloma cells. Int J Cancer. **129**(1): 204-13.

219.   Yue J, Sheng Y, Ren A, Penmatsa S. A miR-21 hairpin structure-based gene knockdown vector. Biochem Biophys Res Commun. **394**(3): 667-72.

220.   Peng K-W, Ahmann GJ, Pham L, Greipp PR, Cattaneo R, Russell SJ. Systemic therapy of myeloma xenografts by an attenuated measles virus. Blood. 2001; **98**(7): 2002-7.

221.   Douglas T, Young M. Viruses: Making Friends with Old Foes. Science. 2006; **312**(5775): 873-5.

222.   Lu X, Humeau L, Slepushkin V, Binder G, Yu Q, Slepushkina T, Chen Z, Merling R, Davis B, Chang Y-N, Dropulic B. Safe two-plasmid production for the first clinical lentivirus vector that achieves >99% transduction in primary cells using a one-step protocol. The Journal of Gene Medicine. 2004; **6**(9): 963-73.

223.   Bosma GC, Custer RP, Bosma MJ. A severe combined immunodeficiency mutation in the mouse. Nature. 1983; **301**(5900): 527-30.

224.   Bosma MJ, Carroll AM. The SCID mouse mutant: definition, characterization, and potential uses. Annu Rev Immunol. 1991; **9**: 323-50.

225.   Mombaerts P, Iacomini J, Johnson RS, Herrup K, Tonegawa S, Papaioannou VE. RAG-1-deficient mice have no mature B and T lymphocytes. Cell. 1992; **68**(5): 869-77.

226.   Schatz DG, Ji Y. Recombination centres and the orchestration of V(D)J recombination. Nat Rev Immunol. **11**(4): 251-63.

227.   Sakaguchi N, Maeda K, Kuwahara K. Molecular mechanism of immunoglobulin V-region diversification regulated by transcription and RNA metabolism in antigen-driven B cells. Scand J Immunol. **73**(6): 520-6.

228.   Hou J, Zhang B, Zhang L, Ding S. [Establishment and biological characteristics of human multiple myeloma cell line CZ-1]. Zhonghua Xue Ye Xue Za Zhi. 2002; **23**(10): 509-13.

229.   Livak KJ, Schmittgen TD. Analysis of relative gene expression data using real-time quantitative PCR and the 2(-Delta Delta C(T)) Method. Methods. 2001; **25**(4): 402-8.

Appendix

Appendix 1

Detection of immunoglobulin light chain gene products

A1.1 Rationale

In order to test the hypotheses put forth for these studies it is important to have reliable systems for accurately measuring differences in levels of LC mRNA and proteins. To do this, several methodologies were adapted and developed that produce accurate and reproducible measurements of LC gene products following exposures to experimental and control siRNAs and shRNA expression systems. Those used for detection of protein included Immunoprecipitation of radiolabeled newly synthesized LC proteins from cell lysates, Enzyme Linked Immunosorbance Assay (ELISA), and fluorescent immunolabeling of intact cells for analysis by flow cytometry; LC mRNA levels were assessed using PCR and Real Time PCR.

A1.2 Detection of LC Gene Expressionby Real time PCR

Cells and culture conditions

Myeloma lines SP2/O-λ6, RPMI 8226, and Bur were maintained as described in Section 3.1. At time of experiments cells were harvested by centrifugation. Supernatants were removed to clean tubes and stored at 4° or -20° until time of assay. If required, cell washes were carried out by resuspending in PBS containing 1% BSA.

Real Time PCR

For each line, cells were lysed, total RNA extracted, and cDNA synthesized by Reverse Transcriptase reaction as described in Sections 3.3 and 3.4. Primers were designed to the LC

product of either SP2/O-λ6 (Fwd 5'AATTTTTTACTGACTCAGCCCC-3', Rev 5'-ACTTGGTCCCTCCGCCGAAAAC-3') or RPMI 8226 (Fwd 5'-gCCCTCAGGGGTTTCTAATC-3', Rev 5'-CTTTGTTTGGAGGGTGTGGT), each of which generated a 100 bp fragment. For the SP2/O-λ6 line, mouse glyceraldehyde 3-phosphate dehydrogenase (mGAPDH; RealTime Primers, LLC.; Fwd 5'-CTGGAGAAACCTGCCAAGTA-3´, Rev 5´-TGTTGCTGTAGCCGT-ATTCA-3´, 223-bp product) was used as reference gene. Likewise human GAPDH (hGAPDH; RealTime Primers, LLC; Fwd 5´-GAGTCAACGCGGATTTGGTCGT-3´, Rev 5´-TTGATT-TTGGAGGGATCTCG-3´, 238-bp product) or human β-actin (hβ-actin; RealTime Primers, LLC; Fwd 5'- GGACTTCGAGCAA- GAGATGG-3', Rev 5'- AgCACTgTgTTggCgTACAg-3') served as the reference genes for the RPMI 8226 line. Real-time PCR reaction was carried out using IQ SYBR Green Supermix (BioRad) containing 400 nM primer mix and 3 µL cDNA following manufacturer's instructions. Amplification was performed in 96-well PCR plates (BioRad) using an ICycler PCR unit and fluorescence detected by an IQ5 Multicolor Real-Time PCR system (BioRad). TAQ activation and denaturation was achieved in 1 cycle at 95°C for 3 minutes which was followed by forty 30-second amplification cycles at 95°C, 63°C, and 72°C. Relative LC mRNA levels for cells in each experimental siRNA treatment group were calculated using the $2^{\Delta\Delta C_T}$ method (229) and reported using cells receiving AllStars siRNA as the reference group.

Optimization of Reactions

The first step in developing the real time PCR conditions used in this study were the design of experimental primer sets. Deduced LC sequences were entered into the NCBI Primer-BLAST primer designing tool (http://www.ncbi.nlm.nih.gov/tools/primer-blast/). For each primer set, BLAST search parameters were set to return PCR products with lengths of between 90-110 bp and

melting temperatures (TM) ranging from 60-70° C. Specificity checks were performed using the refseq mRNA databases for *H. sapiens* and *M. musculus* to avoid amplification of unintended gene products, while search stringency was set so that primers must have had at least 2 bp mismatches to unintended targets.

For each gene target 6-8 primer sets were tested for functionality by Reverse Transctiptase-PCR of selected myeloma cell total RNAs followed by product separation by agarose gel electrophoresis. Amplicons were visualized under UV light following staining with ethidium bromide. Primer sets which failed to amplify any product, or those which generated multiple bands were eliminated from consideration.

Real-time PCR conditions were optimized for the IQ SYBR Green Supermix by ranging the annealing temperature from 60-72° using the temperature gradient curve protocol on the ICycler PCR unit. For each LC product, primer sets were selected which achieved target amplification above thresh hold levels at the lowest cycle number. The presence of single PCR products from each of these sets were confirmed by analysis of melt curves following each reaction.

The final step in selection of PCR primers for LC products was to determine amplification efficiencies for each primer set. This was conducted by setting up 10-fold serial dilutions of LC cDNA followed by analysis by real-time PCR. In the case of each primer selected, the amplification efficiencies were found to be between 90-110%.

Discussion

Real-time PCR was used to determine relative expression of LC mRNA for cell lines SP2/O-λ6 and RPMI 8226 with or without exposure to LC targeting or non-silencing control siRNAs. In the case of these experiments, the fluorescent dye, SYBR Green, was used to measure the amount of double stranded nucleic acids in each reaction. Because the fluorescent signal generated by SYBR

Green is generated as the dye becomes intercalated within double-stranded nucleic acids it is not product dependant amplification specificity is critical. This was initially addressed in the design of PCR primers by using the Primer-BLAST design algorithm which recommended primer sets that were only expected to amplify the LC genes of interest. These expectations were later confirmed by amplifying cDNA generated from either SP2/O-λ6 or RPMI 8226 cells and visualization on agarose gels.

Because real-time PCR steps are kept relatively short (30 sec each), the length of the PCR product can influence reaction efficiency. Thus, we followed recommendations put forth by Bio-Rad and limited our primer sets to generate products of around 100 bp.

Comparisons among treatment conditions in real-time PCR experiments may be influenced by the amount of starting material present in samples. To control for this, a "reference" gene was selected to normalize samples within each experiment. Typically a reference gene measures product levels of a so-called housekeeping gene whose levels may be rationally expected to remain stable among cells. In this case, we used either human or mouse GAPDH and β-actin as our housekeeping genes.

The final consideration in designing a real-time PCR reaction is the relative efficiencies of target versus reference gene amplification efficiencies. This refers to the notion that, under ideal conditions, each cycle of a PCR should exactly double the amount of double stranded material from that found at the start of the reaction. Amplification efficiency is accounted for mathematically by the base in the formula $2^{\Delta\Delta C_T}$. For example, if the efficiency of the reaction is 100%, then the formula for calculating relative expression levels is $2^{\Delta\Delta C_T}$, while if the effiency were lower, say 90% then the formula would be $1.9^{\Delta\Delta C_T}$. If the amplification efficiencies between the gene of interest (GOI) and the reference gene differ significantly, the results will be inaccurate.

A simple test for primer amplification efficiency is to set up a 1:10 dilution curve of cDNAs. Under optimal conditions, subsequent dilutions should generate amplification curves which cross the thresh hold value at exactly 2 cycles difference. In the case of these studies the amplification efficiency of LC primers and reference gene primers were between 90-110%.

A1.3 Detection of LC protein by ELISA

Antibody Selection

Lyophilized patient derived BJPs (κ or λ, respectively) were acquired from the HICP and reconstituted to ~10 µg/ml in PBS, for list see Table 5.1. 100 µl of diluted BJP were added in duplicate wells to the first row of a 96-well high binding ELISA/RIA plates followed by 1:1 serial dilution down plate. Plates were covered and BJPs bound overnight by incubation at 4°. Plates were blocked for 1 h at RT followed by the addition of 100 µl of 10 µg/µl antibody to be tested. Binding to antigen was detected by the addition of either HRP conjugated goat anti-mouse or goat anti-rabbit antisera (Jackson Immunoresearch). Wells with BJP but no antibody served as control.

In another series of experiments tentative primary antibodies (1 µg/µl; 100 µl) were bound to plates as above followed by blocking and addition of serially diluted BJPs. Unconjugated secondary antibodies were added at 1 µg/µl while HRP conjugated secondary antibodies were added at dilutions of 1:2,000-10,000. For a list of antibodies tested see Table 5.2.

Standard Curves

Serial dilution (1:1) of patient derived BJPs with known concentrations were prepared which spanned the dynamic range of ELISAs. Abs_{405} readings were collected using method described in

Table A1.1 BJPs used in developing ELISA assay

Isotype	BJP	Isotype	BJP
λ_1	Houston	κ_1	Galyon
	Locke		Watts
	Cox		**Bur**
λ_2	**Rhea**	κ_3	Dooley
	Levin	κ_4	Lenoir
λ_3	Kirby		
λ_6	JTO		
	Wil		

BJPs in bold were used to generate standard curves in final ELISA

Table A1.2 Antibodies Tested For ELISA

Target	Antibody	Source/ specificity	Vendor	Pass/Fail Bound	Sandwich Pass/Fail Primary	Secondary
$\lambda 6$ (Wil)	55-5F5	Mouse α hλ_6 mAb	HICP	NT	P	NT
	R604	Rabbit α hλ_6 pAb	HICP	NT	NT	P
	15A4	Mouse α hλ_6 mAb	HICP	P	F	F
	9D2	Mouse α hλ_6 mAb	HICP	F		
	15A4	Mouse α hλ_6 mAb	HICP	P	F	F
	14B	Mouse α hλ_6 mAb	HICP	F		
	14C	Mouse α hλ_6 mAb	HICP	F		
Total λ (Rhea) (Cott)	21-3F4	Mouse α hλ mAb	HICP	P	P	P
	18-9G11	Mouse α hλ mAb	HICP	P	P	P
	AO193	Rabbit α hλ pAb	Dako	P	P	P
	Star130P	HRP Rabbit αhλ pAb	AbD Serotec	P	NT	P
	AHI1804	HRP Rabbit αhλ pAb	Invitrogen	P	NT	P
Total κ (Bur)	AO191	Rabbit α hκ pAb	Dako	P	P	NT
	Star127P	HRP Rabbit αhκ pAb	AbD Serotec	P	NT	P

Legend: Antibodies for each ELISA were tested in various combinations using target antigen shown in parenthesis. Pass/Fail Bound refers to reactivity to antigen plated antigen. Sandwich Pass/Fail refers to reactivity of antibody in sandwich format. For non-HRP antibodies, binding was detected using species specific HRP conjugated goat antisera (Jackson ImmunoResearch).

Chapter 3.9 from duplicate wells. Data were entered into Microsoft Excel and fit to either logarithmic or linear regression curves. Calculated R^2 values provided a measure of fit, while the formula of the line was used to calculate LC concentrations from cell supernatant or mouse sera.

ELISA Protocol

For all ELISAs the following standard conditions were used. Primary antibodies were diluted to concentrations of ~10 µg/ml in PBS, and 100 µl of each were added to each well of 96-well high binding ELISA/RIA plates. Antibody binding was accomplished either by incubation overnight at 4° C or for 2 h at 37° C. Plates were blocked with PBS + 1% bovine serum albumin (BSA) for 1 h at room temperature. Antigen and further antibody bindings were carried out by adding 100 ml to each well followed by 1 h incubations at room temperature. Between steps plates were washed 3x in Tris buffered saline containing 0.1% tween20. Plates were developed using ABTS and absorbance read as described in Chapter 3.9.

Final ELISA Formats

Figure 5.1 depicts a graphical representation of the antibodies and standards used for detection of LC products and are reflective of assays reported in Chapter 3.9 and 6.3. A dilution series of standards were included on each plate. Based on initial test plates, standards diluted to encompass either the linear or logarithmic phase of calculated regression curves so that the calculated R^2 for a given line was > 0.9. Figure 5.2 depicts several sample standard curves from individual ELISAs.
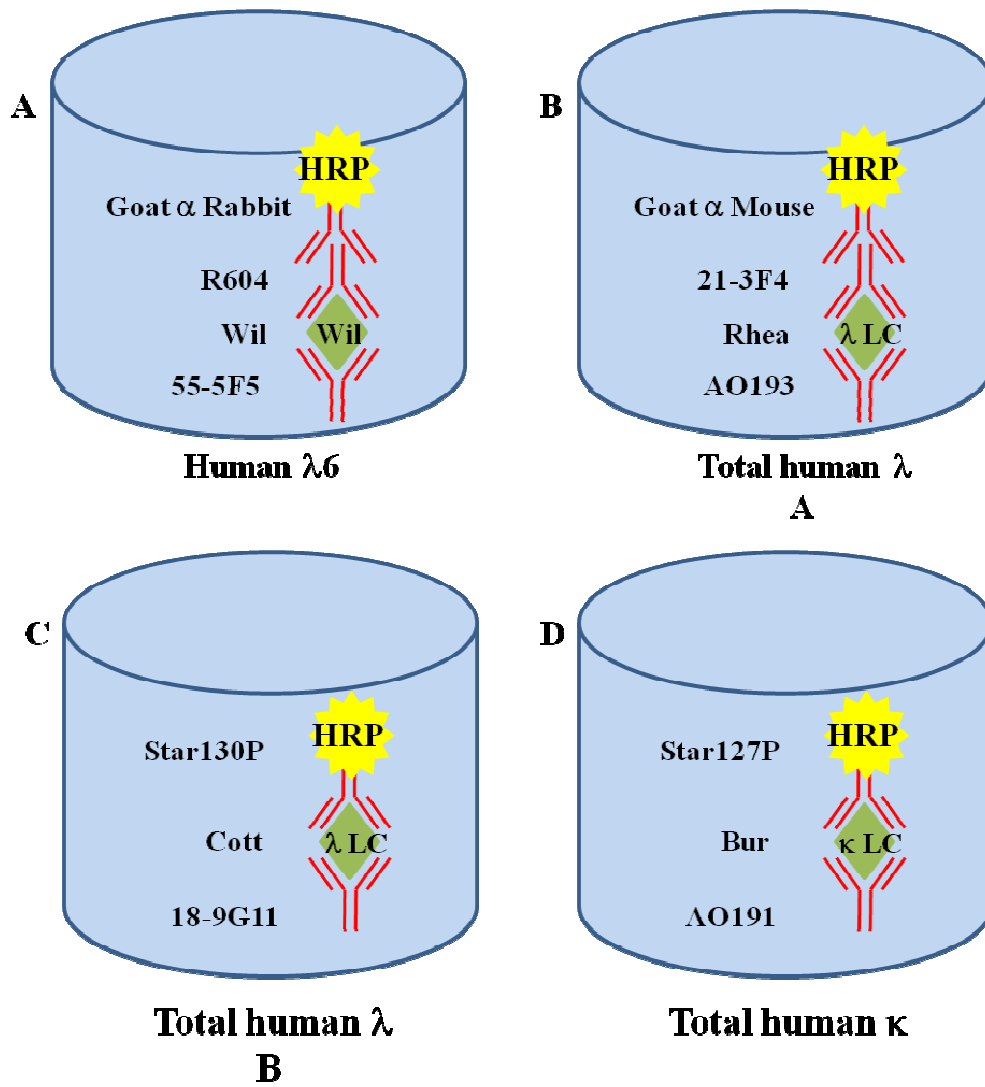
Figure A1.1 Final ELISA Configurations. LC products of cell line SP2/O-λ6 were measured using A) human λ6 ELISA while the LC product of cell line 8226 were mea
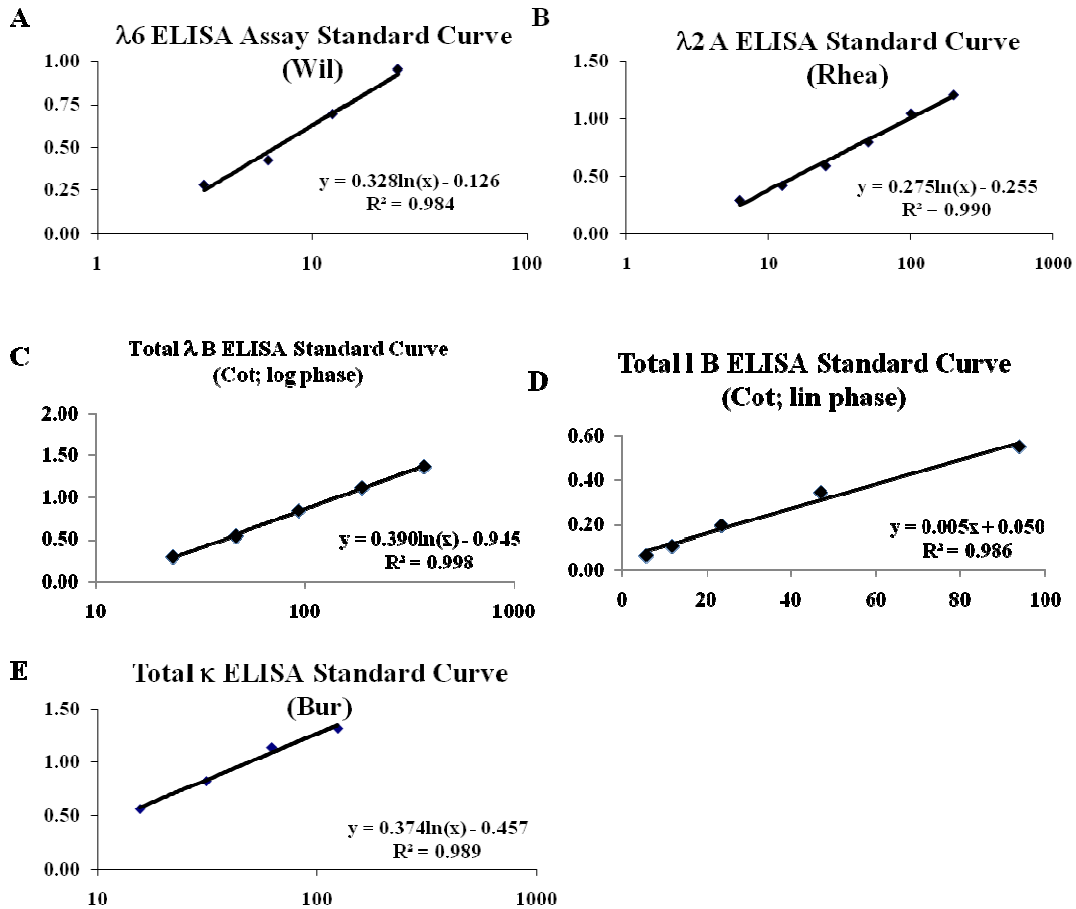
A. λ6 ELISA Assay Standard Curve (Wil)
$y = 0.328\ln(x) - 0.126$
$R^2 = 0.984$

B. λ2 A ELISA Standard Curve (Rhea)
$y = 0.275\ln(x) - 0.255$
$R^2 = 0.990$

C. Total λ B ELISA Standard Curve (Cot; log phase)
$y = 0.390\ln(x) - 0.945$
$R^2 = 0.998$

D. Total l B ELISA Standard Curve (Cot; lin phase)
$y = 0.005x + 0.050$
$R^2 = 0.986$

E. Total κ ELISA Standard Curve (Bur)
$y = 0.374\ln(x) - 0.457$
$R^2 = 0.989$

Figure A.1 2 Sample standard curves from various ELISA formats. Standard curves were generated from A.) Total λ 6 ELISA using patient derived BJP Wil, B.) Total λ ELISA A with BJP Rhea, Total λ ELISA B with Cot standard curve in C.) the log phase or D.) the linear phase, and E.) Total κ ELISA using BJP Bur as a standard. Curves and standards used to generate them were considered valid if unknown samples of interest fell within the dynamic range of the assay and if $R^2 > 0.98$ for the curve.

Vita

Jonathan Phipps is the only child to parents Larry and Judy Phipps of Powder Springs, TN. He is married to Dr. Jada Phipps, DVM, whom he met while attending his undergraduate institution, Lincoln Memorial University. Prior to this, Jonathan had been a graduate of Horace Maynard High School, Maynardville, TN. Following his graduation from Lincoln Memorial Jonathan was awarded a Master's of Science degree by the University of Tennessee for his graduate work in the lab of Dr. Michael Karlstad where he studied the effects of dietary polyunsaturated fatty acids on neutrophil function and hepatocyte membrane phospholipid content. For his Doctor of Philosophy degree, Jonathan worked with Dr. Jonathan Wall and Dr. Daniel Kestler in the laboratory of Dr. Alan Solomon at the University of Tennessee Medical Center in Knoxville, TN.